

**The lower Paleogene shallow-water limestones in the  
Tethyan Himalaya of Tibet and their implications for larger  
foraminiferal evolution, India-Asia collision and PETM-CIE**

Dissertation

zur Erlangung des Doktorgrades der Naturwissenschaften

(Dr. rer. nat.)

am Fachbereich Geowissenschaften

der Universität Bremen

vorgelegt von

**Qinghai Zhang**

Bremen, Oktober, 2012



**Gutachter:**

Prof. Dr. Helmut Willems

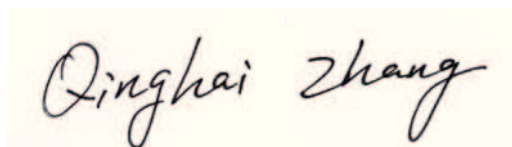
PD Dr. Christian Scheibner



## **-Erklärung-**

Hiermit versichere ich, dass ich

1. die Arbeit ohne unerlaubte fremde Hilfe angefertigt habe,
2. keine anderen als die von mir angegebenen Quellen und Hilfsmittel benutzt habe und
3. die den benutzten Werken wörtlich oder inhaltlich entnommenen Stellen als solche kenntlich gemacht habe.

A handwritten signature in black ink on a light yellow background. The signature reads "Qinghai Zhang" in a cursive, flowing script.

Qinghai Zhang

Bremen, den 20.10.2012

## Preface

The project is part of the Priority Programme 1372 Tibetan Plateau: Formation, Climate, Ecosystems (*TiP*). It was funded by Deutsche Forschungsgemeinschaft (No. Wi725/26) for three years (12. 2008–11.2011), and further supported through a postgraduate scholarship by the University of Bremen for six months (12.2011-05.2012). Additionally, part of field cost in Tibet was financed by Chinese Ministry of Science and Technology (2011CB403101 to Ding Lin) and Chinese Academy of Sciences (KZCX2-YW-Q09-03 to Ding Lin).

The thesis is composed of four first-authorship manuscripts which are published, accepted, or to be submitted for publication in peer-reviewed international scientific journals. These manuscripts are preceded by a general abstract, acknowledgements and introduction, and followed by conclusions and future perspectives.

## TABLE OF CONTENTS

ABSTRACT .....	1
ZUSAMMENFASSUNG .....	3
ACKNOWLEDGEMENTS .....	6
1. Introduction .....	7
1.1 The early Paleogene larger foraminifera .....	7
1.2 Timing of the initial India-Asia continental collision.....	9
1.3 The PETM-CIE .....	11
2. Evolution of the Paleocene-early Eocene larger benthic foraminifera in the Tethyan Himalaya of Tibet, China .....	21
Abstract .....	22
2.1 Introduction .....	23
2.2 Geologic setting and lithostratigraphy .....	24
2.3 Materials and methods .....	25
2.4 Biostratigraphy .....	27
2.5 The Paleocene-early Eocene larger foraminiferal evolution in Tibet .....	37
2.6 Comparison of the Paleocene-early Eocene LBF between the eastern and western Neo-Tethyan Ocean.....	40
2.7 The P-E boundary in the SBZs.....	43
2.8 Conclusions.....	45
3. Depositional environments of the lower Paleogene larger foraminiferal limestones in the Tethyan Himalaya of south Tibet, China .....	52
Abstract .....	53
3.1 Introduction .....	53
3.2 Geologic setting .....	55
3.3 Materials and methods .....	57
3.4 Litho- and bio- stratigraphy of the Zhepure Shan Formation .....	58
3.5 Microfacies description and interpretation .....	59
3.6 An early Paleogene carbonate ramp at Tingri .....	72
3.7 Circum-Tethyan tectonic uplift at the P/E boundary .....	74
3.8 Conclusions.....	76

4. The initial India-Asia continental collision and foreland basin evolution in the Tethyan Himalaya of Tibet: Evidence from stratigraphy and paleontology.....	83
Abstract.....	84
4.1 Introduction .....	84
4.2 Regional stratigraphy .....	86
4.3 Methods .....	90
4.4 Biostratigraphy .....	90
4.5 Paleoenvironmental and paleobathymetric analysis.....	92
4.6 The initial India-Asia continental collision .....	95
4.7 Reinterpretation of timing of provenance change at Sangdanlin .....	98
4.8 A tectonic model for the early Paleogene India-Asia convergence .....	100
4.9 Conclusions.....	102
5. High resolution Paleocene-Eocene carbon isotope excursion in the shallow marine environment of the Tethyan Himalaya (Tibet, China) .....	108
Abstract.....	109
5.1 Introduction .....	109
5.2 Study area, materials, and methods.....	110
5.3 Discussion.....	111
5.4 Conclusions.....	115
6. Conclusions and future perspectives.....	119
6.1 Conclusions.....	119
6.2 Future perspectives.....	120



## ABSTRACT

Fossiliferous limestones in shallow marine environments are important archives for the studies of paleontology, biostratigraphy, paleoenvironment and paleoclimatology as well as geodynamic evolution of their sedimentary basins. In the eastern Tethyan Himalaya, two areas, Tingri and Gamba, expose the best outcrops of the lower Paleogene larger foraminiferal limestones in Tibet. It provides a good chance to study the Paleocene-early Eocene larger foraminiferal evolution, the process of the India-Asia collision and foreland basin evolution, and the response of shallow marine environments to the Paleocene-Eocene Thermal Maximum (PETM) and Carbon Isotope Excursion (CIE).

Following the Opeel Zone's principle, ten Shallow Benthic Zones (SBZs) ranging from SBZ 1 to 10 have been divided from one continuous section at Tingri, and five SBZs comprising SBZ 2, 3, 4, 5, and 7 are recognized from three separate sections at Gamba. During the Paleocene, the Larger Benthic Foraminifera (LBF) were characterized by high diversification of *Lockhartia*, *Kathina*, *Daviesina*, *Miscellanea*, *Ranikothalia*, and *Operculina* in the so-called 'Lockhartia Sea', and in the early Eocene it were *Alveolina*, *Orbitolites*, *Nummulites*, *Assilina*, and *Discocyclina* who dominated the Gamba and Tingri areas. The Paleocene LBF in Tibet showed earlier occurrence of generic and species diversity, and since SBZ 2, some genus (such as *Lockhartia* and *Kathina*) have evolved more than one species within a zonal time slice. It is inconsistent with the monospecific trait of K-strategist genera in Europe. Importantly, the Paleocene/Eocene (P/E) boundary in shallow-water environments is clearly identified at Tingri by measuring carbon isotopes from bulk carbonates, and it is situated in the upper part of SBZ 5 and associated with no evident biotic turnover of benthic foraminiferal communities. Notably, a transient but distinct Larger Foraminiferal Extinction and Origination (LFEO) event has been found in Tibet, which is characterized by the sudden disappearance of all Paleocene lamellar-perforate LBFs, such as *Lockhartia*, *Kathina*, *Daviesina*, *Miscellanea*, *Ranikothalia*, and *Operculina*, and the initial dominance of early Eocene porcellaneous forams of *Alveolina* and *Orbitolites*. The LFEO marks the boundary between SBZ 5 and 6 in Tibet, and it might occur only in the low latitudinal areas of the Neo-Tethyan Ocean. Additionally, the LFEO coincides with the onset of the CIE recovery, and postdates the P/E boundary ~80 kyr according to age models of the PETM-CIE. The synchronicity of the LFEO and the initial recovery of the CIE imply that some possible mechanisms causing the rapid recovery of the CIE probably had also led to the LFEO in shallow-water environments.

Based on the high resolution larger foraminiferal biostratigraphy, eight microfacies types have been recognized from the Zhepure Shan limestones with special emphasis on the

paleoecology of the larger foraminifera. The general development of those microfacies at Tingri can be summarized by a carbonate ramp model with three subdivisions of inner ramp, mid-ramp, and outer ramp. Overall, microfacies analyses indicate that there was a deepening of depositional environment during the Paleocene and early Eocene in Tibet, which was interrupted by a sudden shallowing event at the P/E boundary. In addition to Tibet, the shallowing event has also been recognized from other shallow marine environments surrounding the Neo-Tethyan Ocean by some authors. Together with the opinion of a eustatic rise during the Paleocene-Eocene greenhouse world, the shallowing event may imply that a circum-Tethyan tectonic uplift once took place at the P/E boundary.

Tectonically, the onset of continent-continent collision is accompanied by elimination of oceanic crust and development of a peripheral foreland basin on the subducting continental crust. In Tibet, the lower Paleogene limestones at Gamba and Tingri have been used to study the evolution of the northern Indian continental margin and further to constrain the timing of initial India-Asia collision. Based on our studies of stratigraphy, paleontology, sedimentology, and geochronology at Gamba and Tingri together with other previously published results, we propose that the tectonic uplift occurring at the P/E boundary represents the initial India-Asia continental collision in Tibet and time equivalence between the initial India-Asia collision and the PETM-CIE implies that the former probably also plays an important role in triggering the latter.

The PETM is one of the main focuses in the geoscientific studies during the last 20 years. The magnitude, duration, pattern of the negative CIE are key to constraints on the mass and tempo of light-carbon release during the PETM, which in turn play a crucial roles in determining possible light-carbon sources and mechanisms triggering the PETM. Here we show a high resolution CIE curve from the tropical shallow marine limestones in Tibet, and our results reveal that the pattern of the main CIE in the shallow marine is very similar to that from deep sea (ODP Site 690) except for a larger magnitude and an abrupt recovery in the former. We speculate that the CIE in the entire ocean followed certain regular steps to reach the most negative carbon isotope values during the PETM, and the magnitude of the negative CIE may gradually increase from the deep sea to shallow marine and land. Our work will provide important constraints on testing possible mechanisms triggering the PETM, and improve the current understanding of the PETM-CIE in the shallow marine environments.

## ZUSAMMENFASSUNG

Fossil-führende Flachwasserkalke sind wichtige Archive für Studien zur Paläontologie, Biostratigraphie, zur Rekonstruktion von Paläoklima und –umwelt sowie zur geodynamischen Entwicklung von Sedimentbecken. In zwei Gebieten des östlichen Tethys-Himalaya, in Tingri und Gamba, sind Kalksteine mit Großforaminiferen aus dem unteren Paläogen am besten aufgeschlossen. Sie bieten eine gute Möglichkeit zum Studium der Evolution von Großforaminiferen im unteren Paläogen, der Kollisionsgeschichte zwischen Indien und Asien und der damit verbundenen Entwicklung eines Vorlandbeckens sowie der Reaktionen im flachmarinen Bereich auf das Paläozän-Eozän Temperaturmaximum (PETM) und der entsprechenden Exkursion der Kohlenstoffisotope (CIE).

Nach dem Prinzip der Opperl-Zone wurden zehn benthische Flachwasserzonen (SBZs), von SBZ 1 bis 10, in einem kontinuierlichen Profil in Tingri ausgehalten. Fünf solche Zonen, SBZ 2, 3, 4, 5 und 7, wurden in drei einzelnen Profilen in Gamba erkannt. Während des Paläozän zeichneten sich die benthischen Großforaminiferen (LBF) durch starke Diversifizierung von *Lockhartia*, *Kathina*, *Daviesina*, *Miscellanea*, *Ranikothalia*, und *Operculina* im sogenannten „Lockhartia-Meer“ aus, während im Eozän *Alveolina*, *Orbitolites*, *Nummulites*, *Assilina*, und *Discocyclina* im Gebiet von Gamba und Tingri dominierten. Im Gegensatz zur monospezifischen Entwicklung der K-strategischen Gattungen in Europa tritt im Paläozän in Tibet schon früher eine größere Gattungs- und Artenvielfalt auf, und in einigen Gattungen (wie z.B. in *Lockhartia* und *Kathina*) haben sich ab der SBZ 2 mehr als eine Art entwickelt. Ein wichtiges Ergebnis ist die eindeutige Identifikation der Paläozän-Eozän Grenze in den Flachwasserkalken von Tingri anhand der Kohlenstoffisotopendaten vom Gesamtkarbonat. Diese Grenze befindet sich im oberen Teil der SBZ 5 und zeichnet sich nicht durch einen Umbruch in der Vergesellschaftung benthischer Foraminiferen aus. Ein bemerkenswertes Ereignis eines deutlichen und abrupten Faunenumbruchs (LFEO) mit Aussterben und Neuerscheinen von Arten wurde in Tibet beobachtet, charakterisiert durch das plötzliche Verschwinden aller lamellar-perforierten Großforaminiferen des Paläozän wie z.B. *Lockhartia*, *Kathina*, *Daviesina*, *Miscellanea*, *Ranikothalia*, und *Operculina* und die anfängliche Dominanz der frühen Porzellanschaler des Eozän durch *Alveolina* und *Orbitolites*. Dieses Ereignis (LFEO) markiert die Grenze zwischen SBZ 5 und 6 in Tibet und kommt möglicherweise nur in den niedrigen Breiten der Neotethys vor. Das LFEO ist zeitgleich mit dem Anstieg der Kohlenstoffisotope nach der negativen Exkursion und trat daher etwa 80 kyr nach der Paläozän-Eozän Grenze auf, entsprechend des Altersmodells dieser Exkursion. Das Zusammenfallen der LFEO mit der raschen Normalisierung der Isotopenwerte deuten auf einen gemeinsamen Mechanismus, der sowohl die Kohlenstoffisotope als auch die benthischen Foraminiferen der Flachwasserbereiche beeinflusste.

Mit Hilfe von hochauflösender Biostratigraphie mit Großforaminiferen wurden in den Kalksteinen des Zhepure Shan (Tingri) acht Mikrofaziestypen unterschieden, wobei ein besonderer Schwerpunkt auch auf der Palökologie der Großforaminiferen des Paläozän bis unteren Eozän lag. Ganz allgemein kann die mikrofazielle Entwicklung in Tingri mit dem Modell einer Karbonatrampe beschrieben werden, die in einen inneren, mittleren und äußeren Teil untergliedert war. Die Mikrofaziesanalyse deutet auf einen generellen Vertiefungstrend des Ablagerungsraumes in Tibet während des Paleozän und unteren Eozän, der durch eine plötzliche Verflachung an der Paläozän-Eozän Grenze unterbrochen war. Dieses Verflachungsereignis wurde außer in Tibet auch in anderen Flachwassergebieten der Neotethys beobachtet. Im Hinblick auf die allgemeine Annahme eines globalen eustatischen Meeresspiegelanstiegs während der Treibhauswelt des Paläozän-Eozän könnte das Verflachungsereignis an der Paläozän-Eozän Grenze als tektonische Hebung rund um die Tethys interpretiert werden.

Tektonische Szenarien einer Kontinent-Kontinent Kollision zeichnen sich durch das Verschwinden ozeanischer Kruste aus und werden durch die Entwicklung eines peripheren Vorlandbeckens auf der subduzierten Ozeankruste gekennzeichnet. In Tibet wurden die Kalksteine des Paläogen von Gamba und Tingri benutzt, um die Entwicklung des nördlichen Randes der indischen Kontinentalplatte zu rekonstruieren sowie um den Zeitpunkt der Kollision zwischen Indien und Asien einzugrenzen. Basierend auf unseren Ergebnissen der Untersuchungen zur Stratigraphie, Paläontologie, Sedimentologie und Geochronologie sowie den Daten aus der Literatur schlagen wir vor, dass die tektonische Hebung an der Paläozän-Eozän Grenze den Beginn der Indien-Asien Kontinentalkollision in Tibet repräsentiert. Die zeitliche Übereinstimmung dieser Kollision mit der Kohlenstoffisotopenexkursion am PETM deutet darauf hin, dass letztere möglicherweise mit durch die Kollision ausgelöst wurde.

Das PETM ist eines der zentralen Forschungsthemen der Geowissenschaften der letzten 20 Jahre. Dabei spielen Ausmaß und Ablauf der negativen CIE eine Schlüsselrolle zur Abschätzung der Menge und Geschwindigkeit des freigesetzten isotopisch leichten Kohlenstoffs während des PETM. Dies wiederum ist von großer Bedeutung für das Verständnis möglicher Quellen des isotopisch leichten Kohlenstoffs und der Auslösungsmechanismen des PETM. Unsere hochauflösende CIE-Kurve aus den tropischen Flachwasserkalken von Tibet zeigt in ihrem Ablauf sehr große Ähnlichkeit zu entsprechenden Kurven aus dem tiefen Ozean, allerdings ist die negative Exkursion im Flachwasser wesentlich stärker als im tiefen Wasser. Sie ist bezüglich der Stärke jedoch zu einem gewissen Grade mit den Kurven vergleichbar, die von terrestrischen Profilen publiziert werden. Wir vermuten, dass der CIE des gesamten Ozeans in bestimmten Schritten zum Minimum der Kohlenstoffisotope am PETM abfällt, und die Stärke der Exkursion scheint graduell vom tiefen Ozean hin zum Flachwasser und Land anzusteigen. Unsere Resultate sind ein wichtiger Beitrag zur Überprüfung

möglicher Ursachen des PETMs in der Zukunft und tragen zweifellos zum besseren Verständnis der CIE am PETM in Flachwasserbereichen bei.

## ACKNOWLEDGEMENTS

First of all, my sincere thanks should be given to my doctor's supervisor, Prof. Dr. Helmut Willems. In 2008, he cordially invited me to join his working group and offered me a PhD position to study the area where it was once an ocean during most of the geologic history and now stands highest on the earth – South Tibet. During the past four years, he accompanied me to Tibet two times for carrying out field work, helped me grasp laboratory skills and search for important literature, supported me to do some extra experiments which were not designed in the original project, and encouraged me to attend different kinds of academic courses, workshops, and meetings. In his spare time, he drove me to visit many areas, such as Emden, Langeoog Island, Walsrode, and Worpswede, showing me the most beautiful views and deeply hidden history of the northwest Germany. His carefulness, criticism, and curiosity in doing scientific work and positive attitude towards life will undoubtedly affect me in the future.

Secondly, I owe my gratitude to Prof. Dr. Lin Ding from the Institute of Tibetan Plateau Research, Chinese Academy of Sciences. It was he who firstly led me to enter into Tibetan Plateau and pointed to a clear direction for my studying Tibetan geology. From 2005 to 2008, three years' stay in his working group afforded much knowledge of sedimentary tectonics to me. Thanks also go to the members of his working group, such as Fulong Cai, Di Yang, Yahui Yue, Shun Li, Shuaiquan Fan, Liyun Zhang, Qingzhou Lai, with whom I once had a very pleasant time.

Thirdly, I am grateful to the late Prof. Dr. Lukas Hottinger from the Natural Museum of Basel and PD Dr. Christian Scheibner from the University of Bremen. Prof. Hottinger invited me to his house in the late 2010 and instructed me in his enormous knowledge of larger foraminifera. His assiduity, erudition, and the hospitality from his whole family will be remembered by me forever. Dr. Scheibner has reviewed one of my manuscripts and my dissertation and given me valuable comments and suggestions.

Specially, I thank all members from our working group and some friends in Bremen for providing me the cheerful working and living atmosphere. Anne and Christiane are thanked for their constant laboratory support; Friederike, Jan-Peter, Michaela, and Antonia are thanked for their field assistance in Tibet; Maria, Ines, Dorothee, Walter, Martin, Erna, Pia, Petra, and Monika are thanked for their help on scientific work and daily life. Special thanks are given to my Chinese colleague, Liang Chen, who was once my tutor teaching me how to make life easier in Bremen.

Most importantly, I thank my beloved family, my wife and my parents. You are always the quietest harbour when violent storms attack me.

# 1. Introduction

My study areas – Tingri and Gamba – are located in the Tethyan Himalaya of Tibet, where sedimentary rocks have recorded the history of the initial India-Asia collision and the closure of the Neo-Tethyan Ocean during the early Paleogene. In the thesis, I will mainly focus on the studies of the lower Paleogene limestones, which contain valuable information of the larger foraminiferal evolution, the initial India-Asia collision, and the Carbon Isotope Excursion (CIE) during Paleocene-Eocene Thermal Maximum (PETM).

## 1.1 The early Paleogene larger foraminifera

Foraminifera are non-tissue-forming one-celled marine protozoa (BouDagher-Fadel 2008). Since the Paleozoic, foraminifera have existed in the Ocean and evolved more than 50,000 species (Hottinger 2001). By comparison with other more complicated, multicellular, tissue-forming invertebrate organisms, foraminifera usually have higher potential to be fossilized due to their larger population in the carbonate sediments. As a species, foraminifera showed rapid evolutionary process in the geologic history, and thus have been taken as one of the major biotic groups for the construction of biostratigraphy. Furthermore, foraminifera were also thought to represent 'an ecosystem of their own by being comparatively independent of other biosystems' (Hottinger 1997, 2001), and thus commonly used as excellent ecological indicators to carry out paleoenvironmental interpretation and paleobathymetric reconstruction.

According to their living strategy, foraminifera can be divided into two groups: planktonic and benthic foraminifera. The planktonic foraminifera usually float in the surface of the open ocean, whereas the benthic foraminifera can dwell in all depths of the ocean. The larger foraminifera basically belong to the benthic foraminifera, and they differ from small benthic foraminifera in having more complicated, internal structures and larger sizes ( $>3 \text{ mm}^3$  in volumes or  $>1 \text{ mm}$  in diameter) (Hallock and Glenn 1986; Beavington-Penney and Racey 2004). Consequently, species determination of larger foraminifera has usually been conducted on the thin sections in which their internal structures are exposed. Under most circumstances, random cuttings of larger foraminifera exhibit quite different structures (Fig. 1), and only the axial and/or equatorial cuttings can afford the precise identification to the species level. Considering most fossilized larger foraminifera are preserved in the cemented limestones, to obtain the orientated cuttings of larger foraminiferal shells in randomly polished thin sections is usually a game of luck. So to collect samples densely in the field sections and prepare more thin sections from each sample are indispensable for studies of the larger foraminiferal biostratigraphy in the limestones.

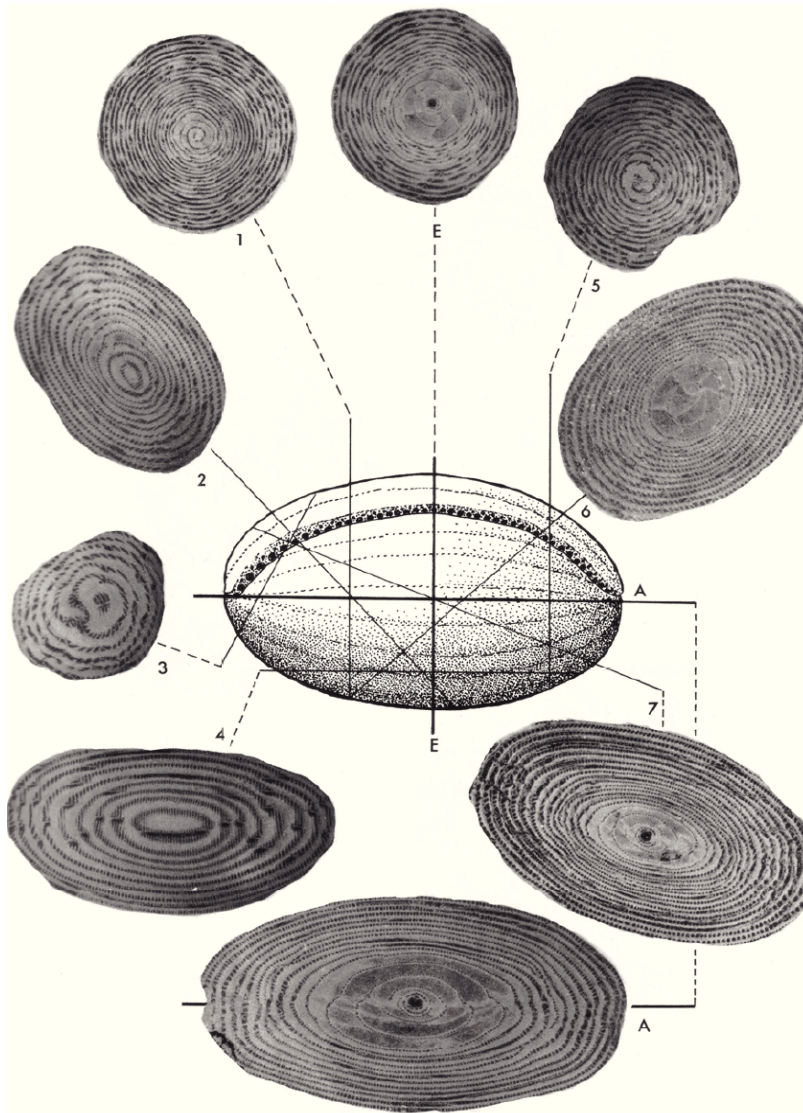


Fig. 1 Aspect of different cuttings of *Alveolina elliptica* (Sowerby), 1840. A and B show axial and equatorial cuttings, respectively, and 1 to 7 represent different oblique and tangential cuttings (from Hottinger 1974).

Theoretically, the term of 'species' in larger foraminifera has been defined by 'quantitative morphological characters which are changing with time in one direction' (Hottinger 2009). However, the morphology of larger foraminifera is affected not only by the internal genetic factor but also by external environmental conditions (Racey 1995), such as temperature, water depth, substrate, water energy, salinity, and so on. So it is rather difficult to assess the relative importance of morphological characters that can indicate the evolutionary trends. As a result, the diagnostic criteria of specific distinction are sometimes variable from different authors.

Apart from the ambiguities in the specific identification, the criteria used to distinguish some sibling genera are not always consistent. For example, Blondeau (1972) divided the Family Nummulitidae into different genera (*Nummulites*, *Assilina*, *Operculina*, *Ranikothalia* etc.) on the basis of the features of 'form of the spire, shape and



arrangement of the septa and chambers'. By contrast, Hottinger (1977) preferred choosing 'shape and arrangement of stolons, sutural canals, and chambers' as the diagnostic features. So, to resolve the above-mentioned questions, long-term taxonomic studies focused on a certain genera are needed, which, however, are not the objectives of the thesis. Therefore, with respect to the determination of the Paleocene and early Eocene larger foraminifera in Tibet, I simply followed the taxonomic descriptions given by Nuttall, Davies, Smout, Hottinger, Schaub etc. (see Chapter 2 for the details), who had once built the milestones in studying the taxonomy of the larger foraminifera in the Neo-Tethyan realm.

Based on the determination of different species of larger foraminifera and the acquisition of their distribution in the sections, sequential biozones defined by the appearance and disappearance of certain species can be recognized, which have been used to designate the Shallow Benthic Zones (SBZ) in the western Neo-Tethyan realm (Serra-Kiel et al. 1998). In Tibet, the construction of the SBZ was mainly built on the sections from the Tingri and Gamba areas. The biozones from the two areas can generally be correlated, and the index fossils of each biozone at Tingri and Gamba are approximately shared. Studies of the early Paleogene larger foraminiferal biostratigraphy in Tibet can be seen in Chapter 2. And in the light of great advantage of larger foraminifera for studying paleobathymetry and paleoecology of their sedimentary environments, the depositional evolution of the Zhepure Shan Formation at Tingri has been discussed in Chapter 3.

## **1.2 Timing of the initial India-Asia continental collision**

The India-Asia collision is the most significant geologic event in the Cenozoic. It caused the closure of the Neo-Tethys equatorial seaway between India and Asia and the formation of high altitude and thick crust of the Tibetan Plateau, which in turn made a strong impact on the global ocean circulation and marine geochemistry (Richter et al. 1992; Chesley et al. 2000; Le Houedec et al. 2012) and the Asian climate and river drainage patterns (Molnar et al. 1993; Clift and Blusztajn 2005). The timing of the initial India-Asia collision is one of the critical parameters for understanding the Tibetan Plateau formation and Himalayan Orogen evolution, and consequently has been paid special attention in the past. In spite of that, proposed ages for the initial India-Asia collision still vary greatly, ranging from the K/Pg boundary (~65 Ma) (Ding et al. 2005; Hu et al. 2012), to the P/E boundary (~56 Ma) (Garzanti 2008; Zhang et al. 2012) or the early Eocene (~50 Ma) (Zhu et al. 2005; Najman et al. 2010), and even to as late as the Eocene/Oligocene boundary (~34 Ma) (Aitchison et al. 2007).

The disagreements on timing of the initial India-Asia collision mainly result from the different understanding of the term ‘the initial India-Asia continental collision’ and correspondingly different working methods adopted. Theoretically, Searle et al. (1997) defined the collision as ‘the transition from marine to continental sedimentation within the suture zone’. By contrast, Rowley (1998) referred to ‘the elimination of Neo-Tethys oceanic lithosphere and the first development of a foreland basin on the Indian continent’ as the initial India-Asia continental collision. In essence, the first definition emphasizes the subaerial contact of the India and Asia plates whereas the second focuses on their subaqueous contact. Actually, the initial contact between the India and Asia continents occurred certainly in the ocean, and subsequently crustal shortening and thickening as well as topographical rising of the Indian and Asian continents drove the seawater out of the northern Indian continent, causing the closure of the eastern Neo-Tethyan Ocean and the India-Asia subaerial contact. Therefore, timing of the subaerial contact indicates only the minimum age of the continental collision while the first subaqueous contact of two continents represents the maximum age of the collision. Consequently, Rowley’s definition is more appropriate for the indication of the initial India-Asia continental collision. Surprisingly, the lag times between the subaerial and subaqueous contacts during the collisions are not always insignificant even over the geologic time scale, such as the Arabia-Eurasia collision in the Persian Gulf where the collision happened since the early Miocene but the marine environment still exists even now (Agard et al. 2005).

Practically, a large variety of geologic methods have been adopted to constrain the age of the initial India-Asia collision, which mainly include (1) an abrupt decrease of the India-Asia convergence rate (Patriat and Achache 1984; Klootwijk et al. 1992; Copley et al. 2010; van Hinsbergen et al. 2011b), (2) paleolatitudinal overlap between the Tethyan Himalaya and the southernmost Lhasa block (Patzelt et al. 1996; Chen et al. 2010; Dupont-Nivet et al. 2010; Liebke et al. 2010; Yi et al. 2011), (3) ultrahigh-pressure metamorphism resulting from the northward subduction of the leading edge of Indian continental margin (de Sigoyer et al. 2000; Leech et al. 2005), (4) the latest marine sediments in the Tethyan Himalaya (Searle et al. 1987; Wang et al. 2002), (5) terrestrial faunal exchange between India and Asia (Jaeger et al. 1989; Clyde et al. 2003; Clementtz et al. 2011), (6) subsidence history of the northern Indian continental shelf (Rowley et al. 1998; Corfield et al. 2005), and (7) regional stratigraphy, sedimentology, and provenance analysis for dating the beginning of provenance change from India to Asia or the initial formation of a forebulge in the Tethyan Himalaya (namely the onset of a foreland basin) (Garzanti et al. 1987; Ding et al. 2005; Zhu et al. 2005; Wang et al. 2011; Hu et al. 2012; Zhang et al. 2012). On one hand, these different methods have improved our understanding of the continent-continent collision; on the other hand, their

theoretical and/or practical limitations on dating the initial India-Asia collision have also caused (at least partly) the present confusion of the proposed collision ages.

Wu et al. (2008) have published a comprehensive review on the timing of the initial India-Asia continental collision, and they pointed out that the sudden slowdown of the India-Asia convergence rate (method 1) may reflect the onset of the continental collision, but the possibility of an intrinsic decrease of the Indian oceanic spreading rate can also not be completely ruled out. Concerning method 2, they thought that the great dispute over the size of 'Greater India' (Ali and Aitchison 2005; van Hinsbergen et al. 2011b) and the lack of enough paleomagnetic data from the Asian continent greatly affected the validity of the method. In reality, although a large number of new paleomagnetic data from the southern Lhasa block have been published in 2010 (Chen et al. 2010; Dupont-Nivet et al. 2010; Liebke et al. 2010; Sun et al. 2010; Tan et al. 2010), their proposed ages for timing of the India-Asia collision varied still greatly from ~60 Ma to ~42 Ma. Moreover, the ultrahigh-pressure rocks have only been reported in the western Himalaya (de Sigoyer et al. 2000; Leech et al. 2005), and the dating methods of eclogites (method 3) either have relatively larger error bars or are questioned by some geologists (O'Brien 2006). Methods 4 and 5 essentially indicate the subaerial contact between the India and Asia, and thus may provide only a minimum age for the collision. Method 6 is highly dependent on the biostratigraphic precision and resolution of the selected sedimentary sections, and it is also affected by the uncertainties from water depth of depositional environments and sea-level fluctuations (Corfield et al. 2005). Therefore, any updates of biostratigraphy, paleoenvironmental interpretations and sea-level changes will influence the calculation of the subsidence history. Exceptionally, method 7 is developed to date the onset of a foreland basin on the Tethyan Himalaya by following Rowley's definition. Theoretically it has the potential to provide the most robust age for the collision, and therefore has been used by us to constrain the initial India-Asia collision in Chapter 4.

### **1.3 The PETM-CIE**

The PETM event was firstly reported by Kennett and Stott in 1991 through their investigations on the cores of Ocean Drilling Project 690, and since that more than 400 papers dealing with the PETM have been published (McInerney and Wing 2011 and references therein). Past studies show that the PETM occurred at ~55-56 Ma (Westerhold et al. 2009; Jaramillo et al. 2010), and lasted for ~120-220 ka (Farley and Eltgroth 2003; Röhl et al. 2007; Aziz et al. 2008; Murphy et al. 2010). The climate, environment and biota during the PETM experienced drastic changes, including a more than 4° to 5°C global warming (Zachos et al. 2003), highly seasonal precipitation (Schmitz and Pujalte 2007), rapid ocean acidification and shallowing of the calcite

compensation depth (Zachos et al. 2005), abrupt reversal of deep-ocean circulation (Nunes and Norris 2006), planktonic foraminiferal diversification (Kelly et al. 1996), nanoplankton extinction and origination (Gibbs et al. 2006), shallow-water larger benthic foraminifera extinction and origination (Zhang et al. submitted), deep-water benthic foraminiferal extinction (Thomas and Shackleton 1996), and mammalian dispersal (Bowen et al. 2002). Most importantly, a sudden and distinct negative CIE has been found globally, from sediments, rocks, fossils, to organic matters both in the ocean (Bains et al. 1999) and on land (Koch et al. 1992). The magnitude and duration of the negative CIE have been adopted to evaluate the mass and tempo of light-carbon release, and those two parameters in turn provide the main constraints on the possible triggers and sources leading to the PETM-CIE. Theoretically, a massive release of  $^{13}\text{C}$ -depleted carbon from the lithosphere to the ocean-atmosphere system has been generally accepted to interpret changes of climate, environment, carbon cycle, and ecosystems. However, some fundamental questions with respect to the PETM-CIE are still in dispute.

- a) Although the CIE curve from ODP 690 (Bains et al. 1999) is generally thought to represent the most complete record of carbon isotopic variations during the PETM, the possibility of incomplete sedimentary records in ODP 690 due to low sedimentation rates and ocean acidification during the PETM (Zachos et al. 2005) still cannot be totally ruled out. Moreover, no two CIE curves having similar structures have been reported until now. Thus, the true, detailed processes of the negative CIE are still unclear;
- b) Both the magnitude (McInerney and Wing 2011 and references therein) and the duration of the negative CIE (Farley and Eltgroth 2003; Röhl et al. 2007; Murphy et al. 2010) are still debated. The disagreements on them have fostered the growth of different hypotheses for not only the onset of the CIE, such as methane hydrate dissociation (Dickens et al. 1997), thermogenic methane from intrusive volcanism (Svensen et al. 2004), desiccation and oxidation of organic matter (Higgins and Schrag 2006), and thawing permafrost at the two poles (DeConto et al. 2012), but also the recovery of the CIE, including terrestrial silicate weathering (Dickens et al. 1997; Kelly et al. 2005) and regrowth of carbon stocks in the biosphere or shallow lithosphere (Bowen and Zachos 2012);
- c) Given that the magnitude and duration of the negative CIE are clear, most assumptions proposed for triggering the PETM-CIE were formulated only to meet the demand of the general mass and rate of light-carbon release, and none of them has been used to explain the detailed variations within the CIE curve;

- d) There is still no solid evidence which is obtained from the geologic records and can directly confirm the exact sources of light-carbon release.

Up to now, the studies of the PETM-CIE from the marine realm were mostly conducted on hemipelagic or pelagic sections from ODP and IODP, where both sediments and fossils are supposed to preserve their original  $\delta^{13}\text{C}$  and  $\delta^{18}\text{O}$  values. However, the stratigraphic thickness of the PETM-CIE from deep oceans is generally thin, with 0.15 m from ODP Site 865 (Kelly et al. 1996), 0.42 and 0.8 m from ODP Sites 999 and 1001 (Bralower et al. 1997), 0.2 m from ODP Site 1051 (Katz et al. 1999), 0.25 m from ODP Site 1209 (Zachos et al. 2003), and ~1 m from ODP Site 690 (Kelly et al. 2005). The thin sedimentary records are caused by low sedimentation rates and carbonate dissolution due to ocean acidification (Zachos et al. 2005), which to some extent impede the further studies of the PETM-CIE.

In Tibet, our preliminary investigations on bulk carbonate  $\delta^{13}\text{C}$  show that the CIE is recorded in a ~9 m thick nodular limestones at Tingri. The thickness is ~9 times thicker than that from ODP 690 and ~6 times than that from the Global boundary Stratotype Section and Point (GSSP) in Dababiya (Aubry et al. 2007), indicating that there was a high sedimentation rate of the shallow-water limestones in the Tingri area during the PETM. Importantly, the similarity of the CIE structures at Tingri and ODP 690 not only confirms, for the first time, the validity of the CIE structures (such as small variations of b, c, d, e, f, g) from ODP 690 (Bains et al. 1999), but also provides an extended sedimentary section for the multidisciplinary studies of the PETM-CIE in the future. Discussions with this respect will be presented in Chapter 5.

## References

- Agard P, Omrani J, Jolivet L, Mouthereau F (2005) Convergence history across Zagros (Iran): constraints from collisional and earlier deformation. *International Journal of Earth Sciences* 94:401-419
- Aitchison JC, Ali JR, Davis AM (2007) When and where did India and Asia collide? *J Geophys Res* 112. doi:10.1029/2006JB004706
- Ali JR, Aitchison JC (2005) Greater India. *Earth Sci Rev* 72:169-188
- Aubry MP, Ouda K, Dupuis C, Berggren WA, Van Couvering JA, Ali J, Brinkhuis H, Gingerich PD, Heilmann-Clausen C, Hooker J, Kent DV, King C, Knox RWOB, Laga P, Molina E, Schmitz B, Steurbaut E, Ward DR (2007) The Global Standard Stratotype-section and Point (GSSP) for the base of the Eocene Series in the Dababiya section (Egypt). *Episodes* 30:271-286

- Aziz HA, Hilgen FJ, Van Luijk GM, Sluijs A, Kraus MJ, Pares JM, Gingerich PD (2008) Astronomical climate control on paleosol stacking patterns in the upper Paleocene–lower Eocene Willwood Formation, Bighorn Basin, Wyoming. *Geology* 36:531-534
- Bains S, Corfield RM, Norris RD (1999) Mechanisms of climate warming at the end of the Paleocene. *Science* 285:724-727
- Beavington-Penney SJ, Racey A (2004) Ecology of extant nummulitids and other larger benthic foraminifera: applications in palaeoenvironmental analysis. *Earth Sci Rev* 67:219-265
- Blondeau A (1972) Les nummulites. De l'enseignement a la recherche des sciences de la terre, Paris:Vuibert, 1-254.
- BouDagher-Fadel MK (2008) Evolution and geological significance of larger benthic foraminifera. *Developments in Palaeontology & Stratigraphy* 21. Elsevier, Amsterdam
- Bowen GJ, Clyde WC, Koch PL, Ting S, Alroy J, Tsubamoto T, Wang Y (2002) Mammalian dispersal at the Paleocene/Eocene boundary. *Nature* 295:2062-2065
- Bowen GJ, Zachos JC (2010) Rapid carbon sequestration at the termination of the Palaeocene-Eocene Thermal Maximum. *Nature Geosci* 3:866-869
- Bralower TJ, Thomas DJ, Zachos JC, Hirschmann MM, Röhl U, Sigurdsson H, Thomas E, Whitney DL (1997) High-resolution records of the late Paleocene thermal maximum and circum-Caribbean volcanism: Is there a causal link? *Geology* 25:963-966
- Chen J, Huang B, Sun L (2010) New constraints to the onset of the India-Asia collision: Paleomagnetic reconnaissance on the Linzizong Group in the Lhasa Block, China. *Tectonophysics* 489:189-209
- Chesley JT, Quade J, Ruiz J (2000) The Os and Sr isotopic record of Himalayan paleorivers: Himalayan tectonics and influence on ocean chemistry. *Earth Planet Sci Lett* 179:115-124
- Clementz M, Bajpai S, Ravikant V, Thewissen JGM, Saravanan N, Singh IB, Prasad V (2011) Early Eocene warming events and the timing of terrestrial faunal exchange between India and Asia. *Geology* 39:15-18
- Clift PD, Blusztajn J (2005) Reorganization of the western Himalayan river system after five million years ago. *Nature* 438:1001-1003

- Clyde WC, Khan IH, Gingerich PD (2003) Stratigraphic response and mammalian dispersal during initial India-Asia collision: Evidence from the Ghazij Formation, Balochistan, Pakistan. *Geology* 31:1097-1100
- Copley A, Avouac J-P, Royer J-Y (2010) India-Asia collision and the Cenozoic slowdown of the Indian plate: Implications for the forces driving plate motions. *J Geophys Res* 115. doi:10.1029/2009jb006634
- Corfield RI, Watts AB, Searle MP (2005) Subsidence history of the north Indian continental margin, Zaskar–Ladakh Himalaya, NW India. *J Geol Soc* 162:135-146
- DeConto RM, Galeotti S, Pagani M, Tracy D, Schaefer K, Zhang T, Pollard D, Beerling DJ (2012) Past extreme warming events linked to massive carbon release from thawing permafrost. *Nature* 484:87-91
- de Sigoyer J, Chavagnac Vr, Blichert-Toft J, Villa IM, Luais Ba, Guillot Sp, Cosca M, Mascle G (2000) Dating the Indian continental subduction and collisional thickening in the northwest Himalaya: Multichronology of the Tso Moriri eclogites. *Geology* 28:487-490
- Dupont-Nivet G, Lippert PC, Van Hinsbergen DJJ, Meijers MJM, Kapp P (2010) Palaeolatitude and age of the Indo–Asia collision: palaeomagnetic constraints. *Geophys J Int* 182:1189-1198
- Dickens GR, Castillo MM, Walker JCG (1997) A blast of gas in the latest Paleocene: Simulating first-order effects of massive dissociation of oceanic methane hydrate. *Geology* 25:259-262
- Ding L, Kapp P, Wan X (2005) Paleocene-Eocene record of ophiolite obduction and initial India-Asia collision, south central Tibet. *Tectonics* 24. doi:10.1029/2004TC001729
- Farley KA, Eltgroth SF (2003) An alternative age model for the Paleocene-Eocene thermal maximum using extraterrestrial  $^3\text{He}$ . *Earth Planet Sci Lett* 208:135-148
- Garzanti E, Baud A, Mascle G (1987) Sedimentary record of the northward flight of India and its collision with Eurasia (Ladakh Himalaya, India). *Geodin Acta* 1:297-312
- Garzanti E (2008) Comment on "When and where did India and Asia collide?" by Jonathan C. Aitchison, Jason R. Ali, and Aileen M. Davis. *J Geophys Res* 113. doi:10.1029/2007jb005276

- Gibbs SJ, Bown PR, Sessa JA, Bralower TJ, Wilson PA (2006) Nannoplankton Extinction and Origination across the Paleocene-Eocene Thermal Maximum. *Science* 314:1770-1773
- Hallock P, Glenn EC (1986) Larger foraminifera: A tool for paleoenvironmental analysis of Cenozoic carbonate depositional facies. *Palaios* 1:55-64
- Higgins JA, Schrag DP (2006) Beyond methane: Towards a theory for the Paleocene-Eocene Thermal Maximum. *Earth Planet Sci Lett* 245:523-537
- Hottinger L (1974) Alveolinids, Cretaceous-Tertiary larger foraminifera. Basel, Switzerland
- Hottinger L (1977) Foraminiferes operculiniformes. *Mémoires du Muséum National D'Histoire Naturelle* 40:1-159
- Hottinger L (1997) Shallow benthic foraminiferal assemblages as signals for depth of their deposition and their limitations. *Bull Soc Géol Fr* 168:491-505
- Hottinger L (2001) Learning from the past. In: R. L-M (ed) *Frontiers of life, vol 4. Discovery and spoliation of the biosphere, vol 2.* Academic Press, London & San Diego, pp 449-477
- Hottinger L (2009) The Paleocene and earliest Eocene foraminiferal family Miscellaneidae: neither nummulitids nor rotaliids. *Notebooks on Geology* 6:1-41
- Hu X, Sinclair HD, Wang J, Jiang H, Wu F (2012) Late Cretaceous-Palaeogene stratigraphic and basin evolution in the Zhepure Mountain of southern Tibet: implications for the timing of India-Asia initial collision. *Basin Res* 24:520-543
- Jaeger JJ, Courtillot V, Tapponnier P (1989) Paleontological view of the ages of the Deccan Traps, the Cretaceous/Tertiary boundary, and the India-Asia collision. *Geology* 17:316-319
- Jaramillo C, Ochoa D, Contreras L, Pagani M, Carvajal-Ortiz H, Pratt LM, Krishnan S, Cardona A, Romero M, Quiroz L, Rodriguez G, Rueda MJ, de la Parra F, Moron S, Green W, Bayona G, Montes C, Quintero O, Ramirez R, Mora G, Schouten S, Bermudez H, Navarrete R, Parra F, Alvaran M, Osorno J, Crowley JL, Valencia V, Vervoort J (2010) Effects of rapid global warming at the Paleocene-Eocene boundary on neotropical vegetation. *Science* 330:957-961
- Katz ME, Pak DK, Dickens GR, Miller KG (1999) The source and fate of massive carbon input during the Latest Paleocene Thermal Maximum. *Science* 286:1531-1533



- Kelly DC, Bralower TJ, Zachos JC, Premoli-Silva I, Thomas E (1996) Rapid diversification of planktonic foraminifera in the tropical Pacific (ODP Site 865) during the late Paleocene thermal maximum. *Geology* 24:423-426
- Kelly DC, Zachos JC, Bralower TJ, Schellenberg SA (2005) Enhanced terrestrial weathering/runoff and surface ocean carbonate production during the recovery stages of the Paleocene-Eocene thermal maximum. *Paleoceanography* 20. doi:10.1029/2005PA001163
- Kennett JP, Stott LD (1991) Abrupt deep-sea warming, palaeoceanographic changes and benthic extinctions at the end of the Palaeocene. *Nature* 353:225-229
- Klootwijk CT, Gee JS, Peirce JW, Smith GM, McFadden PL (1992) An early India-Asia contact: Paleomagnetic constraints from Ninetyeast Ridge, ODP Leg 121. *Geology* 20:395-398
- Koch PL, Zachos JC, Gingerich PD (1992) Correlation between isotope records in marine and continental carbon reservoirs near the Palaeocene/Eocene boundary. *Nature* 358:319-322
- Le Houedec S, Meynadier L, Cogné J-P, Allègre CJ, Gourlan AT (2012) Oceanwide imprint of large tectonic and oceanic events on seawater Nd isotope composition in the Indian Ocean from 90 to 40 Ma. *Geochem Geophys Geosyst* 13. doi:10.1029/2011gc003963
- Leech ML, Singh S, Jain AK, Klempere SL, Manickavasagam RM (2005) The onset of India–Asia continental collision: Early, steep subduction required by the timing of UHP metamorphism in the western Himalaya. *Earth Planet Sci Lett* 234:83-97
- Liebke U, Appel E, Ding L, Neumann U, Antolin B, Xu Q (2010) Position of the Lhasa terrane prior to India–Asia collision derived from palaeomagnetic inclinations of 53 Ma old dykes of the Linzhou Basin: constraints on the age of collision and post-collisional shortening within the Tibetan Plateau. *Geophys J Int* 182:1199-1215
- McInerney FA, Wing SL (2011) The Paleocene-Eocene Thermal Maximum: A perturbation of carbon cycle, climate, and biosphere with implications for the future. *Annu Rev Earth Planet Sci* 39:489-516
- Molnar P, England P, Martinod J (1993) Mantle dynamics, uplift of the Tibetan Plateau, and the Indian monsoon. *Rev Geophys* 31:357-396

- Murphy BH, Farley KA, Zachos JC (2010) An extraterrestrial  $^3\text{He}$ -based timescale for the Paleocene-Eocene thermal maximum (PETM) from Walvis Ridge, IODP Site 1266. *Geochim Cosmochim Acta* 74:5098-5108
- Najman Y, Appel E, Boudagher-Fadel M, Bown P, Carter A, Garzanti E, Godin L, Han J, Liebke U, Oliver G, Parrish R, Vezzoli G (2010) Timing of India-Asia collision: Geological, biostratigraphic, and palaeomagnetic constraints. *J Geophys Res* 115. doi:10.1029/2010jb007673
- Nunes F, Norris RD (2006) Abrupt reversal in ocean overturning during the Palaeocene/Eocene warm period. *Nature* 439:60-63
- O'Brien PJ (2006) The age of deep, steep continental subduction in the NW Himalaya: Relating zircon growth to metamorphic history. Comment on: 'The onset of India-Asia continental collision: Early, steep subduction required by the timing of UHP metamorphism in the western Himalaya' by Mary L. Leech, S. Singh, A.K. Jain, Simon L. Klemperer and R.M. Manickavasagam, *Earth and Planetary Science Letters* 234 (2005) 83-97. *Earth Planet Sci Lett* 245:814-816
- Patriat P, Achache J (1984) India-Eurasia collision chronology has implications for crustal shortening and driving mechanism of plates. *Nature* 311:615-621
- Patzelt A, Li H, Wang J, Appel E (1996) Palaeomagnetism of Cretaceous to Tertiary sediments from southern Tibet: evidence for the extent of the northern margin of India prior to the collision with Eurasia. *Tectonophysics* 259:259-284
- Racey A (1995) Lithostratigraphy and larger foraminiferal (nummulitid) biostratigraphy of the Tertiary of northern Oman. *Micropaleontology* 41:1-123
- Richter FM, Rowley DB, DePaolo DJ (1992) Sr isotope evolution of seawater: the role of tectonics. *Earth Planet Sci Lett* 109:11-23
- Röhl U, Westerhold T, Bralower TJ, Zachos JC (2007) On the duration of the Paleocene-Eocene thermal maximum (PETM). *Geochem Geophys Geosyst* 8. doi:10.1029/2007gc001784
- Rowley DB (1998) Minimum age of initiation of collision between India and Asia north of Everest based on the subsidence history of the Zhepure Mountain Section. *J Geol* 106:229-235
- Schmitz B, Pujalte V (2007) Abrupt increase in seasonal extreme precipitation at the Paleocene-Eocene boundary. *Geology* 35:215-218

- Searle M, Corfield RI, Stephenson BEN, McCarron JOE (1997) Structure of the North Indian continental margin in the Ladakh–Zaskar Himalayas: Implications for the timing of obduction of the Spontang ophiolite, India–Asia collision and deformation events in the Himalaya. *Geol Mag* 134:297-316
- Serra-Kiel J, Hottinger L, Caus E, Drobne K, Ferrandez C, Jauhri AK, Less G, Pavlovec R, Pignatti J, Samso JM (1998) Larger foraminiferal biostratigraphy of the Tethyan Paleocene and Eocene. *Bull Soc Géol Fr* 169:281-299
- Sun Z, Jiang W, Li H, Pei J, Zhu Z (2010) New paleomagnetic results of Paleocene volcanic rocks from the Lhasa block: Tectonic implications for the collision of India and Asia. *Tectonophysics* 490:257-266
- Svensen H, Planke S, Malthe-Sorensen A, Jamtveit B, Myklebust R, Rasmussen Eidem T, Rey SS (2004) Release of methane from a volcanic basin as a mechanism for initial Eocene global warming. *Nature* 429:542-545
- Tan X, Gilder S, Kodama KP, Jiang W, Han Y, Zhang H, Xu H, Zhou D (2010) New paleomagnetic results from the Lhasa block: Revised estimation of latitudinal shortening across Tibet and implications for dating the India-Asia collision. *Earth Planet Sci Lett* 293:396-404
- Thomas E, Shackleton NJ (1996) The Paleocene-Eocene benthic foraminiferal extinction and stable isotope anomalies. In: Knox RWOB, Corfield RM, Dunay RE (eds) *Correlation of the Early Paleogene in Northwest Europe*. Geol Soc London Spec Pub, pp 401-441
- van Hinsbergen DJJ, Kapp P, Dupont-Nivet G, Lippert PC, DeCelles PG, Torsvik TH (2011a) Restoration of Cenozoic deformation in Asia and the size of Greater India. *Tectonics* 30. doi:10.1029/2011tc002908
- van Hinsbergen DJJ, Steinberger B, Doubrovine PV, Gassmüller R (2011b) Acceleration and deceleration of India-Asia convergence since the Cretaceous: Roles of mantle plumes and continental collision. *J Geophys Res* 116. doi:10.1029/2010jb008051
- Wang C, Li X, Hu X, Jansa LF (2002) Latest marine horizon north of Qomolangma (Mt Everest): Implications for closure of Tethys seaway and collision tectonics. *Terra Nova* 14:114-120
- Wang J, Hu X, Jansa L, Huang Z (2011) Provenance of the upper Cretaceous-Eocene deep-water sandstones in Sangdanlin, southern Tibet: Constraints on the timing of initial India-Asia Collision. *J Geol* 119:293-309

- Westerhold T, Röhl U, McCarren HK, Zachos JC (2009) Latest on the absolute age of the Paleocene-Eocene Thermal Maximum (PETM): New insights from exact stratigraphic position of key ash layers +19 and -17. *Earth Planet Sci Lett* 287:412-419
- Wu F, Huang B, Ye K, Fang A (2008) Collapsed Himalayan-Tibetan orogen and the rising Tibetan Plateau. *Acta Petrol Sin* 24:1-30
- Yi Z, Huang B, Chen J, Chen L, Wang H (2011) Paleomagnetism of early Paleogene marine sediments in southern Tibet, China: Implications to onset of the India-Asia collision and size of Greater India. *Earth Planet Sci Lett* 309:153-165
- Zachos JC, Wara MW, Bohaty S, Delaney ML, Petrizzo MR, Brill A, Bralower TJ, Premoli-Silva I (2003) A transient rise in tropical sea surface temperature during the Paleocene-Eocene Thermal Maximum. *Science* 302:1551-1554
- Zachos JC, Röhl U, Schellenberg SA, Sluijs A, Hodell DA, Kelly DC, Thomas E, Nicolo M, Raffi I, Lourens LJ, McCarren H, Kroon D (2005) Rapid acidification of the ocean during the Paleocene-Eocene Thermal Maximum. *Science* 308:1611-1615
- Zhang Q, Willems H, Ding L, Graefe K-U, Appel E (2012) Initial India-Asia continental collision and foreland basin evolution in the Tethyan Himalaya of Tibet: Evidence from stratigraphy and paleontology. *J Geol* 120:175-189
- Zhang Q, Willems H, Ding L (2012) Evolution of the Paleocene-early Eocene larger benthic foraminifera in the Tethyan Himalaya of Tibet, China. *Submitted to Int J Earth Sci*
- Zhu B, Kidd WSF, Rowley DB, Currie BS, Shafique N (2005) Age of initiation of the India-Asia collision in the east-central Himalaya. *J Geol* 113:265-285

First manuscript

## **2. Evolution of the Paleocene-early Eocene larger benthic foraminifera in the Tethyan Himalaya of Tibet, China**

**Qinghai Zhang<sup>1,2</sup>, Helmut Willems<sup>1,3</sup>, Lin Ding<sup>2</sup>**

<sup>1</sup> University of Bremen, Department of Geosciences, D-28359 Bremen, Germany

<sup>2</sup> Key Laboratory of Continental Collision and Plateau Uplift, Institute of Tibetan Plateau Research, Chinese Academy of Sciences, 100085 Beijing, China

<sup>3</sup> Nanjing Institute of Geology and Palaeontology, Chinese Academy of Sciences, 210008 Nanjing, China

Accepted, *International Journal of Earth Sciences*

## Abstract

The Paleocene-early Eocene Larger Benthic Foraminifera (LBF) in the far eastern Neo-Tethyan Ocean of Tibet still remain unknown. Detailed studies on the LBF will not only contribute to the construction of high resolution biostratigraphy for shallow-water limestones in Tibet, but also improve our understanding of the larger foraminiferal evolution in the eastern Neo-Tethyan Ocean. Based on one continuous section at Tingri and three separate sections at Gamba, ten Shallow Benthic Zones (SBZs) ranging from SBZ 1 to 10 have been designated. In Tibet, the Paleocene LBFs are characterized by high diversification of *Lockhartia*, *Kathina*, *Daviesina*, *Miscellanea*, *Ranikothalia*, and *Operculina*. By comparison with those in Europe, the Paleocene LBFs in Tibet evolved much earlier with progressively generic and species diversity during SBZ 2-5. Adult dimorphism and large shell size of some LBFs as well as diversity differentiation between genera and species in the LBFs initiated as early as SBZ 3 in Tibet, suggesting that the occurrence of the Larger Foraminifera Turnover (LFT) was probably not synchronous in the entire Neo-Tethyan Ocean, because the LFT in Europe was generally thought to occur at the beginning of SBZ 5. During the early Eocene, the LBFs were evidently decreased on the generic level and increased on the species level, and some successful genera (*Alveolina*, *Orbitolites*, *Nummulites*, *Assilina*, *Discocyclina*) had gained predominance in the entire Neo-Tethyan Ocean, which is nearly identical to the evolution of the early Eocene LBFs in Europe and indicates a high-degree homogenization of the LBF in the entire Neo-Tethyan Ocean. The Paleocene-Eocene boundary in the shallow-water environments is clearly determined at Tingri, and it is situated in the upper part of SBZ 5 and associated with no evident biotic turnover of shallow benthic foraminiferal communities. Possible diachroneity of the LFT in the Neo-Tethyan Ocean and evident lagging of the Paleocene-Eocene Thermal Maximum (PETM) behind the LFT imply that the LFT could only be the result of a natural evolutionary process and has no linkage with the PETM. Notably, a transient but distinct Larger Foraminiferal Extinction and Origination (LFEO) event has been found in Tibet, characterized by the sudden disappearance of all Paleocene lamellar-perforate LBFs, such as *Lockhartia*, *Kathina*, *Daviesina*, *Miscellanea*, *Ranikothalia*, and *Operculina*, and the initial dominance of early Eocene porcellaneous forms of *Alveolina* and *Orbitolites*. The LFEO marks the boundary between SBZ 5 and 6, and might only occur in the low latitudinal areas of the Neo-Tethyan Ocean. Additionally, the LFEO coincides with the onset of the Carbon Isotope Excursion (CIE) recovery, and postdates the Paleocene-Eocene boundary ~80 kyr according to age models of the CIE. The synchronicity of the LFEO and the initial recovery of the CIE implies that some mechanisms causing the rapid recovery of the CIE probably had also led to the LFEO in the shallow-water environments of the low latitudinal areas.

## 2.1 Introduction

Based mainly on the detailed studies of Paleocene-Eocene *Alveolinids* and *Nummulitids* by Hottinger (1960) and Schaub (1981), 20 Shallow Benthic Zones (SBZs) have been divided for the time interval of Paleocene and Eocene by Serra-Kiel et al. (1998). These SBZs have been used successfully to construct high resolution biostratigraphy in the shallow-water environments where were dominated by the Larger Benthic Foraminifera (LBF) (Scheibner et al. 2005; Drobne et al. 2011). However, the work from Hottinger (1960) and Schaub (1981) was mainly conducted in the western Neo-Tethyan Ocean of Europe. Direct application of the SBZs in the eastern Neo-Tethyan Ocean and regionally stratigraphic correlations of the shallow-water environments between Europe and Asia still remain to some extent ambiguous.

The eastern Neo-Tethyan Ocean was once named 'Ranikot Sea' (Davies 1938) or 'Lockhartia Sea' (Hottinger 1998) mainly owing to high diversity of the Paleocene *Lockhartia* from the Ranikot and Lockhart formations in the Indus basin. Geographically the Lockhartia Sea covers a huge area at least from Tibet in the east to the Persian Gulf in the west (Davies 1938). After a rough investigation on *Alveolina* from Pakistan, Hottinger (1971) came to a conclusion that 'the larger foraminifera contained in these Far Eastern shallow water formations are similar to but not identical with Mediterranean assemblages'. In the recent 20 years, great progresses on larger foraminiferal biostratigraphy have been achieved in India and Pakistan by Butt (1991), Weiss (1993), Jauhri (1996, 1998), Ferrández-Cañadell (2002), and Sameeni and Butt (2004), and a rough SBZ following those in Europe has been tentatively built in the Indus Basin by Afzal et al. (2010).

Compared with India and Pakistan, Tibet was paleogeographically located in the easternmost Neo-Tethyan Ocean during the Paleocene and Eocene, which provides a unique chance to study the Paleocene-Eocene larger foraminiferal evolution. Although systematic descriptions on the Paleocene-Eocene LBF in Tibet has been reported about 20 years ago (He et al. 1976; Zhang 1988; Wan 1990, 1991), a detailed biostratigraphic work following the concept of the SBZs is still missing. Therefore, further investigations on the Paleocene-Eocene LBF in Tibet can not only improve our understanding of the larger foraminiferal evolution in the east, but also consummate the SBZs within the entire Neo-Tethyan Ocean.

This paper presents a first-hand detailed study of the Paleocene-early Eocene LBFs in Tibet, and shows high generic and species diversity of the LBFs during SBZ 2-10 in the eastern Neo-Tethyan Ocean. Our results indicate that the Paleocene LBFs might evolve more early in the east than those in the west, and the occurrence of the Larger

Foraminifera Turnover (LFT) was probably not synchronous in the entire Neo-Tethyan Ocean. Besides, a Larger Foraminiferal Extinction and Origination (LFEO) event is firstly found by us, which occurred at the boundary of SBZ 5 and 6 and coincided with the initial recovery of the Carbon Isotope Excursion (CIE). More importantly, based on a high resolution carbon isotopic variations at the P-E boundary, the P-E boundary in the shallow-water environment has been placed in the upper part of SBZ 5 by us, which conflicts with the opinion that the P-E boundary was located at the boundary between SBZ 4 and 5 (Orue-Etxebarria et al. 2001; Scheibner et al. 2005; Pujalte et al. 2009a, 2009b; Scheibner and Speijer 2009), but is in agreement with the time interval for the P-E boundary recommended by Serra-Kiel et al. (1998) and Hottinger (2001).

## 2.2 Geologic setting and lithostratigraphy

The Tethyan Himalaya of Tibet is bounded to the Lhasa Terrane by the Indus-Yarlung Zangbo Suture (IYS) to the north, and neighbours on the High Himalaya crystalline sequences by the South Tibet Detachment System (STDS) to the south (Yin and Harrison 2000) (Fig. 1). After the Lhasa Terrane rifted from Gondwana supercontinent in the Triassic (Liu and Einsele 1994), the Tethyan Himalaya persisted at the northernmost Indian continent, representing a passive continental margin environment until the end of the Paleocene (Zhang et al. 2012). Paleozoic to Cretaceous marine sedimentary strata are widely exposed within the Tethyan Himalaya, whereas the Paleocene-lower Eocene shallow-water limestones mainly crop out near the counties of Gamba and Tingri.

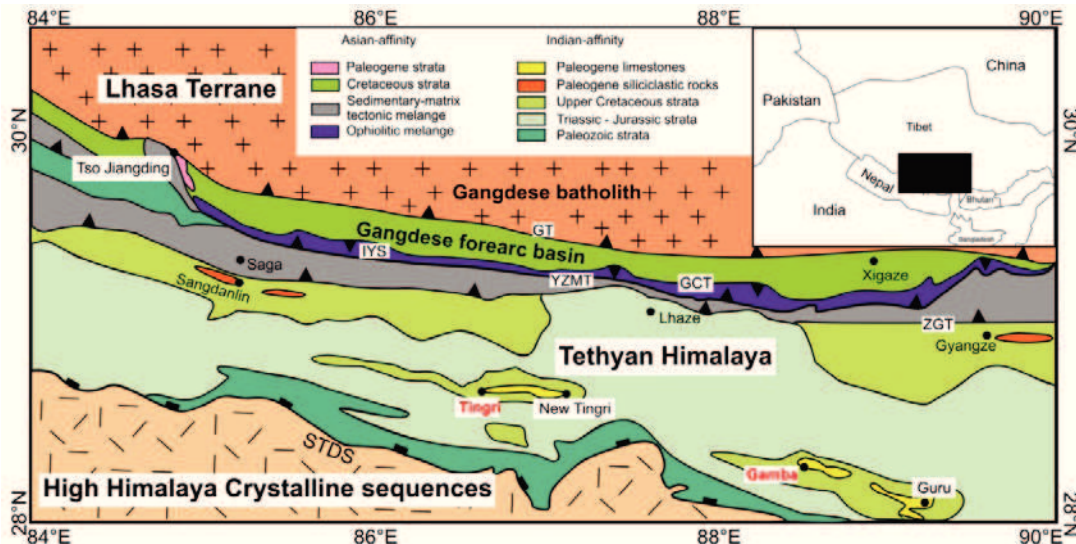


Fig. 1 Schematic geological map of the Tethyan Himalaya showing the study areas of Tingri and Gamba in Tibet, modified from Zhang et al. (2012). Abbreviations: STDS, South Tibet Detachment System; ZGT, Zhongba-Gyangze Thrust; YZMT, Yarlung Zangbo Mantle Thrust; IYS, Indus-Yarlung Zangbo Suture; GCT, Great Counter Thrust; GT, Gangdese Thrust.



At Gamba and Tingri, the Paleocene limestones rich in LBFs were interpreted to represent a carbonate platform on the Indian passive continental margin (Willems 1993; Willems et al. 1996). At the P-E boundary, the India-Asia continental collision led to the flexure of the Indian continental margin and initial development of a foreland basin on the Tethyan Himalaya. Subsequently, owing to the maintenance of tectonic-induced uplift at Gamba and Tingri, the LBFs still highly thrived in these areas until the end of the Ilerdian. At the beginning of the Cuisian, southward migration of the foreland basin and arrival of a foredeep depozone to Gamba and Tingri caused a deepening of the depositional environment, which drowned the early Eocene carbonate ramp and terminated the Paleocene-early Eocene larger foraminiferal evolution in the areas (Zhang et al. 2012).

Lithologically, the entire Paleocene-lower Eocene foraminifera-bearing carbonate sequences are named 'Zhepure Shan Formation' at Tingri and 'Zongpu Formation' at Gamba. Both of them overlie the quartz sandstones of the Jidula Formation and underlie the green marls/shales and lithic-rich sandstones of the Youxia Formation (Willems 1993; Zhu et al. 2005). The Paleocene-lower Eocene carbonate sequence can be subdivided into four members, from bottom to top: the cyclic limestones of Member A, the massive limestones of Member B, the nodular limestones of Member C, and the massive limestones of Member D (Fig. 2). The cyclic limestones comprise 7 cycles, and although the lower part of each cycle is usually covered by weathered carbonate debris, the upward lithological change from marls, nodular limestones to thin-bedded limestones in every cycle can be easily recognised in the field. The massive limestones are ~30-70 m thick and show no evident lithological changes. In the nodular limestones, the nodules and the surrounding matrix contain identical fossil assemblages, and based on paleontological, sedimentological and diagenetic evidence, the nodular limestones were interpreted to have been formed by differential diagenesis but not by allochthonous redeposition (Willems 1993).

## 2.3 Materials and methods

In Tibet, two key locations for studies of the Paleocene-early Eocene LBFs are situated in the surroundings of the Tingri and Gamba County. All the samples presented in the paper were collected from the two areas. At Tingri, one continuous Paleocene-lower Eocene carbonate sequence was measured in 2009 (Section 09ZS), and about 450 samples were taken from the ~400 m thick Zhepure Shan Formation in 2009, 2010 and 2011. Sampling density is ~1-1.5 m/sample at the basal 60 m where the LBFs are relatively barren and ~0.5-1 m/sample for the rest of the section. At Gamba, three separate sections ZP, ZM and F were measured in 1983 and 1992, and they together constitute a ~350 m thick carbonate sequence of the Zongpu Formation which is

lithologically comparable to the Zhepure Shan Formation at Tingri. Totally ~170 samples have been taken at Gamba.

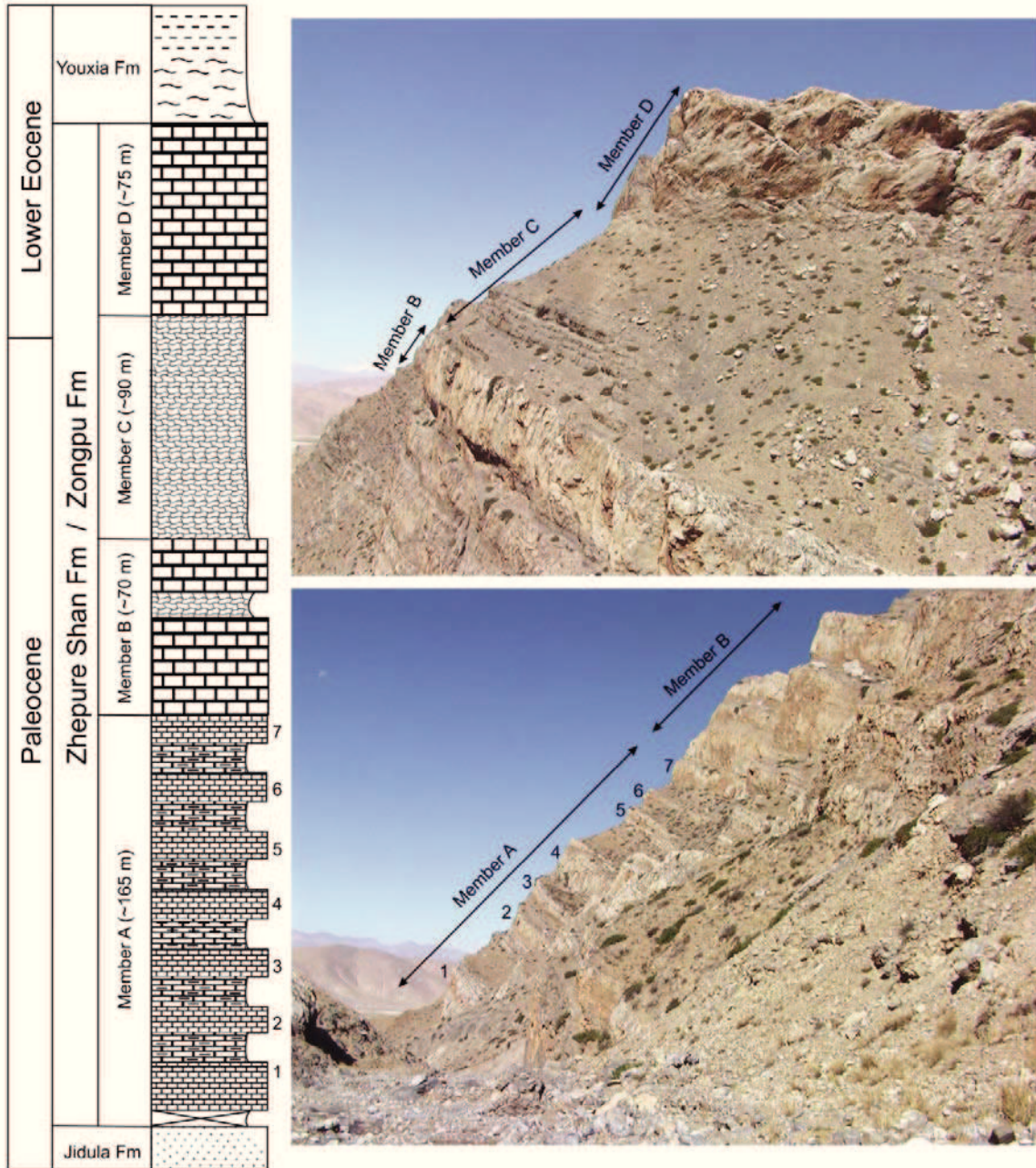


Fig. 2 Generalized lower Paleogene lithological column in Tibet. See fig. 3 for explanations of the lithological symbols.

About 1000 thin sections have been polished from these samples and ~10,000 photomicrographs have been taken to study the Paleocene-early Eocene LBFs. For

some of the late Ilerdian *Nummulites* and *Assilina*, orientated thin sections have been polished from isolated specimens.

Determinations of the Paleocene-early Eocene LBF are mainly based on taxonomic descriptions given by Nuttall (1925), Davies (1927, 1930, 1932, 1940, 1952), Gill (1953), Smout (1954), Hottinger (1960, 1974, 2009), Sen Gupta (1963), He et al. (1976), Dorbne (1977), Caus et al. (1980), Schaub (1981), Leppig (1988), Zhang (1988), Wan (1990, 1991), Butt (1991), Racey (1995), Jauhri (1996, 1998), Hottinger et al. (1998), Ferràndez-Cañadell (2002), Sameeni and Butt (2004), and Cherchi and Schroeder (2005). Especially, Hottinger's unpublished monograph on 'Paleogene rotaliids' greatly contributed to the determination of some Paleocene LBFs. The shallow benthic zones in Tibet are defined by the appearance and disappearance of larger foraminiferal species in the time gradient (Hottinger 2001), essentially following the principle of Opper Zone (Pignatti 1998; Serra-Kiel et al. 1998).

Besides, in order to spike the position of the P-E boundary at Tingri, 372 fresh carbonate rocks with no reworked components or petrographically visible diagenetic alterations or veins from the Zhepure Shan Formation were prepared for measurements of carbon isotopes. The  $\delta^{13}\text{C}$  measurements were conducted on a Finnigan MAT 251 Spectrometer at MARUM (University of Bremen), and the results were calibrated to the PDB with standard deviation of  $<0.05\text{‰}$  for  $\delta^{13}\text{C}$ .

## 2.4 Biostratigraphy

Although no planktonic foraminifera or calcareous nanoplankton has been found from the Zhepure Shan Formation, the recognition of P 6-7 planktonic foraminifera and NP 12 nanoplankton immediately overlying the Zhepure Shan limestones reveals an equivalent age of SBZ 10 for the termination of the LBFs at Tingri (Zhang et al. 2012). At Gamba, P 3 planktonic foraminifera of the *angulata* zone has been reported at the base of the Zongpu Formation (Willems 1993), which is roughly equal to time interval of the top of SBZ 1 and the base of SBZ 2.

Following the Opper Zone's principle and calibrated by the data from planktonic foraminifera, the Zhepure Shan Formation at Tingri can be divided into 10 SBZs ranging from SBZ 1 to 10 (Fig. 3). At Gamba, the Zongpu Formation roughly lasts from SBZ 2 to 7, and the deposition of a conglomerate layer between SBZ 5 and 7 indicates a sedimentary hiatus, accounting for the missing SBZ 6 (Fig. 4). There is no LBF but algae and small benthic foraminifera in SBZ 1 (Fig. 5). The main LBFs dominating time interval of SBZ 2-10 are presented in Figs. 6-9 with their biostratigraphic ranges in Figs. 3-4. The larger foraminiferal zonations are presented in Figs. 10-11 and described as follows.

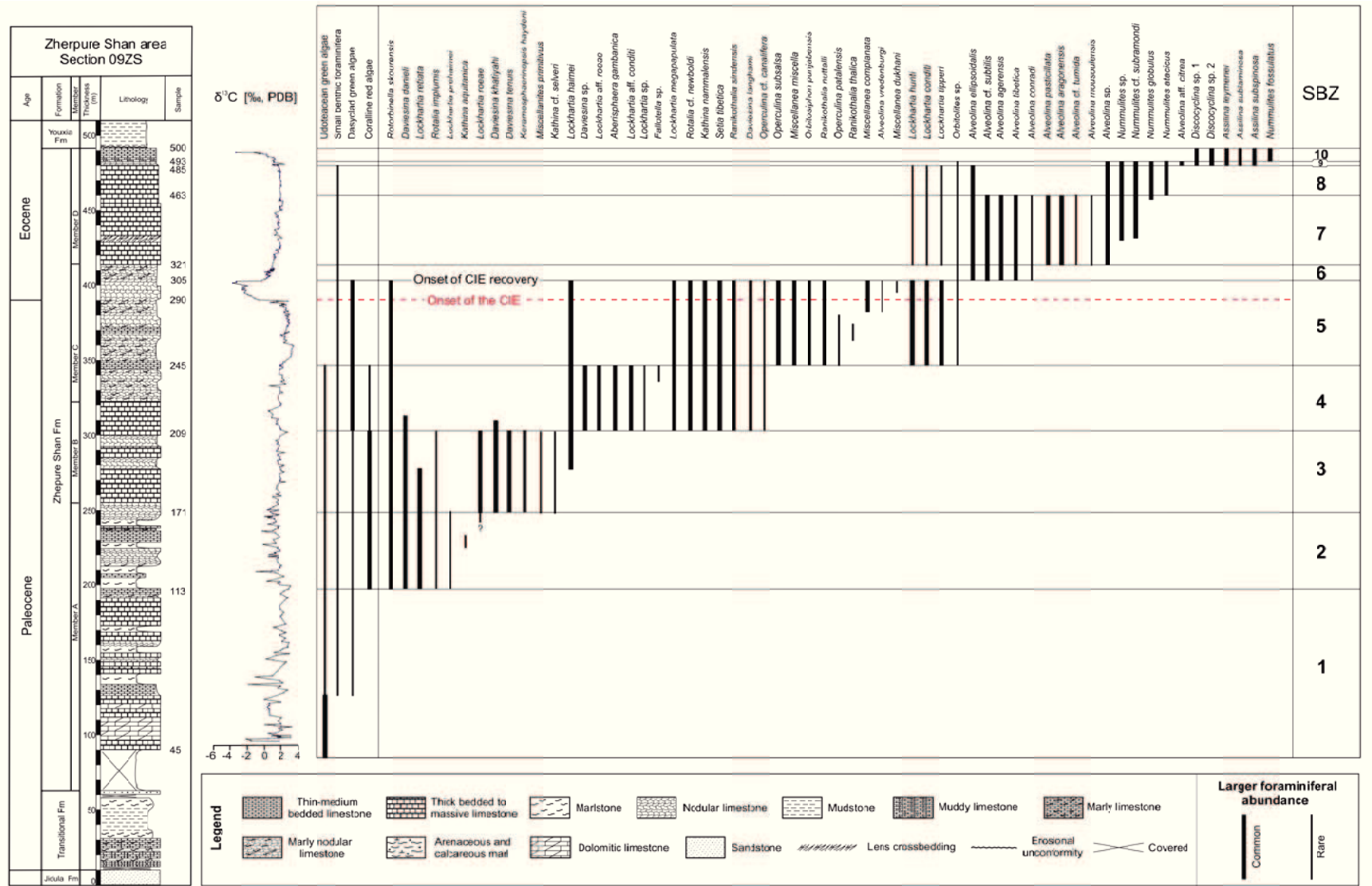
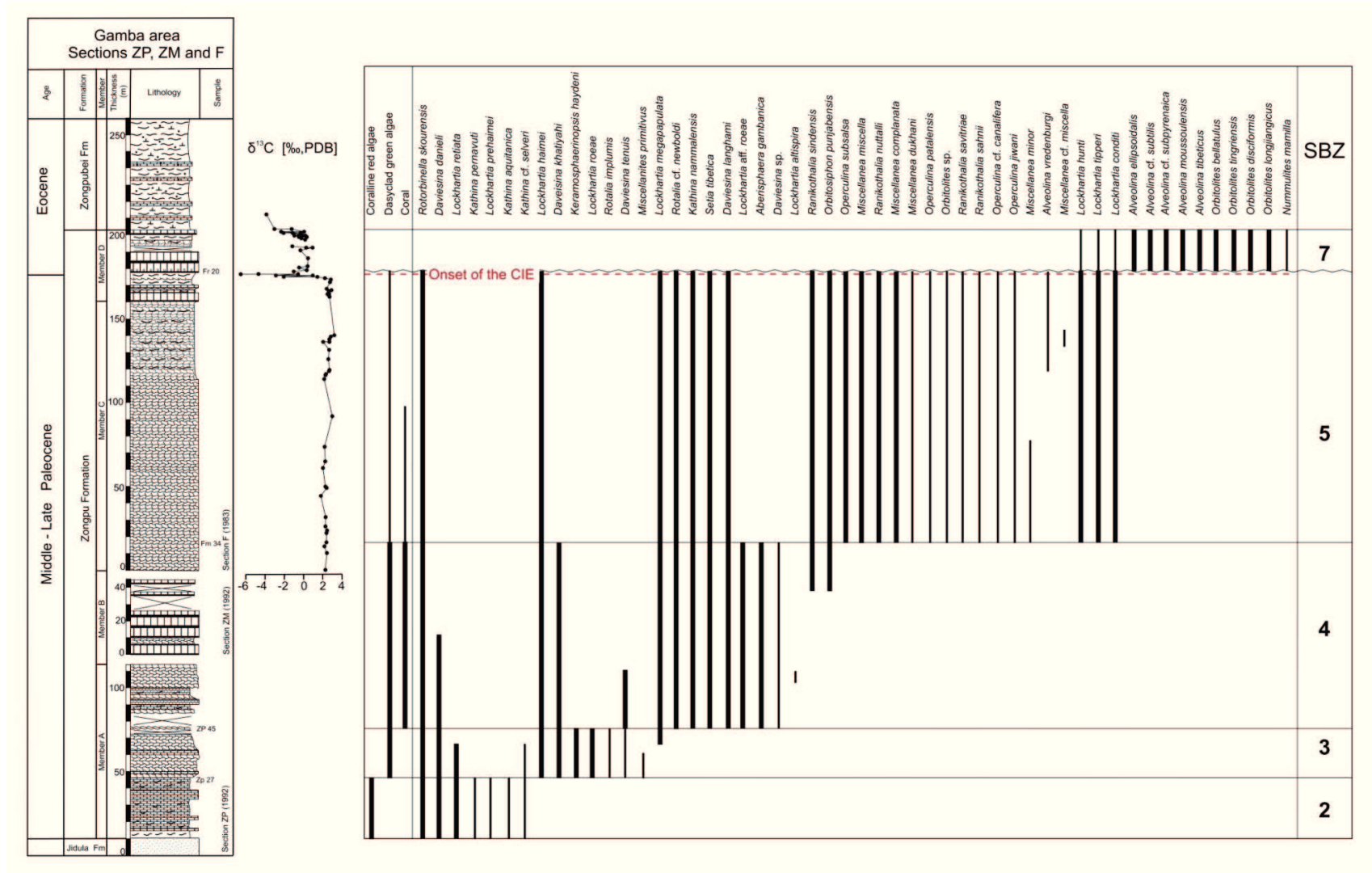


Fig. 3 Larger foraminiferal biostratigraphy and carbon isotopic variations of the Zhepure Shan Formation at Tingri.



The larger foraminiferal evolution

Fig. 4 Larger foraminiferal biostratigraphy of the Zongpu Formation at Gamba. Carbon isotopic curve is from Zhang et al. (2012). See fig. 3 for explanations of the lithological symbols.

## SBZ 1

SBZ 1 is tentatively subdivided into two parts. The lower part (SBZ 1A) is dominated mainly by udoteacean algae *Halimeda*. Small benthic foraminifera (rotalina, miliolina, textularina) and dasycladacean algae start to appear in the upper part (SBZ 1B). No LBFs have been found in SBZ 1 (Fig. 5).

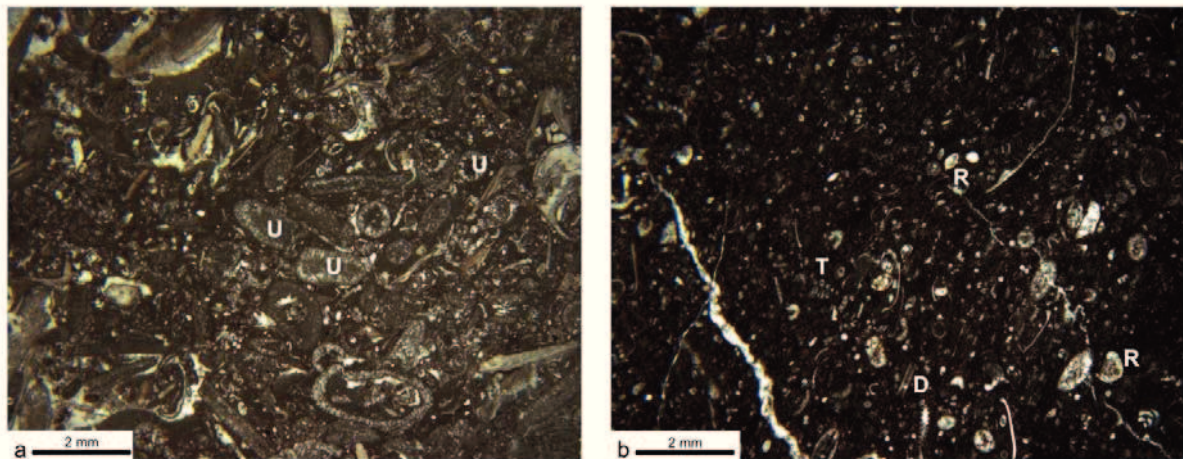


Fig. 5 Thin section photomicrographs of representative microfacies in SBZ 1. (a) Udoteacean algae-dominated packstone in SBZ 1A, sample 52, Tingri; (b) Small benthic foraminifera-dasycladacean algae wackestone in SBZ 1B, sample 91, Tingri. U: Udoteacean algae; R: *Rotaliids*; T: *Textulariids*; D: Dasycladacean algae.

## SBZ 2

The base of SBZ 2 is defined by the first appearance of *Rotorbinella skourensis*, *Rotalia implumis*<sup>1</sup>, *Lockhartia retiata*, *L. prehaimeii*, *Kathina aquitanica*<sup>2</sup>, *K. pernavuti*, *K. cf. selveri*, and *Daviesina danieli*. Among them, the dominant LBFs are *Rotorbinella skourensis*, *Lockhartia retiata* and *Daviesina danieli*.

## SBZ 3

The base of SBZ 3 is defined by the first appearance of *Lockhartia haimeii*, *L. roeae*, *Miscellanites primitivus*, *Keramosphaerinopsis haydeni*, *Daviesina khatiyahi*, and *D. tenuis*. Among them, *Lockhartia haimeii*, *L. roeae*, *Daviesina khatiyahi*, *D. tenuis* and *Keramosphaerinopsis haydeni* dominate SBZ 3. *Keramosphaerinopsis haydeni* can be taken as an index fossil for SBZ 3 owing to its high abundance and limited biostratigraphic range.

<sup>1</sup> From Hottinger's unpublished monograph on 'Paleogene rotaliids'

<sup>2</sup> From Hottinger's unpublished monograph on 'Paleogene rotaliids'



Fig. 6 The Paleocene LBFs in Tibet. (1) *Rotorbinella skourensis* Pfender, 1938. Sample Zm 1, Gamba; (2) *Rotalia implumis* Hottinger. Sample 187, Tingri; (3) *Rotalia* cf. *newboldi* d'Archiac & Haime, 1853. Sample 218, Tingri; (4) *Lockhartia retiata* Sander, 1992. Sample Zp 18, Gamba; (5) *Lockhartia prehaime* Smout, 1954. Sample Zp 10, Gamba; (6) *Lockhartia roeae* Davies, 1930. Sample Zm 10, Gamba; (7) *Lockhartia* aff. *roeae* Davies, 1930. Sample 214, Tingri; (8) *Lockhartia haime* Davies, 1927. Sample Zp 42, Gamba; (9) *Lockhartia altispira* Smout, 1954. Sample Zp 57, Gamba; (10) *Lockhartia* aff. *conditi* Nuttall, 1926. Sample 228, Tingri; (11) *Lockhartia conditi* Nuttall, 1926. Sample 300, Tingri; (12) *Lockhartia hunti* Ovey, 1947. Sample 452, Tingri; (13) *Lockhartia tipperi* Davies, 1926. Sample Fm 40, Gamba; (14) *Lockhartia megapapulata* Hu, 1976. Sample 259, Tingri; (15) *Lockhartia* sp., sample 205, Tingri; (16) *Kathina aquitanica* Hottinger. Sample 140, Tingri; (17) *Kathina pernavuti* Sirel, 1972. Sample Zp 12, Gamba; (18) *Kathina* cf. *selveri* Smout, 1954. Sample 132, Tingri; (19) *Kathina nammalensis* Smout & Haque, 1956. Sample Fr 7, Gamba; (20) *Fallotella* sp., sample 244, Tingri; (21) *Orbitosiphon punjabensis* Davies, 1937. Sample 287, Tingri; (22) *Setia tibetica* Douvillé, 1916. Sample 230, Tingri; (23) *Miscellanites primitivus* Rahaghi, 1983. Sample Zp 30, Gamba; (24) *Daviesina danieli* Smout, 1954. Sample Zp 54, Gamba; (25) *Daviesina khatiyahi* Smout, 1954. Sample Zp 27, Gamba; (26) *Daviesina tenuis* Tambareau, 1967. Sample 200, Tingri; (27) *Daviesina* sp., sample 228; (28) *Daviesina langhami* Smout, 1954. Sample 261, Tingri; (29-30) *Keramosphaerinopsis haydeni* H. Douvillé, 1916. Sample 173 & Zp 38, Tingri & Gamba; (31) *Aberisphaera gambanica* Wan, 1991. Sample Zp 60, Gamba.

#### SBZ 4

The base of SBZ 4 is defined by the first appearance of *Rotalia* cf. *newboldi*, *Lockhartia altispira*, *L. aff. roeae*, *L. aff. conditi*, *Kathina nammalensis*, *Aberisphaera gambanica*, *Setia tibetica*, *Daviesina langhami*, *Ranikothalia sindensis*, and *Operculina* cf. *canalifera*, and the last occurrence of *Rotalia implumis*, *Lockhartia retiata*, *L. roeae*, *Kathina* cf. *selveri*, *Miscellanites primitivus*, and *Keramosphaerinopsis haydeni*. Among them, *Lockhartia haime*, *L. megapapulata*, *L. aff. roeae*, *L. aff. conditi*, *Aberisphaera gambanica*, *Rotalia* cf. *newboldi*, *Kathina nammalensis*, *Setia tibetica*, *Ranikothalia sindensis*, and *Daviesina langhami* appear in high abundance. *Aberisphaera gambanica* can be taken as an index fossil for SBZ 4.

#### SBZ 5

The base of SBZ 5 is defined by the first appearance of *Lockhartia conditi*, *L. tipperi*, *L. hunti*, *Miscellanea miscella*, *M. minor*, *Ranikothalia nuttalli*, *R. savitriae*, *R. thalicus*, *R. sahnii*, *Operculina patalensis*, *O. subsalsa*, *O. jiwani*, and *Orbitolites* sp., and in the upper part of SBZ 5, *M. dukhani*, *M. complanata*, *M. cf. miscella* and *Alveolina vredenburgi* start to appear. The top of SBZ 5 is characterized by the sudden disappearance of all lamellar-perforate LBFs, such as *Miscellanea*, *Operculina*, *Lockhartia*, *Kathina*, and *Daviesina*. The index fossils for SBZ 5 are *Miscellanea miscella*, *Ranikothalia nuttalli*, and *Alveolina vredenburgi*.

#### SBZ 6

The base of SBZ 6 is characterized by the dominance of small benthic foraminifera (mainly *Lenticulina*) together with *Alveolina* and *Orbitolites*. In the lower part of SBZ 6, *Alveolina* and *Orbitolites* are very low in abundance, and in the upper part, *Alveolina*



*ellipsoidalis*, *A. cf. subtilis*, *A. agerensis*, *A. conradi*, *A. tibeticus*, and *Orbitolites* sp. start to appear in higher abundance.

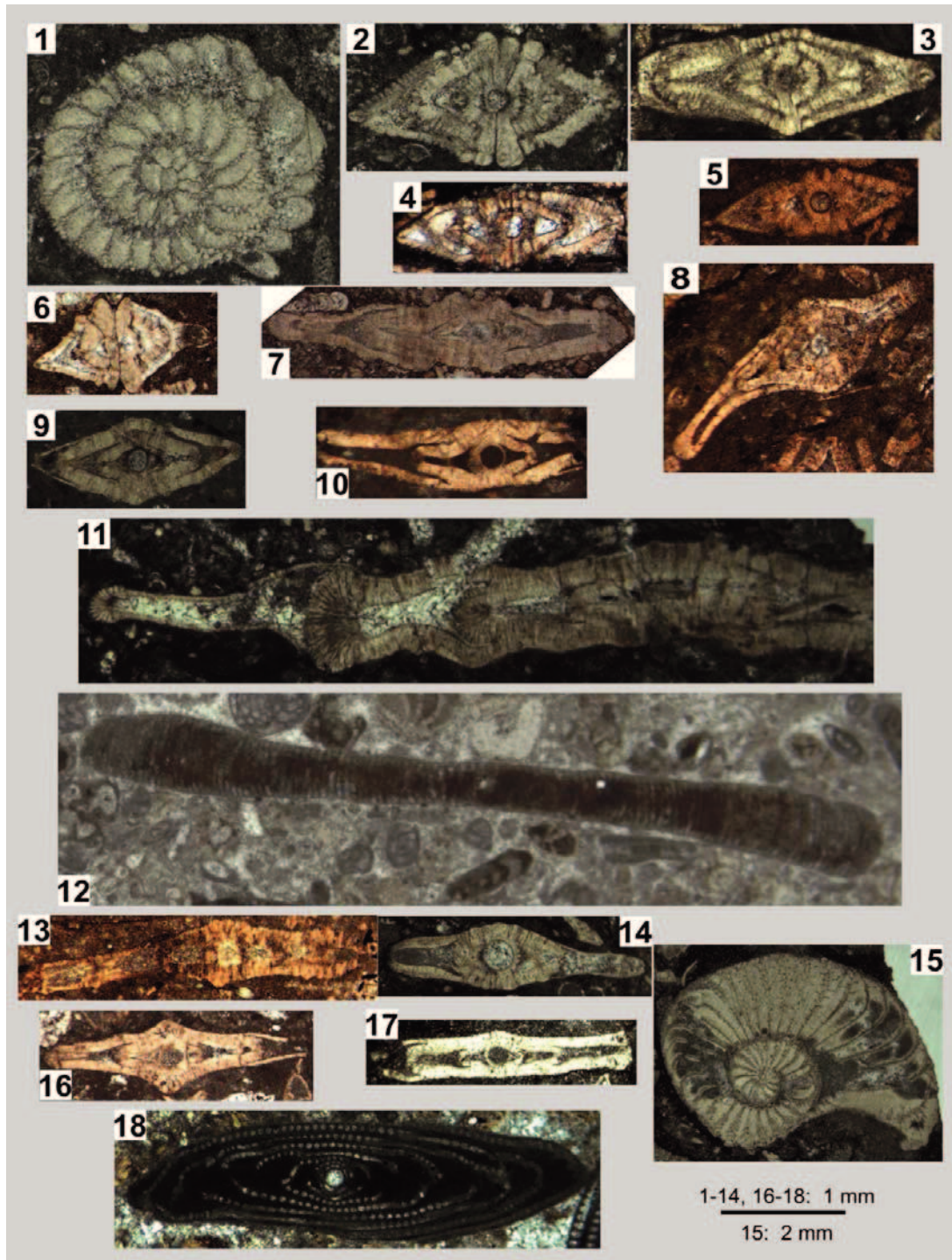


Fig. 7 The Paleocene LBFs in Tibet. (1-2) *Miscellanea miscella* d'Archiac & Haime, 1853. Sample 292 & 298, Tingri; (3) *Miscellanea dukhani* Smout, 1954. Sample 304, Tingri; (4) *Miscellanea complanata* Sheng & Zhang, 1976. Sample Fm 39, Gamba; (5) *Miscellanea minor* Sheng & Zhang, 1976. Sample Fm 5, Gamba; (6) *Miscellanea cf. miscella* d'Archiac & Haime, 1853. Sample Fm 19, Gamba; (7) *Ranikothalia*

*nutalli* Davies, 1927. Sample Fm 21, Gamba; (8) *Ranikothalia sahnii* Davies, 1952. Sample Fm 41, Gamba; (9) *Ranikothalia thalicus* Davies, 1927. Sample 265, Tingri; (10) *Ranikothalia savitriae* Davies, 1952. Sample Fm 49, Gamba; (11) *Ranikothalia sindensis* Davies, 1927. Sample 260, Tingri; (12) *Orbitolites* sp., sample 254, Tingri; (13) *Operculina patalensis* Davies, 1937. Sample Fm 8, Gamba; (14-15) *Operculina subsalsa* Davies, 1937. Sample 285 & 287, Tingri; (16) *Operculina* cf. *canalifera* d'Archiac & Haime, 1853. Sample 228, Tingri; (17) *Operculina jiwani* Davies, 1937. Sample Fr 12, Gamba; (18) *Alveolina vredenburgi* Davies & Pinfold, 1937. Sample 54, Gamba.

## SBZ 7

The base of SBZ 7 is defined by the first appearance of *Alveolina pasticillata*, *A.* cf. *tumida*, *A.* cf. *subpyrenaica*, *A. moussoulensis*, *A. aragonensis*, *A. elliptica nuttalli*, *Orbitolites tingriensis*, *O. bellatulus*, *O. longjiangicus*, and *O. disciformis*, and in the upper part *Nummulites mamilla* and *N. subramondi* appear in low abundance. Generally, *Alveolina* and *Orbitolites* show high abundance in this biozone. *Lockhartia hunti*, *L. conditi*, and *L. tipperi* appear again, but they are very low in abundance and much smaller in size compared with those in SBZ 5.

## SBZ 8

SBZ 8 is dominated by *Nummulites*, and its base is defined by the first appearance of *Nummulites globulus* and *N. atacicus* and the last occurrence of *A. agerensis*, *A. tibeticus*, *A. pasticillata*, and *A. moussoulensis*.

## SBZ 9

SBZ 9 is defined by the first appearance of *Alveolina citrea*, *Discocyclina sowerbyi*, *D. dispansa*, *Assilina leymeriei*, *A. sublamina*, and *A. subspinosa*, and the last occurrence of *Nummulites mamilla*, *N. subramondi*, *N. globulus*, *N. atacicus*. Although *Nummulites* is still high in abundance in the lower SBZ 9, *Assilina* and *Discocyclina* start to gain the dominance of this biozone.

## SBZ 10

This youngest SBZ is defined by the first appearance of *Nummulites fossulata* coexisting with *Discocyclina* and *Assilina*. *Nummulites fossulata* was firstly found in France where it was coexistent with *Nummulites aquitanica* (SBZ 10) and *Nummulites praelucasi* (SBZ 10-11), indicating a possible stratigraphic range of SBZ 10-11 (Cizancourt 1945). Although it has been proposed to represent a Late Cuisian to earliest Lutetian age (SBZ 12-13) in Oman (Racey 1995), it did appear as early as SBZ 10 in Tibet. The SBZ 10 LBFs appear exclusively in the topmost 6 m of the Zhepure Shan Formation, representing the base of SBZ 10.

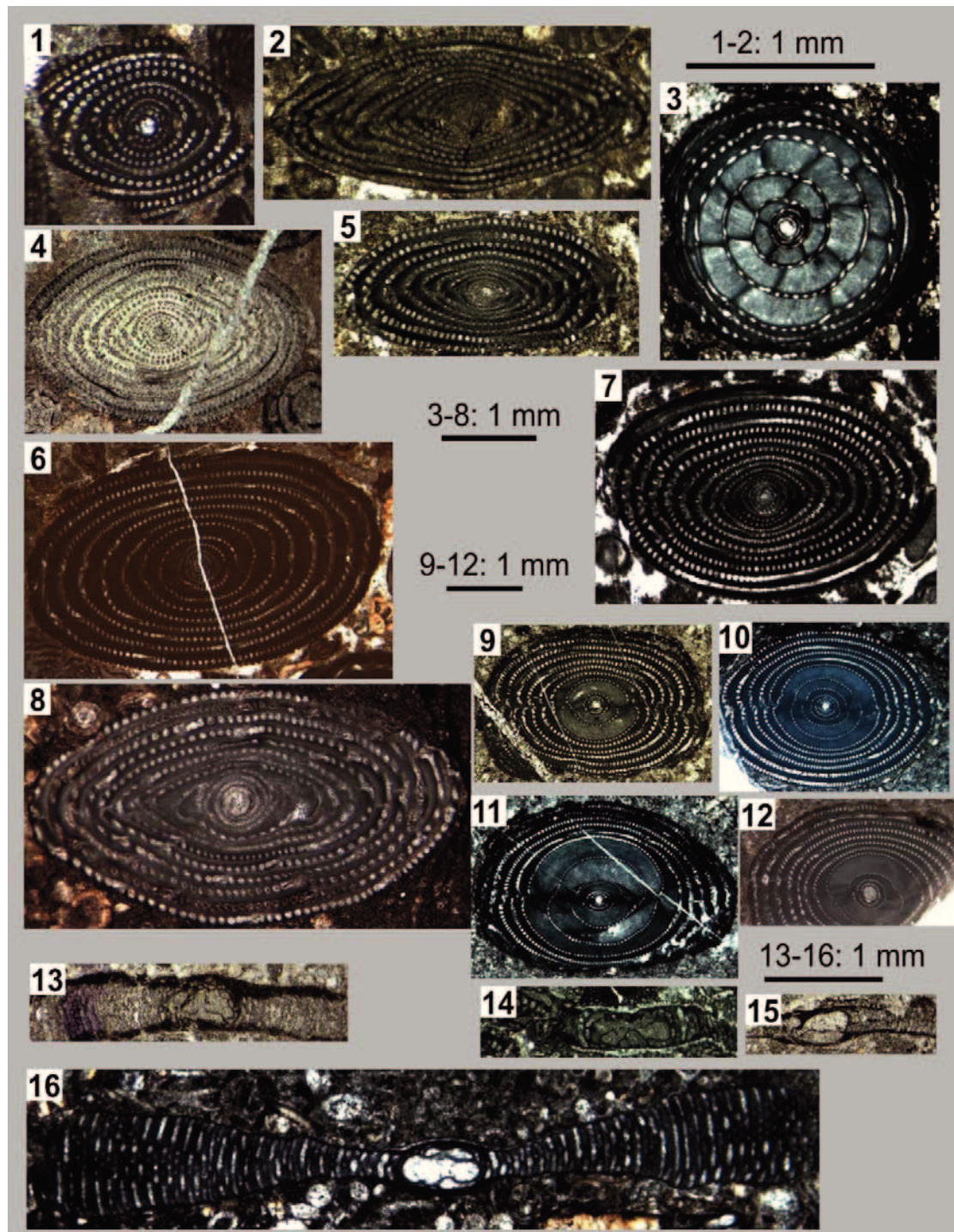


Fig. 8 The early Eocene LBFs in Tibet. (1) *Alveolina* cf. *subtilis* Hottinger, 1960. Sample Fm 55, Gamba; (2) *Alveolina* *agerensis* Gaemers, 1978. Sample 417, Tingri; (3) *Alveolina* *pasticillata* Schwager, 1883. Sample 459, Tingri; (4) *Alveolina* *ellipsoidalis* Schwager, 1883. Sample Fm 28, Gamba; (5) *Alveolina* cf. *tumida* Hottinger, 1960. Sample 432, Tingri; (6) *Alveolina* cf. *subpyrenaica* Leymerie 1846. Sample Fm 25, Gamba; (7) *Alveolina* *moussoulensis* Hottinger, 1960. Sample Fm 25, Gamba; (8) *Alveolina* *conradi* Sameeni & Butt, 2004. Sample 412, Tingri; (9) *Alveolina* *tibeticus* Sheng & Zhang, 1976. Sample 424, Tingri; (10) *Alveolina* *aragonensis* Hottinger, 1960. Sample 439, Tingri; (11) *Alveolina* *elliptica nuttalli* Davies, 1940. Sample 468, Tingri; (12) *Alveolina* *citrea* Drobne, 1977. Sample 490, Tingri; (13) *Orbitolites*

*tingriensis* Zhang, 1988. Sample Fm 25, Gamba; (14) *Orbitolites bellatulus* Zhang, 1988. Sample Ff 35, Gamba; (15) *Orbitolites longjiangicus* Zhang, 1988. Sample Fm 25, Gamba; (16) *Orbitolites disciformis* Zhang, 1988. Sample 481, Tingri.

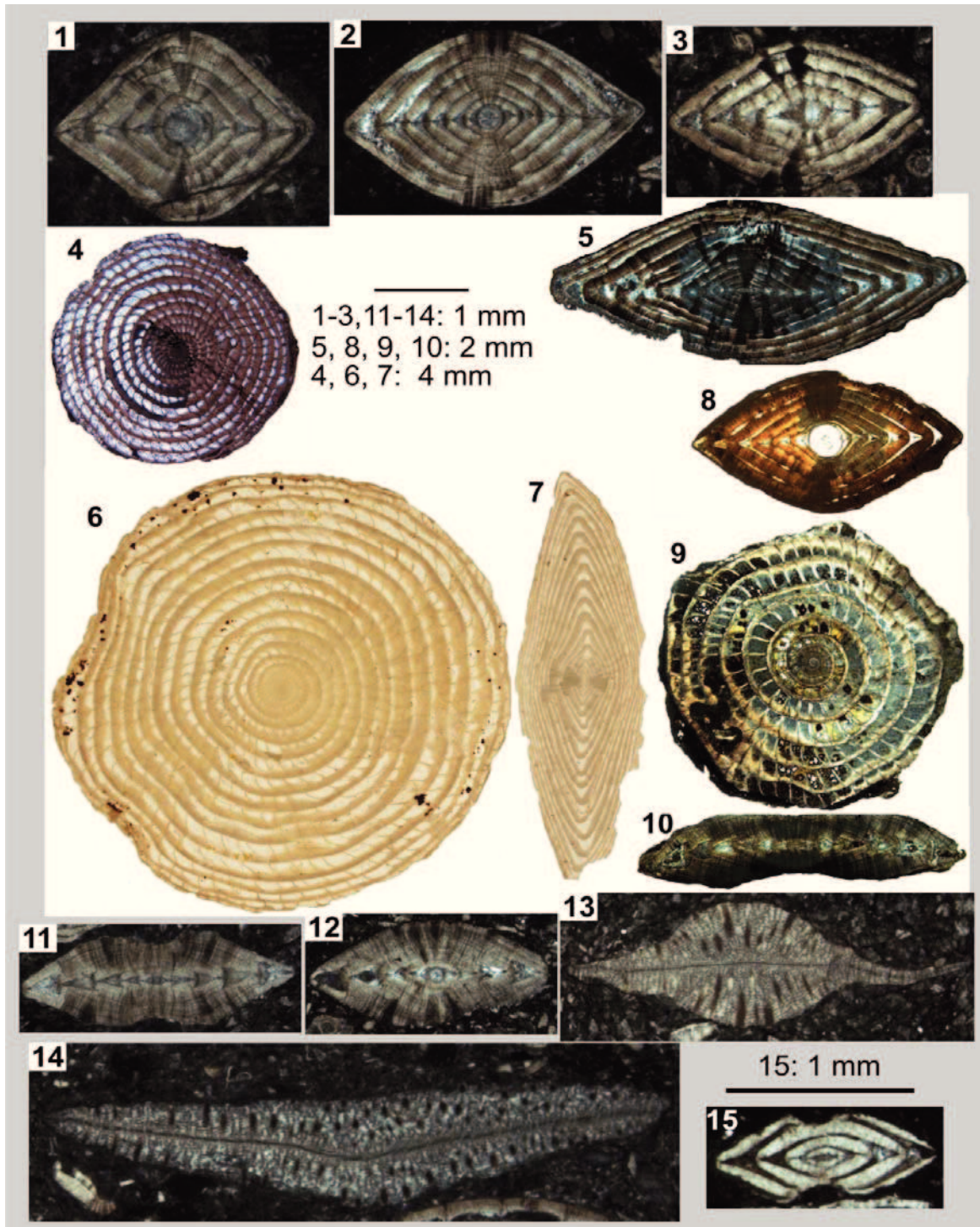


Fig. 9 The early Eocene LBFs in Tibet. (1) *Nummulites subramondi* Harpe, 1883. Sample 471, Tingri; (2) *Nummulites mamilla* Fichtel & Moll, 1803. Sample 482, Tingri; (3-5) *Nummulites globulus* Leymerie, 1846. Sample 478 & isolated specimen, Tingri; (6-8) *Nummulites atacicus* Leymerie, 1846. Isolated specimen,

Tingri; (9-10) *Assilina leymeriei* d'Archiac & Haime, 1853. Isolated specimen, Tingri; (11) *Assilina subspinosa* Davies, 1937. Sample 498, Tingri; (12) *Assilina sublaminosa* Gill, 1953. Sample 492, Tingri; (13) *Discocyclina dispansa* Sowerby, 1840. Sample 499, Tingri; (14) *Discocyclina sowerbyi* Nuttall, 1926. Sample 492, Tingri; (15) *Nummulites fossulata* de Cizancourt, 1946. Sample 493, Tingri.

## 2.5 The Paleocene-early Eocene larger foraminiferal evolution in Tibet

Similar to other shallow marine environments of the Neo-Tethyan Ocean, there is completely no K-strategist LBF in Tibet during the period of SBZ 1, and it was thought to be the result of a mass extinction of the LBFs after the Cretaceous-Tertiary boundary (Hottinger 2001). In SBZ 2, a gradual appearance of some Paleocene LBFs, such as *Rotorbinella*, *Rotalia*, *Lockhartia*, *Kathina*, and *Daviesina*, represents the beginning of generic diversification of the LBF during the evolutionary process. Although the LBFs during this period have been proposed to evolve mainly towards the direction of increasing the number of new genera (Hottinger 2001), some LBFs, such as *Lockhartia* and *Kathina*, did start to develop different species.

The following two biozones (SBZ 3-4) are characterized by progressively generic diversification and distinct species diversity of the LBFs. Some new genera (*Keramosphaerinopsis*, *Miscellanites*, *Aberisphaera*, *Fallotella*, *Setia*, *Ranikothalia*, and *Operculina*) appear in the eastern Neo-Tethyan Ocean, and *Lockhartia* shows high diversity on the species level. The formation of the so-called 'Lockhartia Sea' probably initiates in SBZ 3. At that time, *Keramosphaerinopsis haydeni* (SBZ 3) has already shown distinct adult dimorphism and large shell size (Cherchi and Schroeder 2005) (Fig. 6-29, 30), implying that the advantage of two different life strategies had been taken by some LBFs to adapt environmental changes of seasonality (Hottinger 1998).

In SBZ 5, *Lockhartia*, *Miscellanea*, *Ranikothalia* and *Operculina* exhibit the highest species diversification, and adult dimorphism and large shell dimensions can be easily recognized from those LBFs. Although the abundance and diversity of *Alveolina* and *Orbitolites* are very low in SBZ 5, the existence of *Alveolina vredenburgi* (index fossil of SBZ 5) represents the first appearance of *Alveolina* in Tibet and indicates the beginning of the Ilerdian stage.

In SBZ 6, all Paleocene lamellar-perforate LBF, such as *Lockhartia*, *Kathina*, *Daviesina*, *Miscellanea*, *Ranikothalia*, and *Operculina*, disappear suddenly, and the only two surviving genera, *Alveolina* and *Orbitolites*, gradually dominate this biozone. Since then, most of the early Eocene LBFs in Tibet have also been reported in Europe, which implies the vanishing of the so-called 'Lockhartia Sea' and indicates high-degree homogenization of the early Eocene LBF in the entire Neo-Tethyan Ocean.

Shallow Benthic Zones (SBZ)	Paleocene				Eocene		
	2	3	4	5	6	7	8
<i>Rotorbinnella skourensis</i>							
<i>Rotalia implumis</i>							
<i>Rotalia cf. newboldi</i>							
<i>Lockhartia retiata</i>							
<i>L. megapapulata</i>							
<i>L. prehaimei</i>							
<i>L. haimei</i>							
<i>L. roeae</i>							
<i>L. aff. roeae</i>							
<i>L. altispira</i>							
<i>L. sp.</i>							
<i>L. aff. conditi</i>							
<i>L. conditi</i>							
<i>L. tipperi</i>							
<i>L. hunti</i>							
<i>Kathina aquitanica</i>							
<i>K. permavuti</i>							
<i>K. cf. selveri</i>							
<i>K. nammalensis</i>							
<i>Miscellanites primitivus</i>							
<i>Keramosphaeropsis haydeni</i>							
<i>Aberisphaera gambanica</i>							
<i>Fallotella sp.</i>							
<i>Setia tibetica</i>							
<i>Orbitosiphon punjabensis</i>							
<i>Daviesina danieli</i>							
<i>D. khatiyahi</i>							
<i>D. tenuis</i>							
<i>D. sp.</i>							
<i>D. langhami</i>							
<i>Miscellanea miscella</i>							
<i>M. complanata</i>							
<i>M. dukhani</i>							
<i>M. minor</i>							
<i>M. cf. miscella</i>							
<i>Ranikothalia sindensis</i>							
<i>R. nuttalli</i>							
<i>R. savitriae</i>							
<i>R. thalica</i>							
<i>R. sahnii</i>							
<i>Operculina cf. canalifera</i>							
<i>O. patalensis</i>							
<i>O. subsalsa</i>							
<i>O. jiwani</i>							
<i>Orbitolites sp.</i>							
<i>Alveolina vredenburgi</i>							

Fig. 10 Stratigraphic distributions of the Paleocene LBFs in Tibet.

Shallow Benthic Zones (SBZ)	Early Eocene				
	6	7	8	9	10
<i>Alveolina ellipsoidalis</i>	██████████	██████████	██████████		
<i>A. cf. subtilis</i>	██████████	██████████			
<i>A. agerensis</i>	██████████	██████████			
<i>A. conradi</i>	██████████	██████████			
<i>A. tibeticus</i>	██████████	██████████			
<i>A. pasticillata</i>		██████████			
<i>A. cf. tumida</i>		██████████			
<i>A. cf. subpyrenaica</i>		██████████			
<i>A. moussoulensis</i>		██████████			
<i>A. aragonensis</i>		██████████			
<i>A. elliptica nuttalli</i>		██████████	██████████	██████████	
<i>A. citrea</i>				██████████	
<i>Orbitolites tingriensis</i>		██████████	██████████	██████████	
<i>O. bellatulus</i>		██████████	██████████	██████████	
<i>O. longjiangicus</i>		██████████	██████████	██████████	
<i>O. disciformis</i>		██████████	██████████	██████████	
<i>Nummulites mamilla</i>			██████████	██████████	
<i>N. subramondi</i>			██████████	██████████	
<i>N. globulus</i>			██████████	██████████	
<i>N. atacicus</i>			██████████	██████████	
<i>N. fossulata</i>					██████████
<i>Discocyclus sowerbyi</i>				██████████	██████████
<i>D. dispansa</i>				██████████	██████████
<i>Assilina leymeriei</i>				██████████	██████████
<i>A. sublamnosa</i>				██████████	██████████
<i>A. subspinosa</i>				██████████	██████████

Fig. 11 Stratigraphic distributions of the early Eocene LBFs in Tibet.

SBZ 7-8 are mainly dominated by *Alveolina*, *Orbitolites*, and *Nummulites* with the former two genera thriving in SBZ 7 and the latter one in SBZ 8. Some species of *Lockhartia* appear again but with very low abundance and smaller size. In SBZ 9-10, *Alveolina*, *Orbitolites*, and *Nummulites* are gradually substituted by *Discocyclus* and *Assilina*, which reveals a deepening of the depositional environment (Hottinger 1997) and has been interpreted to be caused by the arrival of a foredeep in the foreland basin (Zhang et al. 2012). Generally, the early Eocene larger foraminiferal evolution in Tibet reflects a complete success of *Alveolina*, *Orbitolites*, *Nummulites*, *Discocyclus* and *Assilina* during the process of the Global Community Maturation (GCM) (Hottinger 2001), and the decline of the LBFs at the very beginning of the Cuisian in Tibet was clearly caused by local tectonic activities owing to the India-Asia collision (Zhang et al. 2012).

## 2.6 Comparison of the Paleocene-early Eocene LBF between the eastern and western Neo-Tethyan Ocean

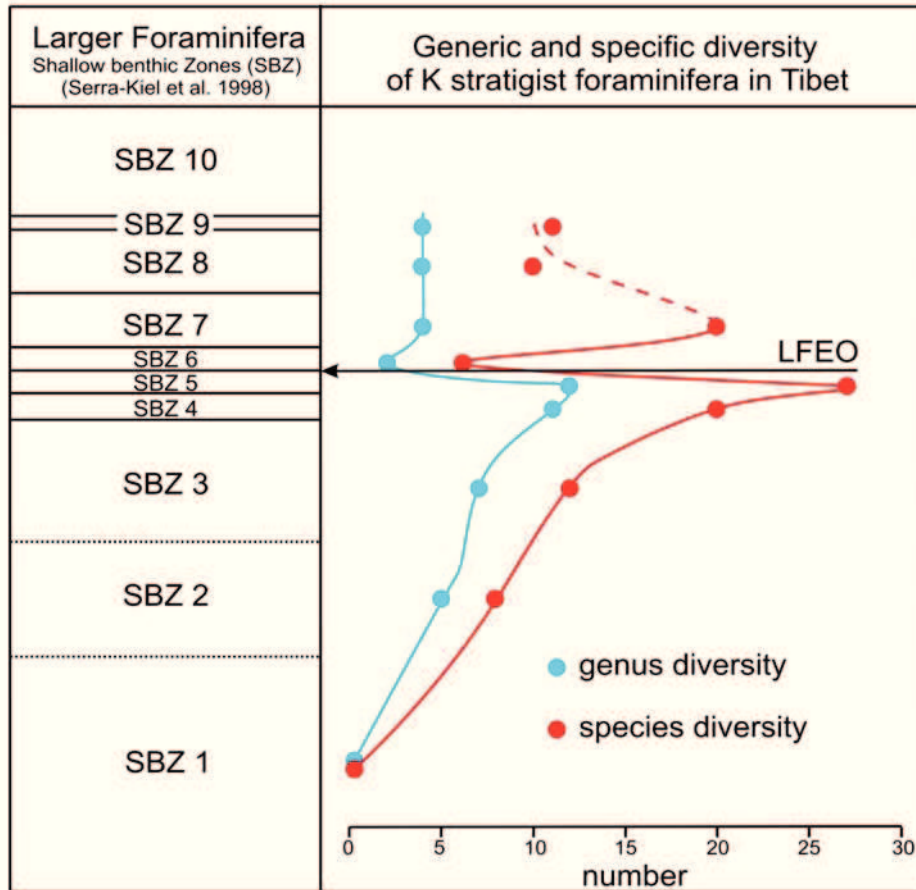


Fig. 12 Evolution of larger foraminiferal generic and species diversity during the Paleocene-early Eocene in Tibet. Note that the red dotted line above SBZ 7 indicates uncertainty of species evolution.

During the early Eocene, the Evolution of the LBFs is similar or nearly identical in the entire Neo-Tethyan Ocean, characterized by the dominance of highly diversified *Alveolina*, *Orbitolites*, *Nummulites*, *Discocyclusina* and *Assilina*. However during the Paleocene, the LBFs show distinct differences between the east (Tibet, Pakistan, India, Persian Gulf) and the west (Spain). In the east, carbonate ramps were mainly dominated by the LBFs, which had been taken as a major carbonate producer for the construction of carbonate ramps. Evolution of the LBFs is characterized by high diversification of *Lockhartia*, *Kathina*, *Daviesina*, *Miscellanea*, *Ranikothalia*, and *Operculina* during SBZ 3-5 and early differentiation between genera and species diversifications since SBZ 3 (Fig. 12). It seems to be that *Lockhartia* and *Kathina* might have only fully evolved in the eastern Neo-Tethyan Ocean. By contrast, carbonate platforms in the west were mainly dominated by corallgal reefs during most time of the Paleocene (Scheibner and Speijer



2008), and *Miscellanea*, *Daviesina*, *Ranikothalia*, *Assilina*, and *Glomalveolina* are some frequently reported genera during SBZ 4-5 (Hottinger 1998).

In the west, the LFT was defined as the 'start of adult dimorphism and large shell size' in the LBF evolution by Hottinger (1998). It took place at the boundary between SBZ 4 and 5, and has been clearly illustrated by the evolution of Ilerdian *Alveolina* and *Nummulites* from the Tresp and Campo sections in Spain (Hottinger and Schaub 1960). However in Tibet, two lines of evidence, early differentiation of diversity between genera and species in the Paleocene LBF and early occurrence of adult dimorphism and large shell size in some LBFs, such as *Keramosphaerinopsis haydeni* (SBZ 3), *Daviesina langhami* (SBZ 4-5), *Miscellanea miscella* (SBZ 5), imply that the Paleocene LBF evolved more early in Tibet than those in the west. As a result, the LFT probably also took place earlier in the east. Given that the LFT in the entire Neo-Tethyan Ocean occurred not synchronously, we support the opinion that the LFT reflects only the result of naturally evolutionary processes, and has no relationship with the Paleocene-Eocene Thermal Maximum (PETM) (Hottinger 1998).

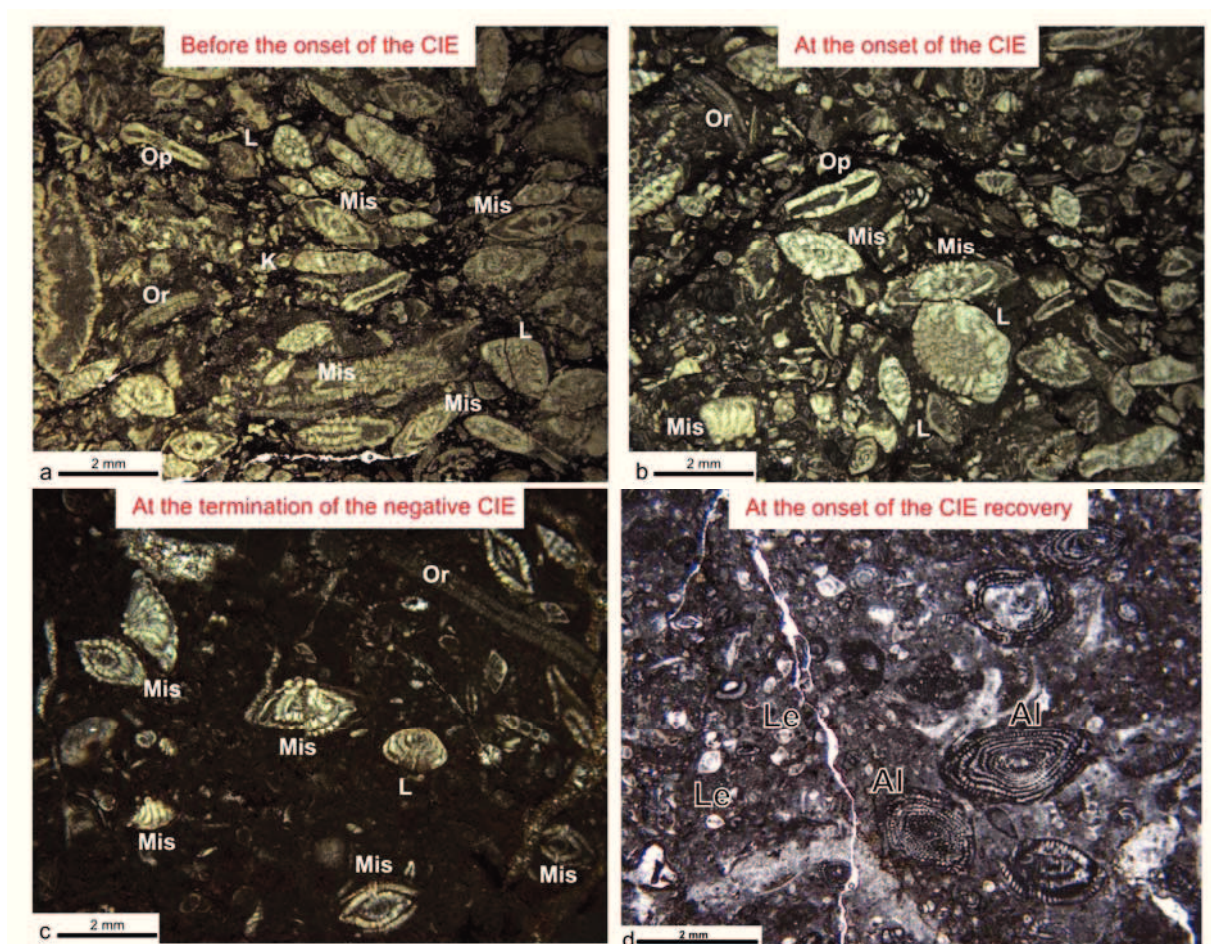


Fig. 13 Thin section photomicrographs showing changes of the larger foraminifera at the P-E boundary. Note that there was no change of larger foraminifera at the onset of the CIE, however, a sudden disappearance of all Paleocene lamellar-perforate LBFs, such as *Miscellanea*, *Ranikothalia*, *Lockhartia*, *Operculina*, *Kathina*, and *Orbitosiphon* and the initial dominance of porcellaneous forams of *Alveolina* occurred at the onset of the CIE recovery, which has been tentatively named 'Larger Foraminiferal Extinction and Origination (LFEO)' by us. All the photomicrographs were taken from the continuous section at Tingri. A: *Alveolina*; K: *Kathina*; L: *Lockhartia*; Le: *Lenticulina*; Mil: *Miliolids*; Mis: *Miscellanea*; Op: *Operculina*; Or: *Orbitosiphon*; R: Rotaliids; T: Textulariids.

At the boundary between SBZ 5 and 6, a distinct LFEO event is found by us for the first time. The LFEO is characterized by the sudden disappearance of all Paleocene lamellar-perforate LBF, such as *Miscellanea*, *Ranikothalia*, *Operculina*, *Lockhartia*, *Kathina*, and *Daviesina*, followed by the initial dominance of porcellaneous forms of *Alveolina* and *Orbitolites* (Figs. 13 c, d). It coincided with the onset of the CIE recovery, and the stratigraphic thickness covering the LFEO at Tingri is less than 30 cm, indicating that the LFEO probably occurred within ~10 kyr and postdated the P-E boundary ~80 kyr according to the age models for the CIE (Röhl et al. 2007; Murphy et al. 2010). The LFEO can be clearly recognized in the Tingri area of Tibet, and it has also been roughly reported in other low latitudinal areas of Pakistan (Afzal et al. 2010), Iran (Bagherpour and Vaziri 2011), Slovenia (Zamagni 2009), and even Egypt (Scheibner et al. 2005; Scheibner and Speijer 2008, 2009). In the middle latitude of Spain, however, it seems there is no interruption of the LBF evolution since *Alveolina* and *Nummulites* started to dominate the shallow water environment in SBZ 5. So, we tentatively speculate that the LFEO probably represents a transient but distinct shallow-water biotic event in the low latitudinal areas of the Neo-Tethyan Ocean. The coincidence of the LFEO and the onset of the CIE recovery implies that the PETM probably had a negligible impact on the LBF, however, some possible mechanisms causing the sudden recovery of the CIE (Bowen and Zachos 2010) might also lead to the LFEO in shallow water environments.

We tentatively ascribe the different evolution of the Paleocene LBF between the east and the west to the latitudinal effect in the Neo-Tethyan Ocean (Scheibner and Speijer 2008). Paleogeographically, the Neo-Tethyan Ocean was located close to the equator to the east and gradually extended into the middle latitude to the west. During the Paleocene, reef-building corals were not able to tolerate the rising temperature in low latitudes during the long-term global warming (Zachos et al. 2001) and retreated from the east to the west in the Neo-Tethyan Ocean (Scheibner and Speijer 2008), which might leave an ecological niche for the LBFs to thrive in the eastern Neo-Tethyan Ocean. Additionally, higher temperature in low latitudinal areas (Sewall et al. 2004) and overall oligotrophic conditions during the Paleocene (Scheibner and Speijer 2008) might accelerate the LBF evolution in the eastern Neo-Tethyan Ocean, leading to early differentiation of genera and species diversification and forming the unique 'Lockhartia

Sea'. However, what on earth resulted in the LFEO and the vanishing of the 'Lockhartia Sea' close to the P-E boundary is still enigmatic.

## 2.7 The P-E boundary in the SBZs

The P-E boundary was officially defined by the beginning of the CIE (Aubry and Ouda 2003), and is located at the base of P 5b and NP 9b in the plankton zones (Dupuis et al. 2003). In the shallow benthic zones, however, there are still two main contrasting opinions concerning the P-E boundary. Serra-Kiel et al. (1998) and Hottinger (1998, 2001) proposed a time interval for the P-E boundary, stretching roughly from the upper part of SBZ 5 to the middle part of SBZ 7. In contrast, Scheibner and Speijer (2009) and Pujalte et al. (2009a, 2009b) suggested to locate the P-E boundary at the transition of SBZ 4 and 5, coinciding with the base of the Ilerdian and the LFT (Fig. 14).

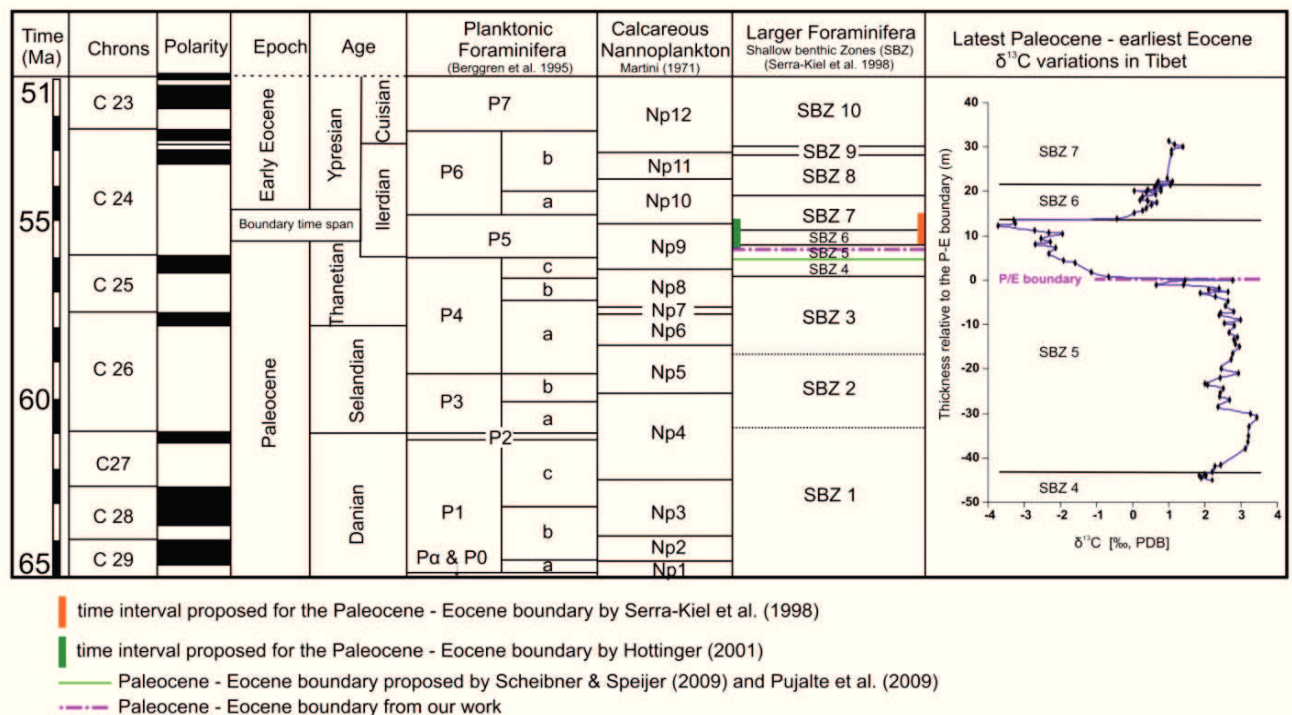


Fig. 14 Comparison of the proposed positions for the P-E boundary in the Shallow Benthic Zones by different authors and carbon isotopic variations close to the P-E boundary at Tingri. The geologic time scale is revised from Berggren et al. (1995), and planktonic foraminifera, calcareous nannoplankton and shallow benthic zones are based on Berggren et al. (1995), Martini (1971) and Serra-Kiel et al. (1998), respectively.

In the western Neo-Tethyan realm, the P-E boundary in the shallow-water environment has been well studied in Spain and Egypt where the upper Paleocene-lower Eocene limestones are relatively well preserved. In Spain, sedimentological studies from some shallow marine sections showed that there was a deposition of non-marine strata close to the P-E boundary (Pujalte et al. 2009a, 2009b). The non-marine strata unconformably

overlie the SBZ 4 strata and underlie the SBZ 5 marine limestones, and thus the boundary between SBZ 4 and 5 (or the base of the Ilerdian) is ambiguous owing to the lack of in-situ LBFs from the non-marine sediments. Notably, the P-E boundary defined by the onset of the CIE is recorded in the upper part of the non-marine strata in spite of poor expression of the CIE from soil carbonate nodules (Schmitz and Pujalte 2003; Pujalte et al. 2009a, 2009b). Therefore, the relationship between the non-marine interval and the base of the Ilerdian is key to constraining the P-E boundary in the shallow benthic zonations. Although the base of the Ilerdian was redefined in the stratotype section of Tremp and was proposed to be placed at the base of the Claret Conglomerate in order to take the base of the Ilerdian as the P-E boundary (Pujalte et al. 2009a), the designation is somehow not reasonable because the foundation of the Ilerdian Stage was originally based on the evolution of the LBFs. Thus, the true base of the Ilerdian can only be spiked through the determination of in-situ LBFs from a complete shallow marine section, not through arbitrary assignment according to the onset of the CIE.

Consequently, it is not suitable to study the relationship of the P-E boundary and the base of the Ilerdian on the basis of the sections with the deposition of non-marine strata at the P-E boundary. In Egypt, Scheibner and Speijer (2009) have investigated the P-E boundary near the Galala Mountain where most of the studied sections recording the upper Paleocene to lower Eocene limestones represent a continental slope environment. In those sections, the SBZ 4 strata defined by *Hottingerina lukasi* (SBZ 4) contain the SBZ 5 index fossils such as *Miscellanea miscella* and *Ranikothalia nuttalli* (Hottinger 1971; Jauhri 1996; Serra-Kiel et al. 1998), and some index species of both SBZ 5 and 6 co-exist in the combinational biozones of SBZ 5/6. The ambiguous zonations among SBZ 4, 5 and 6 in this area probably result from the erosion and/or reworking in the continental slope setting. So, although the authors having studied the Paleocene-Eocene shallow-water platforms in Spain and Egypt proposed that the P-E boundary was coincidentally located at the boundary between SBZ 4 and 5, no convincing evidence from the LBFs has been presented to precisely spike the boundary between SBZ 4 and 5 in these localities. In addition, the distinctness and completeness of the CIEs measured from soil carbonate nodules and bulk limestones in Spain and Egypt were strongly affected by diagenetic overprint and/or low resolution sampling, which to some extent also blurs the recognition of the P-E boundary. Thus, clearly defined SBZs from a continuous shallow marine section with no sedimentary hiatus at the P-E boundary and a high resolution CIE record from the same section are indispensable to clarify the P-E boundary in shallow marine environment.

In the eastern Neo-Tethyan realm of Tibet, the section at Tingri represents the deposition of the complete shallow marine limestones covering the period of the Paleocene to early Eocene. The carbon isotopes measured from bulk limestone show

that an expanded CIE is recorded in a ~9 m thick marine nodular limestone. A high resolution sampling (20 cm/sample) and measurements of carbon isotopes (unpublished data) exhibit nearly identical patterns of the CIE with those from the reference section of ODP 690 (Bains et al. 1999), which implies that a complete sedimentary record at the P-E boundary is preserved at Tingri. The expanded CIE curve clearly shows that the P-E boundary falls into the upper part of SBZ 5 (Fig. 14), which is straddled by biostratigraphic ranges of some typical index fossils of SBZ 5, such as *Alveolina vredenburgi*, *Miscellanea miscella*, and *Ranikothalia nuttalli* (Hottinger 1971; Jauhri 1996; Hottinger et al. 1998; Serra-Kiel et al. 1998), and associated with no evident biotic turnover of the shallow benthic communities (Figs. 13 a, b). Consequently, our results suggest that the P-E boundary should be placed at the beginning of the time intervals recommended by Hottinger (1998, 2001) and Serra-Kiel et al. (1998). Thus, it fits well with the P-E boundary in plankton zones through interzonal correlation schemes provided by Serra-Kiel et al. (1998), but is inconsistent with the work from Scheibner and Speijer (2009) and Pujalte et al. (2009a, 2009b). Additionally, it also suggests that the LFT was only the result of evolutionary processes, and has no relationship with the PETM because the occurrence of the LFT in the entire Neo-Tethyan Ocean clearly predated the drastically climatic and environmental changes during the PETM.

## 2.8 Conclusions

On the basis of our studies of the Paleocene-early Eocene LBFs in Tibet, 10 biozones from SBZ 1 to 10 have been established from the Zhepure Shan Formation at Tingri. At Gamba, the deposition of the Zongpu Formation started from SBZ 2 and terminated in SBZ 7. Totally, 72 species from 19 genera have been identified, and their biostratigraphic ranges in the shallow benthic zones have been tentatively assigned. In Tibet, the Paleocene LBFs show high diversity of *Lockhartia*, *Kathina*, *Daviesina*, *Miscellanea*, *Ranikothalia*, and *Operculina*. The differentiation between genera and species diversity and the beginning of adult dimorphism and large shell size from some LBF took place as early as SBZ 3, indicating that occurrence of the LFT was not synchronous in the entire Neo-Tethyan Ocean and the LFT might take place earlier in the east than in the west. During the early Eocene, some successful genera of *Alveolina*, *Orbitolites*, *Nummulites*, *Assilina*, and *Discocyclina* gained their predominance in the Neo-Tethyan Ocean, and the LBFs showed a high-extent homogenization in the Neo-Tethyan Ocean. In addition, a transient LFEO event has been found by us. It occurred at the boundary between SBZ 5 and 6, and coincided with the beginning of the CIE recovery, implying that some possible mechanisms causing the sudden CIE recovery probably also led to the LFEO in the low latitudinal areas. Importantly, high resolution carbon isotopic variations and well-defined SBZs at Tingri clearly demonstrate that the

P-E boundary is located at the upper part of SBZ 5, not at the boundary between SBZ 4 and 5 proposed by some authors.

## Acknowledgements

The first author is deeply indebted to the late Prof. Lukas Hottinger for his instruction in larger foraminifera, and his generosity and patience to impart knowledge to the young generation together with his erudition will be remembered by us forever. Dr. Christian Scheibner is greatly acknowledged for his illuminating suggestions. Anne Hübner, Christiane Schott, Friederike Wieseler, Jan-Peter Duda, Di Yang, Shuaiquan Fan, and Martin Krogmann are thanked for their assistance in field and laboratory work. The project is part of the Priority Programme 1372 Tibetan Plateau: Formation, Climate, Ecosystems (*TiP*) and is funded by Deutsche Forschungsgemeinschaft (No. Wi725/26), Chinese Ministry of Science and Technology (2011CB403101 to Ding Lin), Chinese Academy of Sciences (KZCX2-YW-Q09-03 to Ding Lin), and Max-Planck Society.

## References

- Afzal J, Williams M, Leng MJ, Aldridge RJ, Stephenson MH (2010) Evolution of Paleocene to early Eocene larger benthic foraminifer assemblages of the Indus Basin, Pakistan. *Lethaia*. doi:10.1111/j.1502-3931.2010.00247.x
- Aubry MP, Ouda K (2003) Introduction to the upper Paleocene-Lower Eocene of the Upper Nile valley. *Micropaleontology* 49:2-4
- Bagherpour B, Vaziri MR (2011) Facies, paleoenvironment, carbonate platform and facies changes across Paleocene Eocene of the Taleh Zang Formation in the Zagros basin, SW-Iran. *Hist Biol*. doi:10.1080/08912963.2011.587185
- Bains S, Corfield RM, Norris RD (1999) Mechanisms of climate warming at the end of the Paleocene. *Science* 285:724-727. doi:10.1126/science.285.5428.724
- Berggren WA, Kent DV, Swisher CC, Aubry MP (1995) A revised Cenozoic geochronology and chronostratigraphy. *SEPM Spec Publ* 54:129-212
- Bowen GJ, Zachos JC (2010) Rapid carbon sequestration at the termination of the Palaeocene-Eocene Thermal Maximum. *Nature Geosci* 3:866-869
- Butt AA (1991) *Ranikothalia sindensis* Zone in late Paleocene biostratigraphy. *Micropaleontology* 37:77-85

- Caus E, Hottinger L, Tambareau Y (1980) Plissements du <<septal flap>> et système de canaux chez *Daviesina*, foraminifères paléocènes. *Eclogae Geol Helv* 73:1045-1069
- Cherchi A, Schroeder R (2005) Revision of *Keramosphaeropsis haydeni* (H. Douvillé), larger foraminifer (Miliolacea) from the Paleocene of southern Tibet (Tethys Himalaya). *Boll Soc Paleontol Ital* 44:175-183
- Cizancourt MD (1945) Nummulites nouvelles ou peu connues d'Aquiiaine. *B Soc Géol Fr* 15:643-655
- Davies LM (1927) The Ranikot beds at Thal (north-west frontier provinces of India). *Quart J Geol Soc* 83:260-290. doi: 10.1144/GSL.JGS.1927.083.01-05.10
- Davies LM (1930) The fossil fauna of the Samana range and some neighbouring areas: Part VI. *Mem Geol Surv India* 15:66-81
- Davies LM (1932) The genera *Dictyoconoides* Nuttall, *Lockhartia* nov. and *Rotalia* Lamarck. *Trans Roy Soc Edin* 57:397-428
- Davies LM (1938) Westward extension of the Ranikot Sea. *Nature* 141:202
- Davies LM (1940) The upper khirthar beds of north-west India. *Quart J Geol Soc* 96:199-230. doi: 10.1144/GSL.JGS.1940.096.01-04.07
- Davies LM (1952) *Ranikothalia sahnii*, N.Sp. and *R. savitriae*, N.Sp.: A possible link between the Paleocene faunas of the east and west Indies. *The palaeobotanist* 1:156-158
- Dorbne K (1977) Alvéolines paléogènes de la Slovénie et de l'Istrie. *Schweiz Paleontol Abh* 99:1-132
- Drobne K, Cosovic V, Moro A, Buckovic D (2011) The role of the Palaeogene Adriatic carbonate platform in the spatial distribution of Alveolinids. *Turk J Earth Sci* 20:721-751
- Dupuis C, Aubry M-P, Steurbaut E, Berggren WA, Ouda K, Magioncalda R, Cramer BS, Kent DV, Speijer RP, Heilmann-Clausen C (2003) The Dababiya Quarry Section: Lithostratigraphy, clay mineralogy, geochemistry and paleontology. *Micropaleontology* 49:41-59. doi:10.2113/49.Suppl\_1.41
- Ferràndez-Cañadell C (2002) New Paleocene orbitoidiform foraminifera from the Punjab Salt Range, Pakistan. *J Foraminifer Res* 32:1-21

- Gill W (1953) The genus *Assilina* in the Laki series (Lower Eocene) of the Kohat Potwar basin, Northwest Pakistan. *Contrib Cushman Found Foraminifer Res* 4:76-84
- He Y, Zhang B, Hu L, Sheng J (1976) Mesozoic and Cenozoic foraminifera from the Mount Julmo Lungma region. In: Scientific team of Tibet investigation from Chinese Academy of Sciences (ed) A report of scientific expedition in the Mount Julmo Lungma Region (1966-1968), Palaeontology. Science press, Beijing, pp 1-124
- Hottinger L (1960) Über Eocäne und Paleocäne Alveolinen. *Eclogae Geol Helv* 53:265-283
- Hottinger L (1971) Larger foraminifera common to Mediterranean and Indian Paleocene and Eocene formations. *Ann Inst Geol Publ Hung* 54:145-151
- Hottinger L (1974) Alveolinids, Cretaceous-Tertiary larger foraminifera. *Schudel*.
- Hottinger L (1997) Shallow benthic foraminiferal assemblages as signals for depth of their deposition and their limitations. *Bull Soc Geol Fr* 168:491-505
- Hottinger L (1998) Shallow benthic foraminifera at the Paleocene-Eocene boundary. *Strata* 9:61-64
- Hottinger L (2001) Learning from the past. In: Levi-Montalcini R (ed) *Frontiers of life*. Academic Press, London & San Diego, pp 449-477
- Hottinger L (2009) The Paleocene and earliest Eocene foraminiferal family *Miscellaneidae*: neither *nummulitids* nor *rotaliids*. *Noteb Geol* 6:1-41
- Hottinger L, Schaub H (1960) Zur Stufeneinteilung das Paleocaens uns das Eocaens. Einführung der Stufen Ilerdien und Biarritzien. *Eclogae Geol Helv* 53:453-479
- Hottinger L, Smeeni SJ, Butt AA (1998) Emendation of *Alveolina vredenburgi* Davies and Pinfold, 1937 from the Surghar range, Pakistan. *Dela-Opera SAZU* 4. razr 34:155-163
- Jauhri AK (1996) *Ranikothalia nuttalli* (Davies), a distinctive early Ilerdian marker, in the Shillong Plateau. In: Pandey J, Azmi RJ, Bhandari A, Dave A (ed) *Contributions to XV Indian Colloquium on Micropalaeontology and stratigraphy*. Allied Printer, Dehra Dun, pp 209-218
- Jauhri AK (1998) *Miscellanea* Pfender, 1935 (foraminiferida) from the south Shillong region, N.E. India. *J Paleontol Soc India* 43:73-83



- Leppig U (1988) Structural analysis and taxonomic revision of *Miscellanea*, Paleocene, larger foraminifera. *Eclogae Geol Helv* 81:689-721
- Liu G, Einsele G (1994) Sedimentary history of the Tethyan basin in the Tibetan Himalayas. *Geol Rundsch* 83:32-61
- Martini E (1971) Standard Tertiary and Quaternary calcareous nannoplankton zonation. In: Farinacci A (ed) *Proceedings of the second Planktonic conference Roma 1970*. Edizioni Tecnoscienza, Rome, pp 739-785
- Murphy BH, Farley KA, Zachos JC (2010) An extraterrestrial  $^3\text{He}$ -based timescale for the Paleocene-Eocene thermal maximum (PETM) from Walvis Ridge, IODP Site 1266. *Geochim Cosmochim Acta* 74:5098-5108
- Nuttall WLF (1925) The Stratigraphy of the Laki Series (Lower Eocene) of parts of Sind and Baluchistan (India); with a description of the larger foraminifera contained in those beds. *Quart J Geol Soc* 81:417-452. doi:10.1144/gsl.jgs.1925.081.01-04.18
- Orue-Etxebarria X, Pujalte V, Bernaola G, Apellaniz E, Baceta JI, Payros A, Nuñez-Betelu K, Serra-Kiel J, Tosquella J (2001) Did the Late Paleocene thermal maximum affect the evolution of larger foraminifers? Evidence from calcareous plankton of the Campo Section (Pyrenees, Spain). *Mar Micropaleontol* 41:45-71
- Patzelt A, Li H, Wang J, Appel E (1996) Palaeomagnetism of Cretaceous to Tertiary sediments from southern Tibet: evidence for the extent of the northern margin of India prior to the collision with Eurasia. *Tectonophysics* 259:259-284
- Pignatti JS (1998) The philosophy of larger foraminiferal biozonation - A discussion. *Dela-Opera SAZU 4 razr* 34:15-20
- Pujalte V, Baceta JI, Schmitz B, Orue-Etxebarria X, Payros A, Bernaola G, Apellaniz E, Caballero F, Robador A, Serra-Kiel J, Tosquella J (2009a) Redefinition of the Ilerdian Stage (early Eocene). *Geol Acta* 7:177-194
- Pujalte V, Schmitz B, Baceta JI, Orue-Etxebarria X, Bernaola G, Dinarès-Turell J, Payros A, Apellaniz E, Caballero F (2009b) Correlation of the Thanetian-Ilerdian turnover of larger foraminifera and the Paleocene-Eocene thermal maximum: Confirming evidence from the Campo area (Pyrenees, Spain). *Geol Acta* 7:161-175
- Racey A (1995) Lithostratigraphy and larger foraminiferal (nummulitid) biostratigraphy of the Tertiary of northern Oman. *Micropaleontology*:1-123

- Röhl U, Westerhold T, Bralower TJ, Zachos JC (2007) On the duration of the Paleocene-Eocene thermal maximum (PETM). *Geochem Geophys Geosyst* 8. doi:10.1029/2007gc001784
- Sameeni SJ, Butt AA (2004) Alveolinid biostratigraphy of the Salt Range succession, Northern Pakistan. *Rev Paleobiol* 23:505-527
- Schaub H (1981) Nummulites et Assilines de la Téthys paléogène Taxinomie, phylogénèse et biostratigraphie. *Schweiz Paleontol Abh* 104:1-236
- Scheibner C, Speijer RP, Marzouk AM (2005) Turnover of larger foraminifera during the Paleocene-Eocene Thermal Maximum and paleoclimatic control on the evolution of platform ecosystems. *Geology* 33:493-496
- Scheibner C, Speijer RP (2008) Late Paleocene–early Eocene Tethyan carbonate platform evolution - A response to long- and short-term paleoclimatic change. *Earth Sci Rev* 90:71-102
- Scheibner C, Speijer RP (2009) Recalibration of the Tethyan shallow-benthic zonation across the Paleocene-Eocene boundary. *Geol Acta* 7:195-214
- Schmitz B, Pujalte V (2003) Sea-level, humidity, and land-erosion records across the initial Eocene thermal maximum from a continental-marine transect in northern Spain. *Geology* 31:689-692
- Sen Gupta BK (1963) A restudy of two common species of *Discocyclina* from India. *Micropaleontology* 9:39-49
- Serra-Kiel J, Hottinger L, Caus E, Drobne K, Ferrandez C, Jauhri AK, Less G, Pavlovec R, Pignatti J, Samso JM (1998) Larger foraminiferal biostratigraphy of the Tethyan Paleocene and Eocene. *Bull Soc Géol Fr* 169:281-299
- Sewall JO, Huber M, Sloan LC (2004) A method for using a fully coupled climate system model to generate detailed surface boundary conditions for paleoclimate modeling investigations: an early Paleogene example. *Global Planet Change* 43 (3-4):173-182
- Smout AH (1954) Lower Tertiary foraminifera of the Qatar Peninsula. British Museum (Natural History), London
- Wan X (1990) Eocene Larger Foraminifera from Southern Tibet. *Rev Esp Micropaleontol* 22:213-238

- Wan X (1991) Palaeocene larger foraminifera from southern Tibet. *Rev Esp Micropaleontol* 23:7-28
- Weiss W (1993) Age assignments of larger foraminiferal assemblages of Maastrichtian to Eocene age in northern Pakistan. *Zitteliana* 20:223-252
- Willems H (1993) Geoscientific investigations in the Tethyan. Universität Bremen, Bremen
- Willems H (1996) Stratigraphy of the Upper Cretaceous and Lower Tertiary strata in the Tethyan Himalayas of Tibet (Tingri area, China). *Geol Rundsch* 85:723-754
- Yin A, Harrison TM (2000) Geologic evolution of the Himalayan-Tibetan Orogen. *Annu Rev Earth Planet Sci* 28:211-280
- Zachos J, Pagani M, Sloan L, Thomas E, Billups K (2001) Trends, rhythms, and aberrations in global climate 65 Ma to present. *Science* 292:686-693
- Zamagni J (2009) Response of a shallow-water ecosystem to the early Paleogene greenhouse environmental conditions. Dissertation, University of Potsdam
- Zhang B (1988) Orbitolites (foraminifera) from Longjiang of Tingri, Xizang. *Acta Micropalaeontol Sin* 5:1-13
- Zhang Q, Willems H, Ding L, Gräfe K-U, Appel E (2012) The initial India-Asia continental collision and foreland basin evolution in the Tethyan Himalaya of Tibet: Evidence from stratigraphy and paleontology. *J Geol* 120:175-189
- Zhu B, Kidd WSF, Rowley DB, Currie BS, Shafique N (2005) Age of initiation of the India-Asia collision in the east-central Himalaya. *J Geol* 113:265-285

Second manuscript

### **3. Depositional environments of the lower Paleogene larger foraminiferal limestones in the Tethyan Himalaya of south Tibet, China**

**Qinghai Zhang<sup>1,2</sup>, Helmut Willems<sup>1,3</sup>, Lin Ding<sup>2</sup>,  
Friederike Wieseler<sup>1</sup>, Jan-Peter Duda<sup>1</sup>**

<sup>1</sup> University of Bremen, Department of Geosciences, D-28359 Bremen, Germany

<sup>2</sup> Key Laboratory of Continental Collision and Plateau Uplift, Institute of Tibetan Plateau Research, Chinese Academy of Sciences, 100085 Beijing, China

<sup>3</sup> Nanjing Institute of Geology and Palaeontology, Chinese Academy of Sciences, 210008 Nanjing, China

To be submitted to *Facies*

## Abstract

The Zhepure Shan Mountain area near Tingri County exposes the most complete sedimentary record of the lower Paleogene limestones in the Tethyan Himalaya of south Tibet, and it provides a good chance to study the evolution of larger foraminifera and their depositional environments. Based on the ~400 m thick limestones of the Zhepure Shan Formation at Tingri and the high resolution biostratigraphy, eight microfacies types have been designated with special emphasis on the paleoecology of the larger foraminifera. Five microfacies types in the Paleocene consist of algal limestones with small benthic foraminifera (MF 1) in SBZ 1, larger rotaliidae packstones with algae (MF 2) in SBZs 2-3, rotaliidae-nummulitidae packstones with algae (MF 3) in SBZ 4, and miscellaneidae-nummulitidae-rotaliidae floatstones with dasycladacean algae (MF 4), and proximal tempestites (MF 5) in SBZ 5. Three microfacies types in the early Eocene are *Alveolina* packstones/floatstones with *Orbitolites* (MF 6) in SBZs 6-7, *Nummulites-Alveolina* floatstones with *Orbitolites* (MF 7) in SBZs 7-8, and *Discocyclina-Assilina* floatstones with *Nummulites* (MF 8) in SBZs 9-10. Generally, the development of the microfacies assemblages can be summarized by a carbonate ramp model with an inner ramp depositing MFs 1, 2, 3, and 6, a mid-ramp with MFs 3, 4, 5, and 7, and an outer ramp with MF 8. Overall, microfacies analyses suggest that there was a deepening of depositional environments during the Paleocene and early Eocene at Tingri, which was interrupted by a sudden shallowing event at the Paleocene/Eocene (P/E) boundary. In addition to the Tingri area of Tibet, the shallowing event has also been reported from other shallow marine environments surrounding the Neo-Tethyan Ocean. Together with the opinion of a eustatic rise at the P/E boundary, the shallowing event may imply that there was a circum-Tethyan tectonic uplift once taking place close to the P/E boundary.

## 3.1 Introduction

During the last decade, special attention has been paid on the lower Paleogene larger foraminiferal limestones in the Neo-Tethyan realm, and some related studies include larger foraminiferal biostratigraphy and biogeography (Özcan et al. 2006; Less et al. 2007; Afzal et al. 2009, 2010; Drobne and Čosović 2009; Scheibner and Speijer 2009; Drobne et al. 2011), sedimentary facies and carbonate platform evolution (Čosović et al. 2004; Scheibner et al. 2007; Scheibner and Speijer 2008; Zamagni et al. 2008; Bagherpour and Vaziri 2011; Höntzsch et al. 2011), response of larger foraminifera to the Paleocene-Eocene Thermal Maximum (PETM) (Hottinger 1998; Scheibner et al. 2005; Zamagni 2009), and the P/E boundary in the Shallow Benthic Zones (SBZs) (Pujalte et al. 2009; Scheibner and Speijer 2009). The growing interest in studying the lower Paleogene larger foraminiferal limestones is partly due to the establishment of the SBZs in 1998 (Serra-Kiel et al. 1998), which makes it possible to study the evolution of

the Paleocene-Eocene carbonate platform with high time resolution. Furthermore, the PETM was a transient warming event with drastic paleoenvironmental perturbations, and has caused different biotic effects on land, in the shallow marine environments and deep seas (e.g., mammalian dispersal, larger foraminiferal extinction and origination, benthic foraminiferal extinction event) (Thomas and Shackleton 1996; Hottinger 1998; Bowen et al. 2002; Zhang et al. submitted). Consequently, to understand the response of the shallow benthic communities to the PETM will contribute to predicting changes of shallow marine ecosystem with anthropogenic global warming in the coming future. In addition, a distinct negative Carbon Isotope Excursion (CIE) associated with the PETM has been recognized globally (McInerney and Wing 2011, and references therein), from paleosol carbonates and mammalian tooth enamel on land (Koch et al. 1992) to sediments and foraminiferal shells in the ocean (Kelly et al. 1996; Bains et al. 1999). Owing to the synchronicity of the CIE in the ocean and on land, the onset of the CIE can represent a globally correlatable chronostratigraphic level, and thus has been adopted to define the P/E boundary (Aubry et al. 2007). According to this geochemical criterion, the P/E boundary occurs in the uppermost part of the Clarkforkian North American Land Mammal age on land (Bowen et al. 2001), the middle part of Zone NP 9 (calcareous nannofossils) and the lower part of Zone P 5 (planktonic foraminifera) in open marine settings (Berggren and Pearson 2005). However in the shallow marine environments, convincing evidence showing the precise location of the P/E boundary within the SBZs is still missing (Serra-Kiel et al. 1998). So, to spike the P/E boundary in the shallow marine environments is also a strong drive for biostratigraphers and paleontologists.

Most of above-mentioned studies on the larger foraminiferal limestones have been conducted in the western Neo-Tethyan realm, such as Spain, Slovenia, Turkey, Iran, and Egypt (Scheibner et al. 2007; Zamagni et al. 2008; Özcan et al. 2010; Bagherpour and Vaziri 2011; Höntzsch et al. 2011). In the east, especially the Tethyan Himalaya of south Tibet, high altitude and abominable climate assuredly impeded the scientific investigations. Therefore, only primary investigations have been conducted on the Paleocene-Eocene limestones in the past, which include systematic descriptions of larger foraminifera and microfacies analyses (He et al. 1976; Zhang 1988; Wan 1990, 1991; Willems 1993; Willems et al. 1996). Unfortunately, microfacies analyses carried out by Willems et al. (1993) were based on some incomplete sections, and the construction of larger foraminiferal biostratigraphy (Willems et al. 1996) was relatively rough compared with the SBZs in the west (Serra-Kiel et al. 1998). Therefore, further microfacies studies with high resolution biostratigraphy are necessary in order to improve our understanding of time-dependent changes of depositional environments at Tingri. Based mainly on a new, complete Paleocene-lower Eocene section (Section 09ZS), we have constructed a high resolution biostratigraphy at Tingri by following the

concept of the SBZs (Zhang et al. submitted). By integrating our new biostratigraphic work, here we will discuss the Paleocene and early Eocene development of microfacies and depositional environments in the Tingri area of Tibet.

### 3.2 Geologic setting

The Tethyan Himalaya lies between the Lhasa Terrane to the north and the High Himalaya to the south (Yin and Harrison 2000), and consists of upper Precambrian to lower Paleogene sedimentary and metasedimentary rocks. Before the initial India-Asia continental collision, the Tethyan Himalaya represents the north-facing Indian passive continental margin, deepening from a shallow shelf environment in the south (e.g., Tingri and Gamba areas) to a continental slope and oceanic basin in the north (e.g., Sangdanlin area) (Liu and Einsele 1994). The India-Asia continental collision at the P/E boundary initiated the development of an underfilled peripheral foreland basin in the Tethyan Himalaya (Rowley 1998; Zhang et al. 2012), causing a flexural subsidence (a foredeep) at the proximal part (e.g., Sangdanlin area) and a flexural uplift (a forebulge) at the distal part (e.g., Tingri and Gamba areas) (DeCelles and Giles 1996). Owing to progressively southward migration of the foreland basin, the distal part of the basin experienced a tectonically-driven subsidence history with firstly shallowing, then deepening, and eventually shallowing processes (DeCelles et al. 1998), and formed vertical superpositions of the so-called 'underfilled trinity' such as in the Alpine foreland basin, representing the sequential dominance by the depozones of the forebulge, the foredeep, and the wedge-top (Sinclair 1997). The lower Paleogene sedimentary strata in the Tethyan Himalaya have been used to perfectly demonstrate the complete geodynamic evolution of the northernmost Indian continent from a passive continental margin to an underfilled peripheral foreland basin (Garzanti et al. 1987; Zhang et al. 2012). After the initial continental collision, continuous convergence between the India and Asia continents caused crustal shortening and uplift of the Himalayan Orogen to the altitude of ~5000 m, which deformed and eroded most of the Paleogene sedimentary strata in the Tethyan Himalaya (Yin and Harrison 2000). As a result, the Paleocene-lower Eocene limestones in south Tibet are only sporadically preserved in the areas near Tingri, Gamba, and Guru (Fig. 1).

The studied Section 09ZS is located at the south flank of the Zhepure Shan Mountain near Tingri County. From the bottom to top, the Section 09ZS consists of the Jidula, Zhepure Shan, Youxia, and Shenkeza formations (Figs. 2 and 3). The lower Danian Jidula Formation is mainly composed of calcareous quartz sandstones, which was interpreted as a seaward prograding delta plain (Willems et al. 1996). Above the Jidula Formation, the Danian-Ilerdian larger foraminiferal limestones of the Zhepure Shan Formation are the focus of this study. Conformably overlying the Zhepure Shan

Formation, the Cuisian Youxia Formation consists of greenish-gray marls and shales intercalated with thin-bedded green-colored sandstone and limestone beds. Marls and shales are rich in planktonic foraminifera and calcareous nannofossils, and tabular sandstone beds having numerous flute casts have recorded the first Asian-derived detritus in the Tingri area (Zhu et al. 2005). Thus, the Youxia Formation was interpreted to have been deposited in an outer shelf environment and represent the arrival of a foredeep depozone to the Tingri area (Zhu et al. 2005). Upward, the Shenkeza Formation is composed of red mudstones and shales interbedded with lens-shaped sandstones, indicative of a continental fluvial channel and floodplain environment. A paleosol horizon at the basal Shenkeza Formation suggests an unconformable contact between the Youxia and Shenkeza formations, which marks the transition from the latest marine sediments to the first continental sediments in the Tethyan Himalaya, and implies changes of depozones from a foredeep to a wedge top in the Tingri area as the result of southward migration of the foreland basin (Zhang et al. 2012).

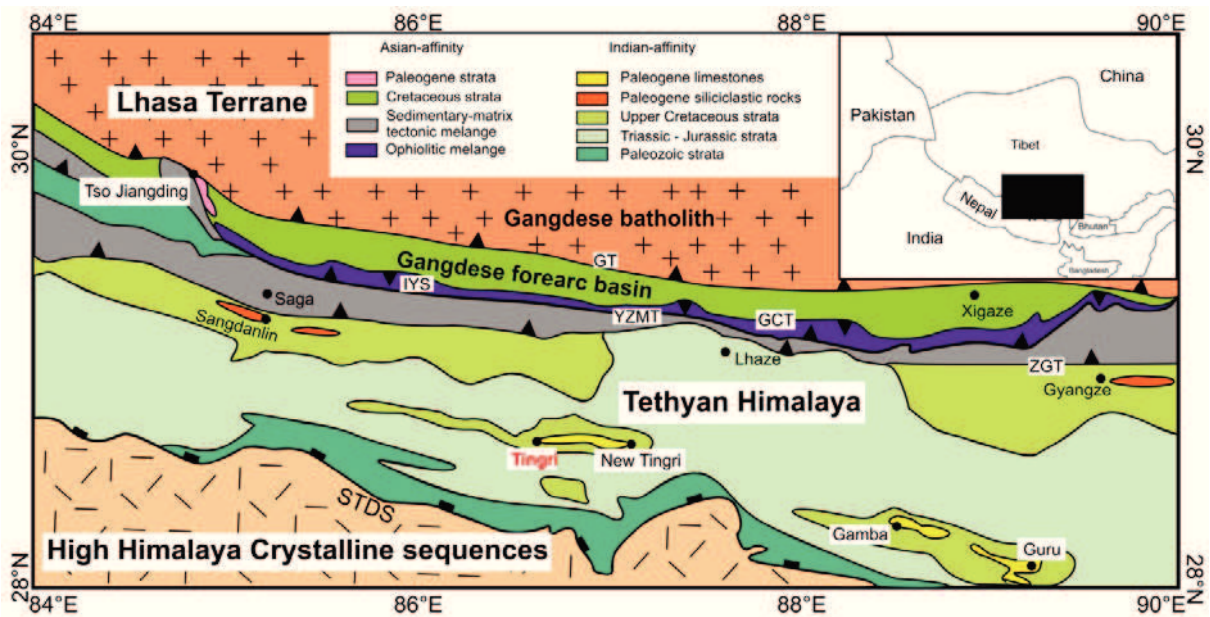


Fig. 1 Schematic geological map of the Tethyan Himalaya showing the study areas of Tingri and Gamba in Tibet, modified from Zhang et al. (2012). Abbreviations: STDS, South Tibet Detachment System; ZGT, Zhongba-Gyangze Thrust; YZMT, Yarlung Zangbo Mantle Thrust; IYS, Indus-Yarlung Zangbo Suture; GCT, Great Counter Thrust; GT, Gangdese





Fig. 2 Satellite image (from Google Earth) showing the locations of the Jidula, Zhepure Shan, Youxia, and Shenkeza formations in Section 09ZS near the Zhepure Shan Mountain.

### 3.3 Materials and methods

The Section 09ZS has been logged and described in 2009. About 450 limestone samples from the Zhepure Shan Formation have been collected for polishing thin sections. The samples are named after Arabic numbers consecutively from 1 to 321 and then from 408 to 500, and the absence of sample numbers between 322 and 407 is owing to our sampling strategy. In the laboratory, at least one thin section has been prepared from each sample, and most of the thin sections have relatively bigger sizes (9 cm × 6 cm or even larger) in order to fully investigate textural and compositional features of the samples. Textural classifications originally proposed by Dunham (1962) and later expanded by Embry and Klovan (1971) are adopted to describe the samples. Through transmitted-light microscopy, four categories (rare, few, common, abundant) have been used to evaluate relative abundance of carbonate grains in thin sections. Determination of microfacies types is mainly based on rock textures, fossil assemblages (mainly calcareous algae and larger benthic foraminifera), and other biogenic and abiogenic carbonate particles (Flügel 2004). Owing to the limited space of a figure suitable for publication purpose, only representative samples used for microfacies analysis are presented in Figs. 4-7. All samples and thin sections used for this study are placed in the Department of Geosciences, University of Bremen, Germany.

### 3.4 Litho- and bio- stratigraphy of the Zhepure Shan Formation

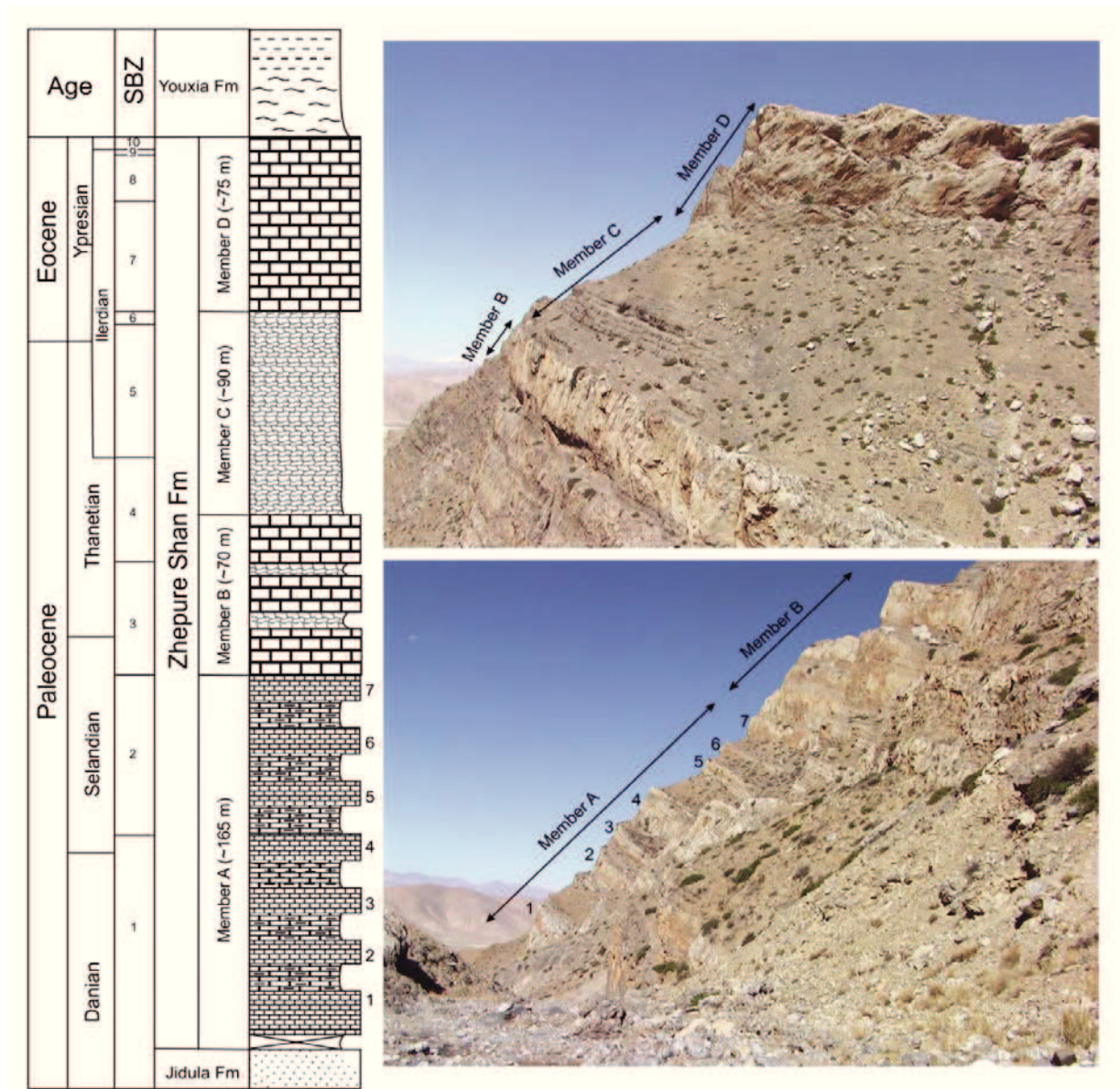


Fig. 3 Generalized lower Paleogene lithological column at Tingri with the biostratigraphy adopted from Zhang et al. (submitted). Photos are taken from the eastern side of the section. See Fig. 7 for explanations of the lithological symbols.

The carbonate sequence of the Zhepure Shan Formation in Section 09ZS is ~ 400 m thick, and consist of four lithologically distinct members, including cyclic limestones of Member A, massive limestones of Member B, nodular limestones of Member C, and massive limestones of Member D from the bottom to top (Fig. 3).

Member A is ~165 m thick with its base covered by weathered sedimentary debris, and therefore the contact between the underlying Jidula Formation and the overlying

Zhepure Shan Formation is unclear. The cyclic limestones comprise 7 cycles, and the thickness of each cycle is ~15-25 m except for the first cycle at the base having a thickness of >40 m. Each cycle is composed of lithologically soft marls and/or nodular limestones in the lower part and nodular limestones and/or medium to thickly bedded or massive limestones in the upper part. Compared with the limestones in the upper part, soft marls in the lower part are susceptible to physical erosion, which results in morphologically clear-cut concave surfaces in the lower part and forms visually striking cyclic limestones (Fig. 3). The lithological changes from marls, nodular limestones, to medium to thickly bedded or massive limestones in each cycle indicate that there is an upward decrease of clay contents and increase of carbonate contents. Member B is ~70 m thick and comprises mainly grey massive limestones with intercalations of medium to thickly bedded nodular limestones. Member C has a thickness of ~90 m, and consists of nodular limestones and a few thin and medium limestone beds. Vertically, several morphologically distinct sedimentary packages with the thicknesses of ~1-10 m can be recognized. The typical limestone assemblage in the package comprises matrix-supported nodular limestone at the bottom, nodular limestone with fitted fabric type in the middle, and nodular limestone with layering beds or thinly to medium bedded limestone at the top. The transition between different limestones is gradational. Member D is ~75 m thick and its majority is dominated by monotonous massive limestones. The top of Member D includes a ~4 m nodular limestone layer, which is overlain by ~6 m thinly bedded marly limestones. Continuing upwards, green marls and sandstones of the Youxia Formation rest conformably upon Member D.

The biostratigraphy of the Zhepure Shan Formation is mainly based on the determination of larger benthic foraminifera. Following the Opper Zone's principle and the concept of SBZ proposed by Serra-Kiel et al. (1998), totally 10 SBZs ranging from SBZ 1 to 10 have been divided. Member A represents the time interval of SBZs 1-2, and Member B belongs to SBZ 3 and the lower part of SBZ 4. Upwards, the upper part of SBZ 4, and SBZs 5-6 are all contained in Member C with the P/E boundary in the upper part of SBZ 5. In the end, Member D represents time interval from SBZ 7 to the lowermost of SBZ 10. (Fig. 3) (Zhang et al. submitted).

### **3.5 Microfacies description and interpretation**

#### **MF 1 Algal limestones with small benthic foraminifera**

##### **Description**

MF 1 occurs at the lower part of Member A with a thickness of ~105 m, including the first four cycles of the cyclic limestones. Biostratigraphically it belongs to SBZ 1 (Fig. 4). MF

1 consists of poorly sorted udoteacean algal (mainly *Halimeda* and *Ovulites*) floatstones and grainstones in the first cycle (Fig. 8A and B) and dasycladacean algal wackestones and grainstones with small benthic foraminifera in the overlying three cycles (Fig. 8C). In the first cycle, *Ovulites* and large skeletal grains of *Halimeda* (~2-12 mm long) with micrite envelopes are quite abundant, and echinoderms, gastropods, bivalves, and ostracods are some main subordinate organisms, which appear also frequently and sometimes have relatively high abundance. Selective dolomitization is a quite distinctive diagenetic phenomenon in this interval, occurring mainly in the matrix of floatstones and forms euhedral dolomite rhombohedrons. In the overlying three cycles, dasycladacean green algae (e.g., *Cymopolia*) and small benthic foraminifera with porcellaneous-walled miliolina, conical agglutinated textulariina, and hyaline-walled rotaliina start to take the place of *Halimeda* in spite of their low abundance. Both abundance and diversity of subordinate organisms decrease, and ostracods is the only one appearing continuously. Finely broken thalli of erect, articulated coralline red algae (e.g., *Jania*) with a few *Lockhartia* and *Kathina* occur at the upper boundary of MF 1. In the entire MF 1, occurrences of terrestrial quartz and peloids as well as fecal pellets are common, and coral exists but with very low abundance and frequency. In addition, geopetal fabrics can occasionally be recognized in some grainstones.

### **Interpretation**

MF 1 is interpreted to have been formed in a coastal, nutrient-rich, open, shallow lagoon with a nearby sand shoal. Udoteacean and dasycladacean green algae are mostly common in a normal saline, low-energy environment with water depths of a few meters and with sand or mud bottoms (Wray 1977; Flügel 2004), and the diversification of the Paleocene *Halimeda* was also thought to indicate a nutrient-rich, open lagoonal environment (Dragastan and Herbig, 2007). The co-existence of dominant floatstones/wackestones and subordinate grainstones points to a generally low but sometimes high energy environment, and implies alternating dominance of environment by the lagoon and the sand shoal. Frequent occurrences of detrital quartz imply that the lagoon was close to a shoreline and affected by terrestrial influx, causing the nutrient-rich condition in the lagoon.



## MF 2 Larger rotaliidae packstones with *Keramosphaerinopsis* and algae

### Description

MF 2 occurs in the upper part of Member A and the lower part of Member B, which biostratigraphically represents the time interval of SBZ 2 and 3 (Fig. 5). MF 2 is characterized by lamellar-perforate larger rotaliidae packstones with calcareous algae. Dominant components of the rotaliidae in MF 2 are composed of *Lockhartia*, *Kathina*, *Rotalia*, *Rotorbinella*, and *Daviesina* in SBZ 2 (Fig. 8D) and with an addition of porcellaneous *Keramosphaerinopsis* in SBZ 3 (Fig. 8E). Although smaller benthic foraminifera still occur frequently, MF 2 is gradually taken over by so-called 'K-strategist' larger foraminifera (Hottinger 1983). Generally, calcareous algae thriving in MF 1 are still relatively abundant in MF 2 except that the content of *Halimeda* shows an up-section decrease. Moreover, coralline red algae occur quite frequently by comparison with those in MF 1. The occurrences of echinoderms, gastropods, bivalves, and ostracods with high frequency and low abundance can be recognized, and corals in colony can be found occasionally. The input of terrestrial detrital quartz is still quite frequent, and peloids, ooids, and fecal pellets are some common non-skeletal carbonate grains.

### Interpretation

Larger foraminifera are referred to a certain group of benthic foraminifera usually having complex internal structures and larger size with  $> 3 \text{ mm}^3$  in volumes or  $> 1 \text{ mm}$  in diameter (Hallock and Glenn 1986). They prefer to shallow ( $< 120\text{-}140 \text{ m}$ ), warm, oligotrophic marine environment, and many, if not all, larger foraminifera harbor symbiotic algae in their chamber endoplasm. Different classes of symbiotic algae preferentially utilize different light quality (including intensity and wavelength) (Leutenegger 1984), and so depth distributions of larger foraminifera are mainly constrained by light throughout its impact on symbiotic algae. Consequently, larger symbiont-bearing foraminifera are regarded as a good indicator for bathymetric analyses (Hottinger 1997). During the early to middle Paleocene, the co-occurrence of *Lockhartia*, *Rotalia* and *Daviesina* was interpreted to indicate the shallower part of the upper photic zone with water depth of  $< 40 \text{ m}$  (Hottinger 1997). The existence of a large number of *Keramosphaerinopsis* also points to a relatively shallow, well-lit environment because the porcellaneous imperforate walls are composed of optically cryptocrystalline lathes, rods or needles of magnesium calcites arranged randomly in the outer wall layer, which functions as inhibition of strong light penetration and specially adapts for very shallow marine environment (Hottinger 2006). Although frequent occurrences of coralline red algae are indicative of a relatively agitated water body, the dominant limestone



texture of packstones and well preserved fossils in MF 2 show that there was still a low to moderate energy environment. The existence of detrital quartz probably reveals that the depositional environment is still affected by terrestrial input. Collectively, MF 2 is interpreted as the offshore part of an inner ramp with water depth of < 40 m.

### **MF 3 Rotaliidae-nummulitidae packstones with *Aberisphaera* and algae**

#### **Description**

MF 3 occurs in the upper part of Member B and the lower part of Member C, which biostratigraphically represents the time interval of SBZ 4 (Fig. 6). The main biota in MF 3 include *Lockhartia*, *Kathina*, *Rotalia*, *Rotorbinella*, *Daviesina*, *Aberisphaera*, *Setia*, *Ranikothalia*, *Operculina*, *Fallotella*, and *Orbitosiphon* (Fig. 8F and G). Occurrences of corallinacean red algae and udoteacean green algae are gradually decreasing up-section, and other subordinate organisms in MF 3 are quite similar to those in MF 2. With respect to non-skeletal grains, a decrease of detrital quartz content and increase of fecal pellets can be seen by comparison with those in MF 2.

#### **Interpretation**

The larger foraminiferal assemblage in MF 3 exhibits a mixture of some major foraminifera from MF 2 and MF 4. Common occurrences of fecal pellets imply that the environment has low water energy, normal oxygen concentration, and reduced sedimentation rate, which are favorable for normal activities of fecal pellet producers (Flügel 2004). By comparison with the depositional environments of MF 2 and MF 4, MF 3 represents a transitional setting between an inner ramp and a mid-ramp environment.

### **MF 4 Miscellaneidae-nummulitidae-rotaliidae floatstones with dasycladacean algae**

#### **Description**

MF 4 occurs in the upper part of Member C, and biostratigraphically represents the time interval of SBZ 5 (Fig. 6). MF 4 is characterized by larger miscellaneidae-nummulitidae-rotaliidae assemblages together with dasycladacean algae. Major larger foraminifera consist of *Lockhartia*, *Kathina*, *Rotalia*, *Rotorbinella*, *Setia*, *Ranikothalia*, *Operculina*, *Orbitosiphon*, and *Miscellanea* (Figs. 8H and 9C). Importantly, *Alveolina* and *Orbitolites*, two porcellaneous-walled larger foraminifera dominating mainly the Eocene Neo-Tethyan Ocean, have firstly appeared in MF 4. *Alveolina* are very low both in abundance and frequency, and fragmentary skeletons of *Orbitolites* mainly appear at the base of MF 4 (Fig. 8H). Both abundance and frequency of udoteacean green algae and corallinacean red algae decrease greatly, and dasycladacean algae are the only group



of calcareous algae which still thrived in the latest Paleocene. In spite of low frequency, corals (e.g. *Actinacis cognata?*) still existed in the larger foraminifera-dominated shallow marine environment.

### Interpretation

In the late Paleocene, the co-occurrence of *Lockhartia*, *Daviesina*, *Ranikothalia*, and *Miscellanea* is indicative of deeper part of the upper photic zone with water depth of ~40-80 m (Hottinger 1997). Although *Alveolina* and *Orbitolites* are generally thought to inhabit in a shallower water body (less than 40 m), most of them are quite fragmentary and mainly distributed in the lower part of MF 4 where the tempestites in MF 5 have formed. Therefore, it probably implies that *Alveolina* and *Orbitolites* in MF 4 have experienced syndepositional reworking and are transported from some neighboring shallower areas to the deeper-water places. So, MF 4 is interpreted as to indicate a relative deeper mid-ramp environment.

### MF 5 Alternating layers of densely packed grainstones and mudstones

#### Description

MF 5 occurs in the middle part of Member C, and is sandwiched within the lower part of MF 4 (Fig. 6). A few millimeter thick intercalations of light-colored bioclast-dominated grainstone beds and dark-colored lime mudstone beds with a distinct boundary are the major feature of MF 5, and sometimes isolated mudstone lithoclasts are scattered in the grainstone beds and form centimeter-sized irregular-shaped micrite clasts (Fig. 9A and B) or vice versa. Grainstones are composed of chaotic accumulations of carbonate grains with highly variable sizes, including non-skeletal grains of peloids and relatively well-preserved skeletal grains from ecologically mixed biota, such as corallinacean red algae, small miliolids, *Lockhartia*, *Daviesina*, *Miscellanea*, *Ranikothalia*, *Operculina*, *Orbitolites*, and other subordinate organisms. Mudstones are devoid of fossils.

#### Interpretation

MF 5 is interpreted to represent proximal tempestites deposited in a mid-ramp environment where storm wave might have affected the sedimentary environment. The alternating layers indicate rapidly changing hydrodynamic environments, and probably result from periodically storm-driven turbiditic redeposition of the shallower-water bioclasts into a low-energy, relatively deeper-water environment. The admixture of mud- or grainstone clasts may indicate an escape structure caused by benthic organisms as reaction to episodically turbiditic material input. In comparison with mud-dominated distal



tempestites, coarse-grained grainstones with bioclast-supported fabric in MF 5 exhibit distinct proximal features of storm beds (Flügel 2004).

### **MF 6 *Alveolina* packstones/floatstones with *Orbitolites***

#### **Description**

MF 6 ranges from the topmost 10 m of Member C to the lower 20 m of Member D, which biostratigraphically represents SBZ 6 and the lower part of SBZ 7 (Figs. 6 and 7). MF 6 is mainly dominated by the porcellaneous-walled, lenticular- and oval-shaped *Alveolina* admixed with subordinate flat, disc-shaped *Orbitolites* and small benthic foraminifera (Fig. 9D and E). By comparison with the Paleocene microfacies types, MF 6 contains almost no hyaline-walled larger foraminifera and calcareous algae. The distinct change of the larger foraminiferal assemblage from MF 4 (Fig. 9C) to MF 6 (Fig. 9D) was called 'Larger foraminiferal extinction and origination' (Zhang et al. submitted). Generally, in the lower part of MF 6, *Alveolina* are formed with relatively small sizes and fine regular coilings and without flosculinizations (the thickening of the basal wall in the equatorial region of the test). Their original morphology is distorted by diagenetic compaction and their internal structures are obscured by meteoric diagenesis. With respect to small benthic foraminifera, numerous tiny, biconvex-shaped, hyaline-walled rotaliids (e.g., *Lenticulina*) occur in great amount (Fig. 9D). Detrital quartz and fecal pellets occur frequently, however, other subordinate biota are very rare. In the upper part of MF 6, diagenetic overprints on *Alveolina* decrease largely, and cylindrical *Alveolina* with large sizes and flosculinizations start to appear in high abundance (Fig. 9E). Colonial corals can be seen, and the only one surviving Paleocene larger foraminifera, *Lockhartia*, starts to re-appear again, however, with small sizes, low abundance and highly reduced specific diversity.

#### **Interpretation**

Paleoecological studies on the Eocene *Alveolina* in the Neo-Tethyan realm have suggested that the existence of in situ *Alveolina* is indicative of a shallow inner ramp with water depth of less than 40 m, especially when it is associated with *Orbitolites* (Hallock and Glenn 1986; Hottinger 1997; Beavington-Penney and Racey 2004, and references therein). Besides, test shapes of larger foraminifera are thought to be a compromise between hydrodynamic factors and light, and therefore thick, lenticular or oval shapes of larger foraminiferal tests are interpreted to be formed for adapting strong light and turbulence in a shallower marine environment (Hallock and Glenn 1986). Thus, MF 6 at Tingri is interpreted to represent a well-lit, agitated, inner ramp setting.



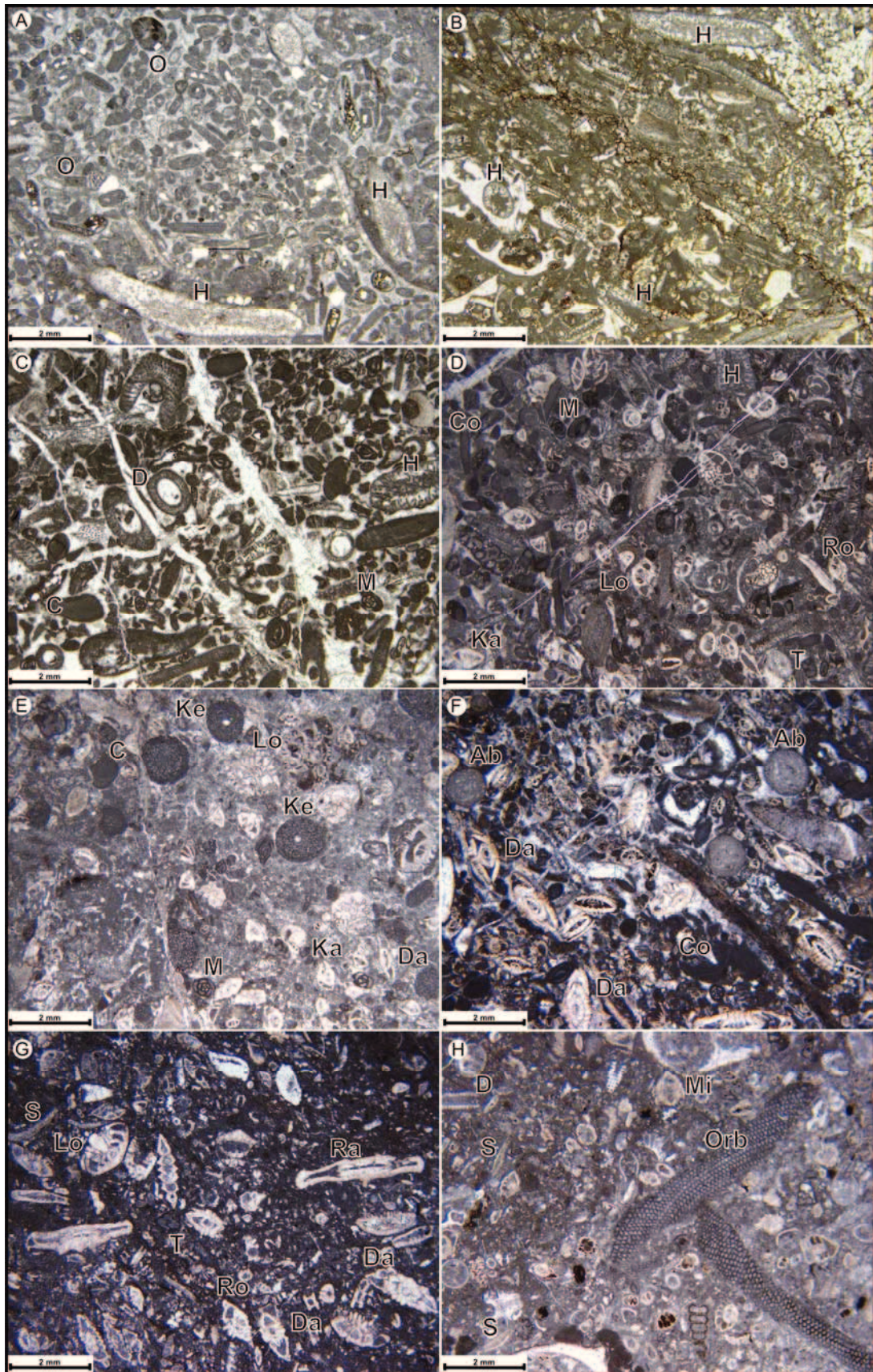


Fig. 8 Photomicrographs showing the representative microfacies and dominant fossil components during the Paleocene (SBZ 1-5) at Tingri. **a** Sandy *Halimeda*-*Ovulites* grainstone of MF 1, sample 09ZS48. **b** *Halimeda* floatstone of MF 1, sample 09ZS51. **c** Algal grainstone with small benthic foraminifera of MF 1, sample 09ZS110. **d** *Lockhartia*-*Kathina*-*Rotalia*/*Rotorbinella* packstone with algae of MF 2, sample 09ZS144. **e** *Lockhartia*-*Kathina*-*Daviesina*-*Keramosphaerinopsis* packstone of MF 2, sample 09ZS173. **f** *Daviesina*-*Aberisphaera* packstone of MF 3, sample 09ZS216. **g** *Daviesina*-*Lockhartia*-*Ranikothalia*-*Setia* packstone of MF 3, sample 09ZS228. **h** *Orbitolites*-*Miscellanea*-*Setia*-*Rotalia* floatstone of MF 4, sample 09ZS254. Abbreviations in Figs. 8 and 9: Ab, *Aberisphaera*; Al, *Alveolina*; As, *Assilina*; Co, Coral; C, Corallinacean algae; D, Dasycladacean algae; Da, *Daviesina*; Di, *Discocyclus*; H, *Halimeda*; Ka, *Kathina*; Ke, *Keramosphaerinopsis*; Lo, *Lockhartia*; Le, *Lenticulina*; M, Miliolina; Mi, *Miscellanea*; Nu, *Nummulites*; Orb, *Orbitolites*; Or, *Orbitosiphon*; O, *Ovulites*. Ra, *Ranikothalia*; Ro, *Rotalia*/*Rotorbinella*; S, *Setia*; T, *Textulariina*.

## MF 7 *Nummulites*-*Alveolina* floatstones with *Orbitolites*

### Description

MF 7 occurs in the main body of Member D, and represents the biostratigraphic range of the upper SBZ 7 and SBZ 8 (Fig. 7). Limestones in MF 7 show distinctly bimodal textures, with large foraminiferal tests (up to several centimeters) floating in a matrix of fine carbonate muds. The major biotic assemblage in MF 7 is composed of spherical, thick-walled *Nummulites* and *Alveolina* (Fig. 9F). In spite of frequent occurrences of fragmentary *Orbitolites*, their abundance in MF 7 is obviously less than those of *Nummulites* and *Alveolina*. The Eocene *Lockhartia* which re-appears in MF 6 still exists in MF 7, however, small rotaliids once thriving in MF 6 have lost their ubiquity. Dasycladacean and corallinacean algae appear again, and a few planktonic foraminifera can occasionally be seen at the top of MF 7.

### Interpretation

Studies on some extant symbiont-bearing larger foraminifera show that habitat of nummulitids hosting diatoms as symbiotic algae has the highest flexibility of depth distribution, because blue and green lights preferably utilized by diatoms have more variable penetration depth (between 0 and 130 m) than red, yellow, and green lights used by chlorophyceans and rhodophyceans as well as dinophyceans (Leutenegger 1984). Therefore, *Nummulites* usually have a wider ecological range, and may indicate a mid-ramp setting when associated with *Alveolina* and *Orbitolites* (Racey 1994) and an outer ramp environment when associated with *Assilina* and *Discocyclus* (Luterbacher 1998). Besides, the existence of a few planktonic foraminifera may be an indicator of a deeper environment. Collectively, the larger foraminiferal assemblage of *Nummulites* and *Alveolina* in MF 7 is thus interpreted to indicate a typical mid-ramp environment with water depth of ~40-80 m (Hottinger 1997).

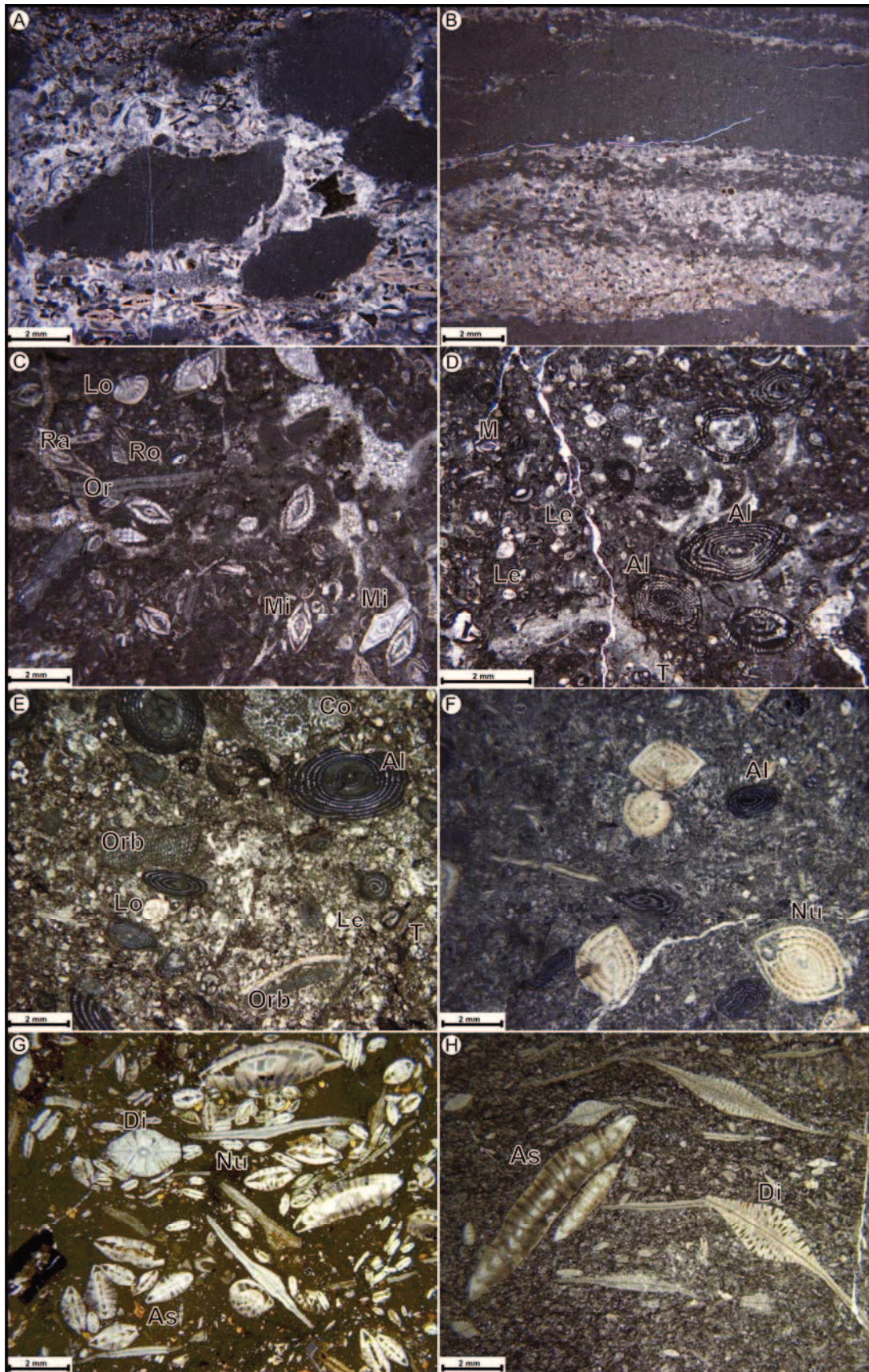


Fig. 9 Photomicrographs showing the representative microfacies and dominant fossil components during the latest Paleocene to early Eocene (SBZ 5-10) at Tingri. **a** Polymict limestone breccia of MF 5, sample 09ZS264. **b** Interlayering of fossil-rich grainstone and fossil-poor mudstone of MF 5, sample 09ZS265. **c** *Miscellanea-Orbitosiphon-Ranikothalia-Lockhartia* floatstone of MF 4, sample 09ZS304. **d** *Alveolina* packstone with small *Rotaliina* (such as *Lenticulina*) of MF 6, sample 09ZS307. **e** *Alveolina-Orbitolites* floatstone of MF 6, sample 09ZS419. **f** *Nummulites-Alveolina* floatstone of MF 7, sample 09ZS468. **g** *Assilina-Discocyclus* floatstone with thin-walled *Nummulites* (*Nummulites fossulata*) of MF 8, sample 09ZS493. **h** *Discocyclus-Assilina* floatstone of MF 8, sample 09ZS500.

### **MF 8 *Discocyclus-Assilina* floatstones with *Nummulites***

#### **Description**

MF 8 occurs at the topmost ~6-7 m of Member D, which biostratigraphically represents SBZ 9 and the base of SBZ 10 (Fig. 7). The floatstones in MF 8 is dominated by the predominant *Discocyclus* and *Assilina* with subordinate *Nummulites* (Fig. 9G and H). With ~1 m thickness of the base of MF 8, the co-existence of predominant *Nummulites* and subordinate *Alveolina*, *Assilina* and *Discocyclus* represents the transition between MF 7 and MF 8. Upwards, *Alveolina* and *Orbitolites* disappear completely, and *Nummulites* decreases dramatically in abundance. Large, thick-walled, spherical-shaped *Nummulites* with high specific diversity in MF 7 are substituted by the small-sized, thin-walled *Nummulites fossulata* (Fig. 9G). Moreover, very fine detrital quartz with good sorting and high abundance are evenly distributed in the matrix of the floatstones.

#### **Interpretation**

The Eocene elongate *Discocyclus* and *Assilina* with thin-walled *Nummulites* was interpreted to live in the lower photic zone with water depth of ~80-120 m (Hottinger 1997), indicating an outer ramp environment (Gilham and Bristow 1998; Luterbacher 1998; Racey 1994). The thinning of chamber walls in lamellar-perforate foraminifera was thought to be caused by a slow-down of the biomineralisation process, which in turn resulted from an increase of dissolved CO<sub>2</sub> in the water due to the decreasing rates of turbulence with the deepening of depositional environments (Hottinger 1997). Thus, MF 8 represents an outer ramp environment with the water depth of ~80-120 m.

### **3.6 An early Paleogene carbonate ramp at Tingri**

A carbonate ramp usually refers to a carbonate depositional system, which is attached to a shoreline at one end and extends to a basin at the other end through a very low-gradient slope (< 1°) (Burchette and Wright 1992). It differs from a carbonate platform in having no distinct slope break (Flügel 2004). As the contemporary sedimentary strata depositing between the shallow marine environments (such as Tingri and Gamba) and deep ocean (such as Sangdanlin and Gyangze) are completely eroded by the India-Asia collision and the subsequent uplift of the Himalayan Orogen, the evidence indicating



whether there was a distinct slope break or not in the Tethyan Himalaya is therefore not existent. However, carbonate ramps are generally thought to be common in times when frame- and reef-building organisms were rare (Flügel, 2004), and many studies have adopted carbonate ramp models to interpret the Paleogene larger foraminifera-dominated carbonate buildups in the Neo-Tethyan realm (Beavington-Penney and Racey, 2004 and references therein; Čosović et al. 2004; Zamagni et al. 2008; Afzal et al. 2011; Bagherpour and Vaziri, 2011; Höntzsch et al. 2011). Consequently, we tentatively use the standard carbonate ramp model with subdivisions of an inner ramp, mid-ramp and outer ramp (Burchette and Wright 1992) to describe the depositional environments of the Zhepure Shan Formation at Tingri (Fig. 10).

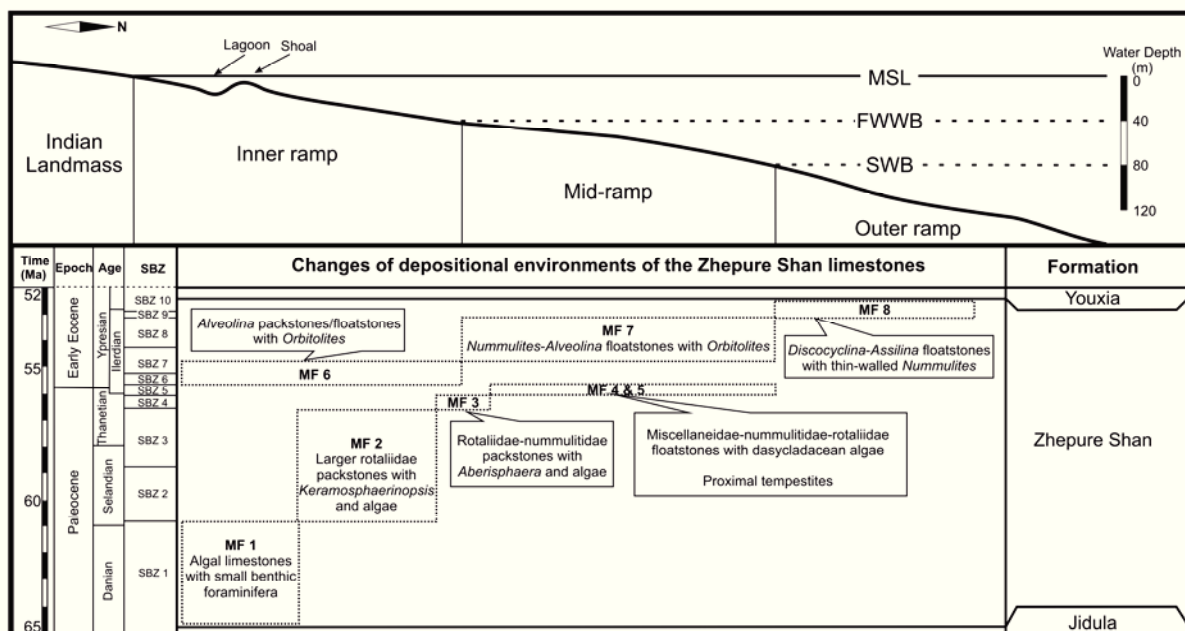


Fig. 10 A schematic carbonate ramp model showing changes of depositional environments of the Zhepure Shan Formation from the Paleocene to early Eocene. MSL: Mean sea level; FWWB: Fair-weather wave base; SWB: Storm wave base.

In the earliest Danian, deposition of the Jidula sandstones containing the *Skolithos* ichnofacies at Tingri were thought to represent the formation of a seaward prograding delta plain (Willems et al. 1996). Afterwards, calcareous algal limestones with small benthic foraminifera in MF 1 are indicative of the nutrient-rich, open-marine, shallow lagoon and sand shoal in an inner ramp with water depth of a few meters. The lagoon was closely attached to the Indian landmass to the south and frequently affected by the influx of terrestrial quartz from the hinterland. During the Selandian and early Thanetian, some larger foraminifera (mainly rotaliidae) including *Lockhartia*, *Rotalia/Rotorbinella*, *Kathina*, *Daviesina*, and *Keramosphaerinopsis* appeared gradually and finally dominated MF 2. Those larger foraminifera probably inhabited the lower part of the inner ramp with

water depth less than 40 m, and represented the earliest recovery of the Paleocene larger foraminifera after the K/T mass extinction in the Neo-Tethyan Ocean. At Tingri, MF 3 is characterized by a mixture of dominant larger benthic foraminifera of rotaliidae from MF 2 and nummulitidae from MF 4, and thus indicates a transitional environment between them. In the latest Paleocene, highly diversified larger benthic foraminifera of miscellaneidae and nummulitidae as well as rotaliidae in MF 4 together with interlayered tempestites (MF 5) suggest a mid-ramp environment with water depth of ~40-80 m.

During the early Eocene, the Zhepure Shan limestones were dominated successively by three larger foraminiferal assemblages, which are the *Alveolina-Orbitolites* assemblage, the *Nummulites-Alveolina-Orbitolites* assemblage, and the *Discocyclina-Assilina-Nummulites* assemblage. Many former studies on the early Eocene larger foraminifera in the western Neo-Tethyan Ocean (Beavington-Penney and Racey, 2004 and references therein) agreed that those three larger foraminiferal assemblages usually inhabited the inner ramp, mid-ramp, and outer ramp, respectively, and indicated a steadily deepening trend of depositional environments from less than 40 m to ~120 m (Hottinger 1997). In the end, the carbonate ramp at Tingri was drown at the very beginning of the Cuisian owing to the continually deepening of depositional environments triggered by the India-Asia collision (Zhang et al. 2012), and the Zhepure Shan limestones were eventually covered by the green sandstones and mudstones/marls of the Youxia Formation from an outer shelf environment (Zhu et al. 2005).

### **3.7 Circum-Tethyan tectonic uplift at the P/E boundary**

Microfacies analyses from Section 09ZS at Tingri show that gradually deepening processes of depositional environments occurred both in the Paleocene and early Eocene, which, however, had been interrupted by an abrupt and short-termed shallowing event close to the P/E boundary. The shallowing event is revealed by the sudden change of larger foraminiferal assemblages from the relatively deeper-water dwellers of *Miscellanea-Ranikothalia-Operculina-Lockhartia-Kathina-Daviesina* in MF 4 to the shallower-water dwellers of *Alveolina-Orbitolites* in MF 6. The changes of larger foraminiferal assemblages have been referred as 'Larger Foraminiferal Extinction and Origination' (Zhang et al. submitted), and are to be found in many low paleolatitudinal areas of the Neo-Tethyan Ocean (~0°-30°N), including the Tethyan Himalaya of Tibet, the lower Indus basin of Pakistan (Afzal et al. 2010), the Oman Mountains of northern Oman (Haynes et al. 2010), the southern Galala Mountains area of Egypt (Scheibner et al. 2005), the Zagros basin of Iran (Bagherpour and Vaziri, 2011), and the Kastamonu region of Northern Turkey (Özgen-Erdem et al. 2005). In the middle paleolatitudinal areas (>~30°N), the shallowing of depositional environments has also been reported in the northwestern Adriatic carbonate platform of Slovenia and the Pyrenean platform of

Spain. In Slovenia, the upper Paleocene Trstelj Formation is composed of *Assilina*, *Discocyclus*, and Lacazinids admixed with red algae, and indicates a mid-ramp environment. Upwards it is superimposed by the lower Eocene *Alveolina-Nummulites* Limestone formed on an inner ramp (Zamagni et al. 2008). In Spain, the shallowing event is expressed through a more explicit way by the deposition of continental beds between the uppermost Paleocene and the lowermost Eocene shallow marine carbonates in the Campo and Tremp sections (Scheibner et al. 2007; Pujalte et al. 2009). Collectively, we tentatively assume that there was a circum-Tethyan shallowing event during the latest Paleocene to earliest Eocene (Fig. 11).

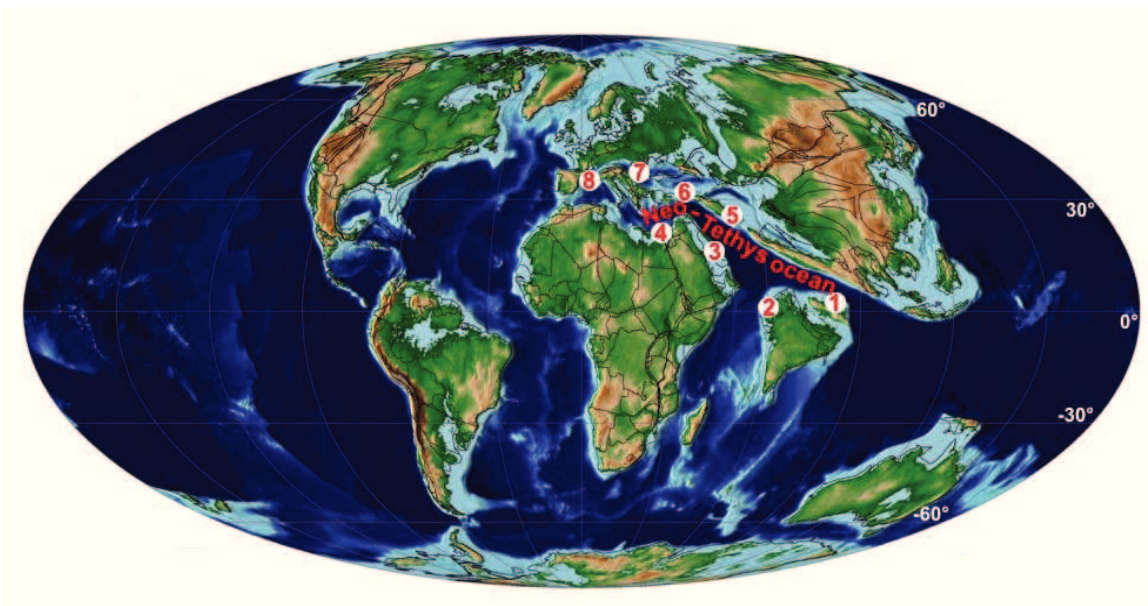


Fig. 11 The global paleogeographic map at the P/E boundary (Scotese 2011) with numbers showing the locations of some major shallow marine carbonate depositions on the periphery of the Neo-Tethyan Ocean. 1: Tibet; 2: Pakistan; 3: Oman; 4: Egypt; 5: Iran; 6: Turkey; 7: Slovenia; 8: Spain.

In Tibet, the shallowing event and associated changes of larger foraminiferal assemblages coincide with the well-known negative CIE during the PETM (Zhang et al. submitted). And in Egypt, time equivalence between changes of larger foraminiferal assemblages and the CIE has once been taken as the main evidence arguing for the assumption that drastically climatic changes of the PETM led to the larger foraminiferal turnover (Scheibner et al. 2005). Moreover, studies on the P/E boundary in Spain showed that the CIE was recorded in the continental beds overlying the uppermost Paleocene shallow marine sediments, revealing the synchronicity of the shallowing event and the PETM-CIE. So, we conclude that the circum-Tethyan shallowing event occurred close to the P/E boundary.

At the P/E boundary, a eustatic rise has been recognized by studying dinoflagellate cysts, grain size fractions, and organic biomarkers in some widely separated sections from the Arctic Ocean, New Jersey shelf, western United States, North Sea, Russia, the southern Tethyan margin, and New Zealand (Sluijs et al. 2008). Because the duration of the PETM-CIE (~100-200 kyr) was relatively short over the geologic time scale (Röhl et al. 2007; Murphy et al. 2010), and both the circum-Tethyan shallowing event and the eustatic rise coincided with the PETM-CIE. Thus, we may speculate that there is time equivalence between the shallowing event and the eustatic rise. Consequently, the shallowing event in the context of a global transgression suggests that a circum-Tethyan tectonic uplift probably occurred at the P/E boundary and caused the widespread shallowing events surrounding the Neo-Tethyan Ocean.

### 3.8 Conclusions

Totally, eight microfacies types have been recognized in the Zhepure Shan Formation at Tingri. Among them, five facies in the Paleocene consist of algal limestones with small benthic foraminifera, larger rotaliidae packstones with algae, rotaliidae-nummulitidae packstones with algae, and miscellaneidae-nummulitidae-rotaliidae floatstones with dasycladacean algae, and proximal tempestites. Three facies in the early Eocene include *Alveolina* packstones and floatstones with *Orbitolites*, *Nummulites-Alveolina* floatstones with *Orbitolites*, and *Discocyclina-Assilina* floatstones with *Nummulites*.

A carbonate ramp model is adopted to summarize the development of microfacies and depositional environments, and a general deepening of depositional environments has been revealed by changes from an inner ramp to a mid-ramp in the Paleocene, and from an inner ramp, through a mid-ramp, to an outer ramp in the early Eocene. Notably, a shallowing event taking place close to the P/E boundary had interrupted the deepening processes. Contemporary shallowing events have also been reported from other areas surrounding the Neo-Tethyan Ocean. Combined with the opinion of a eustatic rise at the P/E boundary, the shallowing event has been tentatively assumed to represent a circum-Tethyan tectonic uplift occurring at the P/E boundary.

### Acknowledgements

Di Yang, Shuaiquan Fan, Anne Hübner, and Christiane Schott are thanked for their assistance in the field and the laboratory. The project is part of the Priority Programme 1372 Tibetan Plateau: Formation, Climate, Ecosystems (*TiP*) and is funded by Deutsche Forschungsgemeinschaft (No. Wi725/26), Chinese Ministry of Science and Technology (2011CB403101 to Ding Lin), and Chinese Academy of Sciences (KZCX2-YW-Q09-03 to Ding Lin).

## References

- Afzal J, Willems M, Aldridge R (2009) Revised stratigraphy of the lower Cenozoic succession of the Greater Indus Basin in Pakistan. *J Micropalaeontol* 28:7-23
- Afzal J, Williams M, Leng MJ, Aldridge RJ, Stephenson MH (2010) Evolution of Paleocene to Early Eocene larger benthic foraminifer assemblages of the Indus Basin, Pakistan. *Lethaia*. doi:10.1111/j.1502-3931.2010.00247.x
- Afzal J, Williams M, Leng MJ, Aldridge RJ (2011) Dynamic response of the shallow marine benthic ecosystem to regional and pan-Tethyan environmental change at the Paleocene-Eocene boundary. *Palaeogeogr Palaeoclimat Palaeoecol* 309:141-160
- Aubry MP, Ouda K, Dupuis C, Berggren WA, Van Couvering JA, Ali J, Brinkhuis H, Gingerich PD, Heilmann-Clausen C, Hooker J, Kent DV, King C, Knox RWOB, Laga P, Molina E, Schmitz B, Steurbaut E, Ward DR (2007) The Global Standard Stratotype-section and Point (GSSP) for the base of the Eocene Series in the Dababiya section (Egypt). *Episodes* 30 (4):271-286
- Bagherpour B, Vaziri MR (2011) Facies, paleoenvironment, carbonate platform and facies changes across Paleocene Eocene of the Taleh Zang Formation in the Zagros basin, SW-Iran. *Hist Biol*. doi:10.1080/08912963.2011.587185
- Bains S, Corfield RM, Norris RD (1999) Mechanisms of climate warming at the end of the Paleocene. *Science* 285:724-727
- Beavington-Penney SJ, Racey A (2004) Ecology of extant nummulitids and other larger benthic foraminifera: applications in palaeoenvironmental analysis. *Earth Sci Rev* 67:219-265
- Berggren WA, Pearson PN (2005) A revised tropical to subtropical paleogene planktonic foraminiferal zonation. *J Foramin Res* 35 (4):279-298
- Bowen GJ, Koch PL, Gingerich PD, Norris RD, Bains S, Corfield RM (2001) Refined isotope stratigraphy across the continental Paleocene-Eocene boundary on Polecat Bench in the northern Bighorn basin. In: Gingerich PD (ed) *Paleocene-Eocene stratigraphy and biotic change in the Bighorn and Clarks Fork basins, Wyoming*. University of Michigan papers on Paleontology 33, pp 73-88
- Bowen GJ, Clyde WC, Koch PL, Ting S, Alroy J, Tsubamoto T, Wang Y (2002) Mammalian dispersal at the Paleocene/Eocene boundary. *Nature* 295:2062-2065

- Burchette TP, Wright VP (1992) Carbonate ramp depositional systems. *Sediment Geol* 79:3-57
- Ćosović V, Drobne K, Moro A (2004) Paleoenvironmental model for Eocene foraminiferal limestones of the Adriatic carbonate platform (Istrian Peninsula). *Facies* 50:61-75
- DeCelles PG, Giles KA (1996) Foreland basin systems. *Basin Res* 8:105-123
- DeCelles PG, Gehrels GE, Quade J, Ojha TP (1998) Eocene-early Miocene foreland basin development and the history of Himalayan thrusting, western and central Nepal. *Tectonics* 17 (5):741-765
- Dragastan ON, Herbig H-G (2007) *Halimeda* (green siphonous algae) from the Paleogene of (Morocco) -Taxonomy, phylogeny and paleoenvironment. *Micropaleontology* 53:1-72
- Drobne K, Ćosović V (2009) Palaeobiogeography of the Late Cretaceous to Paleogene larger Miliolids from tropical to subtropical sea belts (Neotethys to Caribbean). *Bull Soc Géol Fr* 180 (4):317-331
- Drobne K, Ćosović V, Moro A, Bucković D (2011) The role of the Palaeogene Adriatic carbonate platform in the spatial distribution of Alveolinids. *Turk J Earth Sci* 20:721-751
- Dunham RJ (1962) Classification of carbonate rocks according to depositional texture. In: Ham WE (ed) *Classification of carbonate rocks*. Am Assoc Petrol Geol Mem 1:108-121
- Embry AF, Klovan JE (1971) A late Devonian reef tract on northeastern Banks Island, northwestern Territories. *Bull Can Petrol Geol* 19: 730-781
- Flügel (2004) *Microfacies of carbonate rocks: analysis, interpretation, and application*. Springer, Heidelberg Dordrecht London New York
- Garzanti E, Baud A, Mascle G (1987) Sedimentary record of the northward flight of India and its collision with Eurasia (Ladakh Himalaya, India). *Geodin Acta* 1:297-312
- Gilham RF, Bristow CS (1998) Facies architecture and geometry of a prograding carbonate ramp during the early stages of foreland basin evolution: Lower Eocene sequences, Sierra del Cadí, SE Pyrenees, Spain. In: Wright VP, Burchette TP (eds) *Carbonate ramps*. Geol Soc London Spec Pub 149, pp181-203

- Hallock P, Glenn EC (1986) Larger foraminifera: A tool for paleoenvironmental analysis of Cenozoic carbonate depositional facies. *Palaios* 1 (1):55-64
- Haynes JR, Racey A, Whittaker JE (2010) A revision of the Early Palaeogene nummulitids (Foraminifera) from northern Oman, with implications for their classification. In: Whittaker JE, Hart MB (eds) *Micropalaeontology, Sedimentary Environments and Stratigraphy: A Tribute to Dennis Curry (1912-2001)*. *Micropalaeontol Soc Spec Pub*, pp 29-89
- He Y, Zhang B, Hu L, Sheng J (1976) Mesozoic and Cenozoic foraminifera from the Mount Julmo Lungma region. In: Scientific team of Tibet investigation from Chinese Academy of Sciences (ed) *A report of scientific expedition in the Mount Julmo Lungma Region (1966-1968)*, *Palaeontology*. Science press, Beijing, pp 1-124
- Höntzsch S, Scheibner C, Kuss J, Marzouk A, Rasser M (2011) Tectonically driven carbonate ramp evolution at the southern Tethyan shelf: the lower Eocene succession of the Galala Mountains, Egypt. *Facies* 57:51-72
- Hottinger L (1983) Processes determining the distribution of larger foraminifera in space and time. *Utrecht Micropaleont Bull* 30:239-253
- Hottinger L (1997) Shallow benthic foraminiferal assemblages as signals for depth of their deposition and their limitations. *Bull Soc Géol Fr* 168 (4):491-505
- Hottinger L (1998) Shallow benthic foraminifera at the Paleocene-Eocene boundary. *Strata* 9:61-64
- Hottinger L (2006) Illustrated glossary of terms used in foraminiferal research. *Carnets de Géologie* 2:1-126
- Kelly DC, Bralower TJ, Zachos JC, Premoli-Silva I, Thomas E (1996) Rapid diversification of planktonic foraminifera in the tropical Pacific (ODP Site 865) during the late Paleocene thermal maximum. *Geology* 24 (5):423-426
- Koch PL, Zachos JC, Gingerich PD (1992) Correlation between isotope records in marine and continental carbon reservoirs near the Palaeocene/Eocene boundary. *Nature* 358:319-322
- Less G, Özcan E, Báldi-Beke M, Kollányi K (2007) Thanetian and early Ypresian orthophragmines (Foraminifera: Discocyclinidae and Orbitoclypeidae) from the

- central western Tethys (Turkey, Italy and Bulgaria) and their revised taxonomy and biostratigraphy. *Riv Ital Paleontol S* 113 (3):419-448
- Leutenegger S (1984) Symbiosis in benthic foraminifera; specificity and host adaptations. *J Foramin Res* 14 (1):16-35.
- Liu G, Einsele G (1994) Sedimentary history of the Tethyan basin in the Tibetan Himalayas. *Geol Rundsch* 83:32-61
- Luterbacher H (1998) Sequence stratigraphy and the limitations of biostratigraphy in the marine Paleogene strata of the Tremp Basin (central part of the southern Pyrenean foreland basins, Spain). In: De Graciansky PC, Hardenbol J, Jacquin T, Vail PR (eds) *Mesozoic and Cenozoic sequence stratigraphy of European basins*. Soc Sediment Geol Spec Pub 60, pp 303-309
- McInerney FA, Wing SL (2011) The Paleocene-Eocene Thermal Maximum: A perturbation of carbon cycle, climate, and biosphere with implications for the future. *Annu Rev Earth Planet Sci* 39:489-516
- Murphy BH, Farley KA, Zachos JC (2010) An extraterrestrial  $^3\text{He}$ -based timescale for the Paleocene-Eocene thermal maximum (PETM) from Walvis Ridge, IODP Site 1266. *Geochim Cosmochim Acta* 74:5098-5108
- Özcan E, Less G, Baldi-Beke M, Kollányi K, Kertész B (2006) Biometric analysis of middle and upper Eocene Discocyclinidae and Orbitoclypeidae (Foraminifera) from Turkey and updated orthophragmine zonation in the Western Tethys. *Micropaleontology* 52 (6):485-520
- Özcan E, Less G, Okay AI, Baldi-Beke M, Kollányi K, Yılmaz İÖ (2010) Stratigraphy and larger foraminifera of the Eocene shallow-marine and olistostromal units of the southern part of the Thrace Basin, NW Turkey. *Turk J Earth Sci* 19:27-77
- Özgen-Erdem N, İnan N, Akyazi M, Tunoğlu C (2005) Benthonic foraminiferal assemblages and microfacies analysis of Paleocene–Eocene carbonate rocks in the Kastamonu region, Northern Turkey. *J Asian Earth Sci* 25:403-417
- Pujalte V, Baceta JI, Schmitz B, Orue-Etxebarria X, Payros A, Bernaola G, Apellaniz E, Caballero F, Robador A, Serra-Kiel J, Tosquella J (2009) Redefinition of the Ilerdian Stage (early Eocene). *Geol Acta* 7:177-194
- Racey A (1994) Biostratigraphy and palaeobiogeographic significance of Tertiary nummulitids (foraminifera) from northern Oman. In: Simmons MD (ed)



- Micropalaeontology and hydrocarbon exploration in the Middle East. Chapman & Hall, pp 343-370
- Röhl U, Westerhold T, Bralower TJ, Zachos JC (2007) On the duration of the Paleocene-Eocene thermal maximum (PETM). *Geochem Geophys Geosyst* 8. doi:10.1029/2007gc001784
- Rowley DB (1998) Minimum age of initiation of collision between India and Asia north of Everest based on the subsidence history of the Zhepure Mountain section. *J Geol* 106:229-235
- Scheibner C, Speijer RP, Marzouk AM (2005) Turnover of larger foraminifera during the Paleocene-Eocene Thermal Maximum and paleoclimatic control on the evolution of platform ecosystems. *Geology* 33 (6):493-496
- Scheibner C, Rasser MW, Mutti M (2007) The Campo section (Pyrenees, Spain) revisited: Implications for changing benthic carbonate assemblages across the Paleocene-Eocene boundary. *Palaeogeogra Palaeoclimat Palaeoecol* 248:145-168
- Scheibner C, Speijer RP (2008) Late Paleocene-early Eocene Tethyan carbonate platform evolution - A response to long- and short-term paleoclimatic change. *Earth Sci Rev* 90:71-102
- Scheibner C, Speijer RP (2009) Recalibration of the Tethyan shallow-benthic zonation across the Paleocene-Eocene boundary. *Geol Acta* 7:195-214
- Scotese, CR (2011) The PALEOMAP Project PaleoAtlas for ArcGIS, Vol. 1; Cenozoic paleogeographic and plate tectonic reconstructions, Arlington, Texas
- Serra-Kiel J, Hottinger L, Caus E, Drobne K, Ferrandez C, Jauhri AK, Less G, Pavlovec R, Pignatti J, Samsó JM (1998) Larger foraminiferal biostratigraphy of the Tethyan Paleocene and Eocene. *Bull Soc Géol Fr* 169 (2):281-299
- Sinclair HD (1997) Tectonostratigraphic model for underfilled peripheral foreland basins: An Alpine perspective. *Bull Geol Soc Am* 109 (3):324-346
- Sluijs A, Brinkhuis H, Crouch EM, John CM, Handley L, Munsterman D, Bohaty SM, Zachos JC, Reichert G, Schouten S, Pancost RD, Sinninghe Damste JS, Welters NLD, Lotter AF, Dickens GR (2008) Eustatic variations during the Paleocene-Eocene greenhouse world. *Paleoceanography* (23). doi:10.1029/2008PA001615

- Thomas E, Shackleton NJ (1996) The Paleocene-Eocene benthic foraminiferal extinction and stable isotope anomalies. In: Knox RWOB, Corfield RM, Dunay RE (eds) Correlation of the Early Paleogene in Northwest Europe. Geol Soc London Spec Pub, pp 401-441
- Wan X (1990) Eocene larger foraminifera from southern Tibet. *Rev Esp Micropaleontol* 22 (1):213-238
- Wan X (1991) Palaeocene larger foraminifera from southern Tibet. *Rev Esp Micropaleontol* 23 (2):7-28
- Willems H (1993) Geoscientific investigations in the Tethyan. Universität Bremen, Bremen
- Willems H (1996) Stratigraphy of the upper Cretaceous and lower Tertiary strata in the Tethyan Himalayas of Tibet (Tingri area, China). *Geol Rundsch* 85:723-754
- Wray JL (1977) Calcareous algae. Elsevier Scientific publishing company, Amsterdam, Oxford, New York
- Yin A, Harrison TM (2000) Geologic evolution of the Himalayan-Tibetan Orogen. *Annu Rev Earth Planet Sci* 28:211-280
- Zamagni J, Mutti M, Košir A (2008) Evolution of shallow benthic communities during the Late Paleocene–earliest Eocene transition in the Northern Tethys (SW Slovenia). *Facies* 54 :25-43
- Zamagni J (2009) Response of a shallow-water ecosystem to the early Paleogene greenhouse environmental conditions. Dissertation, University of Potsdam
- Zhang B (1988) Orbitolites (foraminifera) from Longjiang of Tingri, Xizang. *Acta Micropalaeontol Sin* 5:1-13
- Zhang Q, Willems H, Ding L, Gräfe K-U, Appel E (2012) The initial India-Asia continental collision and foreland basin evolution in the Tethyan Himalaya of Tibet: Evidence from stratigraphy and paleontology. *J Geol* 120:175-189
- Zhang Q, Willems H, Ding L (2012) Evolution of the Paleocene-early Eocene larger benthic foraminifera in the Tethyan Himalaya of Tibet, China. *Submitted to Int J Earth Sci*
- Zhu B, Kidd WSF, Rowley DB, Currie BS, Shafique N (2005) Age of initiation of the India-Asia collision in the east-central Himalaya. *J Geol* 113:265-285

Third manuscript

## **4. The initial India-Asia continental collision and foreland basin evolution in the Tethyan Himalaya of Tibet: Evidence from stratigraphy and paleontology**

**Qinghai Zhang<sup>1,2</sup>, Helmut Willems<sup>1,3</sup>, Lin Ding<sup>2</sup>, Kai-Uwe Gräfe<sup>1</sup>, Erwin Appel<sup>4</sup>**

<sup>1</sup> University of Bremen, Department of Geosciences, D-28359 Bremen, Germany

<sup>2</sup> Key Laboratory of Continental Collision and Plateau Uplift, Institute of Tibetan Plateau Research, Chinese Academy of Sciences, 100085 Beijing, China

<sup>3</sup> Nanjing Institute of Geology and Palaeontology, Chinese Academy of Sciences, 210008 Nanjing, China

<sup>4</sup> University of Tübingen, Institute for Applied Geosciences, 72076 Tübingen, Germany

Published in *The Journal of Geology* (2012) Volume 120, pp. 175-189, doi:  
10.1086/663876

Received May 31, 2011; accepted September 15, 2011

## Abstract

The onset of continent-continent collision is accompanied by elimination of oceanic crust and development of a peripheral foreland basin on the subducting continental crust. However, owing to the progressively southward migration of the foreland basin, the appearance of flexural uplift (forebulge) will predate that of flexural subsidence (foredeep) at the distal location (such as Gamba and Tingri). Consequently, to trace and date the forebulge may provide a better constraint on the India-Asia collision. At Gamba and Tingri, our studies on the stratigraphy, paleontology, and paleoenvironment show that depositional cessation of the limestones occurred at Shallow Benthic Zone 7 (SBZ 7, ~54-55 Ma) in the Gamba area and at the base of SBZ 10 (~52.8 Ma) in the Tingri area. At Gamba, a conglomerate layer within the upper Zongpu Formation is proposed to represent formation of the forebulge at the onset of the foreland basin, and coincidence of the conglomerate layer with the Carbon Isotope Excursion (CIE) provides a precise age of ~56 Ma (the Paleocene/Eocene boundary) for the possible initial India-Asia continental collision. Our results not only provide a reliable and precise age for the India-Asia collision but, for the first time, report time equivalence between the India-Asia collision and the CIE in Tibet.

## 4.1 Introduction

After more than 30 years of intense international geoscientific attention, the questions of when and where the initial India-Asia continental collision occurred as well as the size of 'Greater India' before the initial collision are still in dispute. Proposed ages for the onset of this collision range from ~65 Ma (Ding et al. 2005; Cai et al. 2011) or even earlier (Willems et al. 1996), to ~55-50 Ma (Garzanti et al. 1987; Searle et al. 1997; Zhu et al. 2005; Green et al. 2008; Najman et al. 2010), and even as late as ~34 Ma (Aitchison et al. 2007). Models for the collision vary from diachronous, starting from Ladakh in the west (Rowley 1998) or south central Tibet in the middle (Ding et al. 2005), to synchronous across the entire northern Indian continental margin (Zhu et al. 2005; Green et al. 2008). The question of diachroneity or synchronicity depends on the reliable and accurate dating of the initial collision. Moreover, authors arguing for a relatively larger 'Greater India' have usually preferred an earlier collision age (Patzelt et al. 1996), and vice versa. Consequently, reliable and precise dating of the initial India-Asia collision is the key to solving these collision-related questions.

The various dates for the initial collision result from different definitions of the term 'initial India-Asia continental collision' and the correspondingly different working methods adopted. Plate-motion (Patriat and Achache 1984), paleomagnetism (Chen et al. 2010; Liebke et al. 2010), stratigraphic, sedimentological, paleontological, and structural

evidence (Garzanti et al. 1987; Searle et al. 1988; Willems et al. 1996; Clementz et al. 2011), as well as subsidence history of the northern Indian continental shelf (Rowley 1998; Corfield et al. 2005), and subduction-related magmatism and metamorphism (Leech et al. 2005; St-Onge et al. 2010) have all been used to constrain the collision. During the last decade, Rowley's definition of the initial India-Asia continental collision (Rowley 1998) – the time of elimination of Neo-Tethys oceanic lithosphere and the first development of a foreland basin on the Indian continent – has become generally accepted, and the expected onset of a foreland basin has been used to constrain the initial continental collision.

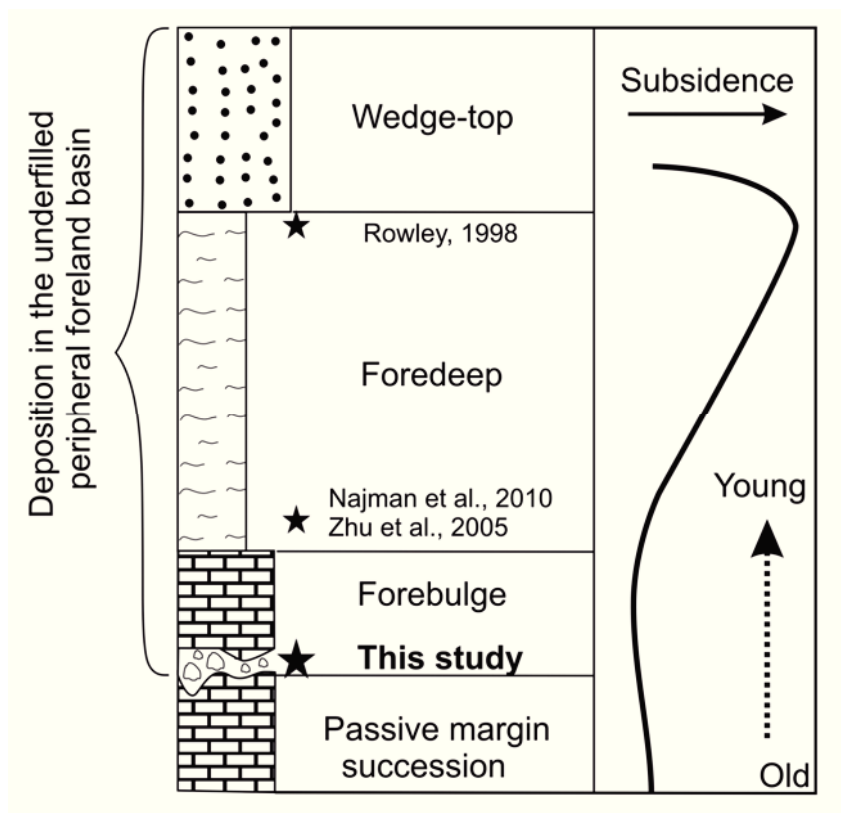


Fig. 1 The idealized sedimentary sequences in an underfilled peripheral foreland basin, showing vertical superpositions of different depozones and subsidence history resulting from migration of a foreland basin towards the craton (revised from Sinclair (1997) and DeCelles et al. (1998)). Stars represent the ages proposed to constrain the India-Asia collision by different authors, and see Fig. 3 for explanations of the symbols.

When continent-continent collision started, development of a peripheral foreland basin on the subducting continental plate would cause flexural subsidence (foredeep) at the proximal location and flexural uplift (forebulge) at the distal location (DeCelles and Gile 1996). As a result, timing of the initial collision can be obtained by dating the occurrence of either the foredeep in the proximal location (such as the northern Tethyan Himalaya) or the forebulge in the distal location (such as the southern Tethyan Himalaya). However,

deep water siliciclastic rocks in the foredeep are usually devoid of diagnostic fossils, which may hinder the construction of high resolution biostratigraphy (such as Wang et al. 2011's studies at Sangdanlin). In contrast, shallow-water limestones rich in fossils in the forebulge (such as Gamba and Tingri) can provide high-resolution biostratigraphy and therefore may better constrain the onset of a peripheral foreland basin.

In the south Tethyan Himalaya, evidence of the earliest Asian-derived detritus (Zhu et al. 2005; Najman et al. 2010) and accelerated tectonic subsidence (Rowley 1998) has been proposed to indicate the arrival of the foredeep and thus the India-Asia collision. However, a considerable lag time between the initial collision and those events may exist, because the foredeep and related flexural subsidence would firstly occur in the northern Tethyan Himalaya and then move to the southern Tethyan Himalaya as the foreland basin was migrating southward (DeCelles et al. 1998). By an alternate method, the larger foraminifera-bearing limestones underlying the foredeep deposition probably represent the forebulge deposits that resulted from flexural uplift; thus, these limestones can be used to better constrain the initial India-Asia continental collision. Consequently, one of the most direct and precise ways to constrain the onset of a peripheral foreland basin marking the India-Asia collision is to identify the forebulge at the distal location and date it with high resolution (Sinclair 1997) (Fig. 1).

## **4.2 Regional stratigraphy**

The Tethyan Himalaya is situated on the northern Indian continental margin. It is sandwiched between the Lhasa Terrane to the north and the High Himalaya to the south (Yin and Harrison 2000) (Fig.2). Structurally it can be subdivided into the southern and northern zones by the Lhagoi Kangri anticline (Ding et al. 2005). Paleozoic to lower Paleogene marine sedimentary strata are widely exposed in the Tethyan Himalaya, and the spatial distribution of carbonates and shales in the south and pelites and turbiditic mudstones in the north suggests a northward deepening environment from continental shelf to slope, and ultimately to deep sea (Liu and Einsele 1994).

### **Gangdese forearc region and the Northern Tethyan Himalaya**

To the north of the Indus-Yarlung Tsangpo suture zone, the northern subduction of Neo-Tethyan oceanic crust beneath the Asian continent resulted in the formation of the middle-late Cretaceous Gangdese forearc basin, which was filled by the hemipelagic shales and sandsheets of the Xigaze Group (Dürr 1996). Overlying the Xigaze Group are the upper Maastrichtian larger foraminifera-bearing limestones of the Qubeiya Fm. The Quxia conglomerate, unconformably resting on the Qubeiya Fm, was proposed to indicate an arc-continental collision or the India-Asia continental collision at the

Cretaceous-Paleogene (K/Pg) boundary (Ding et al. 2005). The Paleocene to lower Eocene Jilazi Fm is made up of larger foraminiferal limestones and coarse sandstones and is unconformably overlain by the upper Oligocene-lower Miocene continental Gangrinboche conglomerate (Fig. 3).

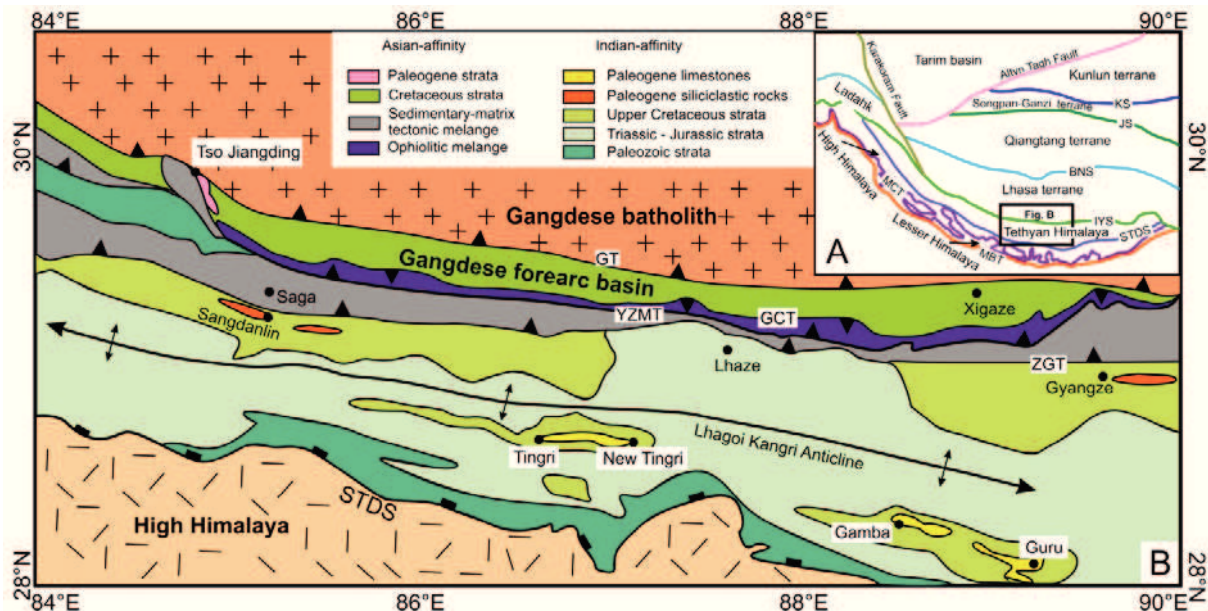


Fig. 2 (A) Inset map with major tectonic units and boundaries in Tibet. (B) Schematic geological map of the Tethyan Himalaya of Tibet showing the study areas of Tingri and Gamba, modified from Ding et al. (2005). Abbreviations: MBT, Main Boundary Thrust; MCT, Main Central Thrust; STDS, South Tibet Detachment System; ZGT, Zhongba-Gyangze thrust; YZMT, Yarlung Zangbo Mantle thrust; IYS, Indus-Yarlung Zangbo Suture; GCT, Great Counter thrust; GT, Gangdese thrust; BNS, Bangong Nujiang Suture; JS, Jinsha Suture; KS, Kunlun Suture.

In the northern Tethyan Himalaya, although a newly published stratigraphy at Sangdanlin by Wang et al. (2011) is inconsistent with the former stratigraphic work (Ding et al. 2005), a general consensus has been reached. The upper Cretaceous-Paleocene quartz-rich sandstones, siltstones, and shales have been sourced from the Indian continent, and a deeper water environment was revealed by the intercalated layers of radiolarian-bearing cherts. Upwards, the lower-middle Eocene sediments show a coarsening upwards trend from shales to pebbly sandstones, whereby the Asian-derived detritus is proposed to indicate the onset of the India-Asia collision (Ding et al. 2005; Wang et al. 2011) (Fig. 3).

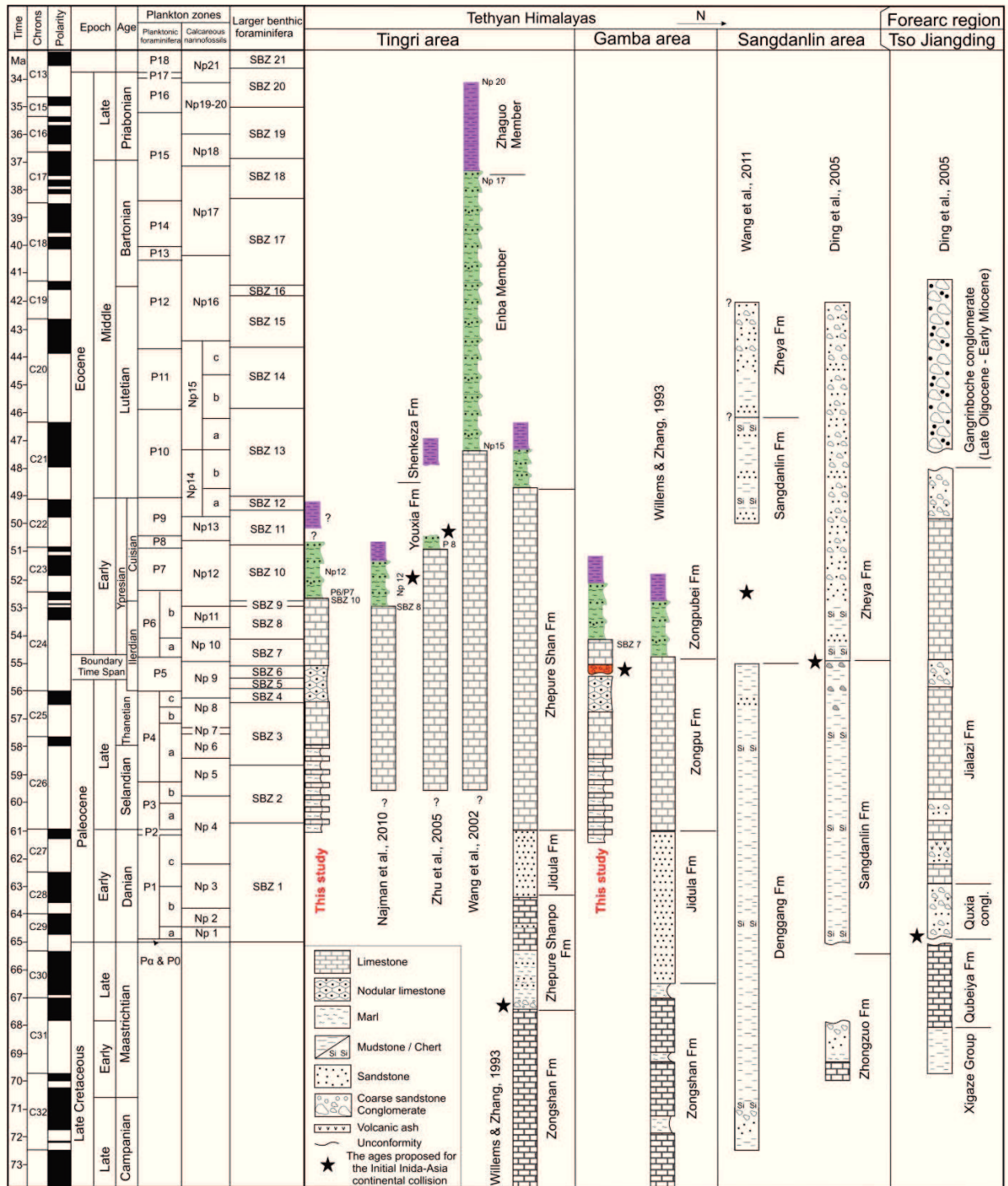


Fig. 3 Integrated chrono- and biostratigraphic time scale with sections from Tingri and Gamba of the southern Tethyan Himalaya (Najman et al., 2010; Wang et al., 2002; Willems and Zhang, 1993a; Willems, 1993b; Willems et al., 1996; Zhu et al., 2005), Sangdanlin of the northern Tethyan Himalaya (Ding et al., 2005; Wang et al., 2011) and Tso Jiangding of the forearc region (Ding et al., 2005). The biozonations of planktonic foraminifera, calcareous nanofossils, and larger benthic foraminifera are adopted from Berggren et al. (1995), Martini (1971), and Serra-Kiel et al. (1998), respectively. Time scale is based on Berggren et al. (1995).



## Southern Tethyan Himalaya

Our two working areas are located within the southern Tethyan Himalaya, near the towns of Tingri and Gamba. At Gamba, the upper Cretaceous limestones and calcareous marls of the Zongshan Fm, rich in planktonic and epiplanktonic organisms indicative of an open continental shelf environment (Willems and Zhang 1993a), are overlain by the upper Maastrichtian to lower Paleocene shoreface deposits of the Jidula Fm, which comprise Indian-derived quartz sandstones. At Tingri, however, about 225 m of sandstone turbidites and mixed carbonate-siliciclastic reworked sediments of the Zhepure Shanpo Fm are sandwiched between the Zongshan and Jidula Fms. The Zhepure Shanpo Fm are interpreted to have been deposited in locally restricted submarine fans on a continental slope and to represent the onset of the India-Asia collision (Willems et al. 1996) (Fig. 3).

Larger foraminifera-bearing marine limestones above the Jidula Fm are relatively well preserved at Tingri and Gamba. At Tingri, limestone sequences of the Zhepure Shan Fm (about 450 m thick) form a continuous lithological section composed of four lithologically distinct members. At the base, cyclic limestones consist of seven cycles, each of which is composed of a transition from calcareous marls, sometimes nodular, to limestones. These are overlain by the first massive limestones. Continuing upwards, the nodular limestones and the overlying second massive limestones represent the upper part of the Zhepure Shan Fm. At Gamba, although the limestones of the Zongpu Fm have undergone deformation and faulting during the India-Asia collision, the stratigraphic combination of several isolated lithological columns reveals limestone sequences similar to those at Tingri.

On top of the Paleogene limestone sequences, green marls and siltstones and red mudstones and siltstones are exposed. At Tingri, the green beds, with disputed stratigraphic ages from late Ypresian to Bartonian (Fig. 3), were interpreted to have been deposited in a marine outer-shelf environment (Zhu et al. 2005). The red beds above are the subject of even more controversy, regarding not only their age but also their depositional environment (Wang et al. 2002; Zhu et al. 2005), which has resulted in different names for the two sedimentary sequences. Thus, the green and red beds were named the Enba and Zhaguo members, respectively, by Wang et al. (2002) and the Youxia and Shenkeza Fms by Zhu et al. (2005). We suggest adopting the stratigraphic nomenclatures proposed by Zhu et al. (2005), owing to their proper sedimentological interpretations and relatively accurate age determination (Fig. 3).

At Gamba, our investigations are mainly based on section F, measured by Willems and Zhang (1993). The lithological column at Tingri has been investigated by several authors

and was called the 'Qumiba section' by Wang et al. (2002) and Najman et al. (2010) and the 'Shenkeza section' by Zhu et al. (2005). More detailed geological description of the Gamba and Tingri areas can be found in these publications.

### 4.3 Methods

About 70 samples from the Zongpu Fm at Gamba and 430 samples from the Zhepure Shan Fm at Tingri were collected during field trips in 1983, 1986, and 2009. About 800 thin sections were prepared and ~7000 light-microscope photos were taken for the construction of the larger foraminiferal biostratigraphy and paleoenvironmental analysis. To obtain additional biostratigraphic information from the Tingri area, two samples at the boundary between the Zhepure Shan and Youxia Fms were washed and sieved to collect planktonic foraminifera, and smear slides of 15 samples from the Youxia Fm were prepared for the investigation of calcareous nannofossils.

Through careful inspection under the microscope, about 70 fresh carbonate rocks of the Zongpu Fm without reworked components or petrographically visible diagenetic alterations or veins were prepared for measurements of carbon isotopes. The  $\delta^{13}\text{C}$  measurements were conducted on a Finnigan MAT 251 Spectrometer at MARUM (University of Bremen), and the results were calibrated to the PDB with standard deviation of  $<0.05\text{‰}$ .

### 4.4 Biostratigraphy

Our biostratigraphic work is based on the determination of larger foraminifera, planktonic foraminifera and calcareous nannofossils, mainly focusing on the limestones of the Zhepure Shan and Zongpu Fms and the marls of the Youxia Fm. For the limestone sequences, the concept of the Shallow Benthic Zonation (SBZ) (Serra-Kiel et al. 1998) was adopted to describe the larger foraminiferal biostratigraphy. For the planktonic foraminifera and calcareous nannofossils, we have used the biozonations proposed by Berggren et al. (1995) and Martini (1971), respectively.

#### Larger foraminifera

In the eastern Neo-Tethys (Pakistan, India, Tibet), the larger foraminiferal assemblage of *Miscellanea miscella* and *Ranikothalia nuttalli* represents SBZ 5 (Jauhri 1996; Hottinger 2009). In Tibet, SBZ 6 is dominated by very primitive *Alveolina* species with small sizes and fine regular coilings. The frequent appearances of *Alveolina* with flosculinizations (the thickening of the basal wall in the equatorial region of the test) represent SBZ 7. In SBZ 8-9, *Nummulites* start to dominate the carbonate ramp with the coexistence of

*Alveolina*, and the assemblage of *Assilina*, *Nummulites* and *Discocyclina* indicates SBZ 10 (Fig. 4).

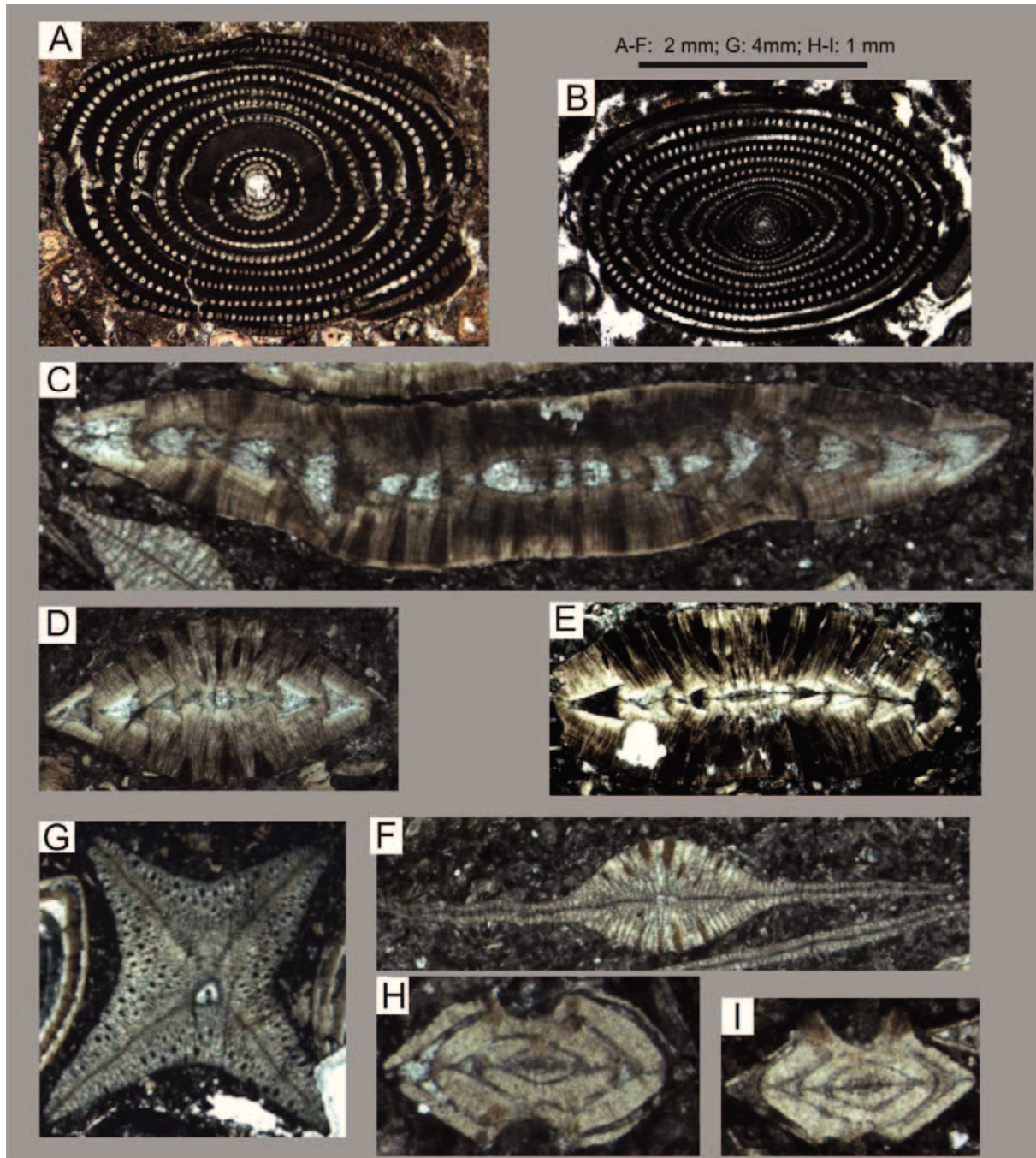


Fig. 4 Photomicrographs of diagnostic larger foraminifera from the topmost limestones of the Zongpu Fm at Gamba (A-B) and the Zhepure Shan Fm at Tingri (C-I). (A) *Alveolina ovicula* (Nuttall), Sample Fm 25; (B) *Alveolina moussoulensis* (Hottinger), Sample Fm 25; (C) *Assilina granulosa* (d'Archiac); (D) *Assilina sublamnosa* (Gill); (E) *Assilina laminosa* (Gill); (F) *Discocyclina dispansa* (Sowerby); (G) *Discocyclina sowerbyi* (Nuttall); (H-I) *Nummulites fossulata* (de Cizancourt). Note that larger foraminifera from Tingri occurring only within the uppermost 6 m of the Zhepure Shan Fm indicate the base of SBZ 10, and

*Alveolina ovicula* and *A. moussoulensis* at Gamba represent SBZ 7. See Fig 9B. for their precise locations in the section.

At Tingri, *Assilina granulosa* (d'Archiac), *A. sublaminosa* (Gill), *A. laminosa* (Gill), *Discocyclina dispansa* (Sowerby), *D. sowerbyi* (Nuttall), and *Nummulites fossulata* (de Cizancourt) appear exclusively within the uppermost 6 m of the Zhepure Shan Fm, representing the base of SBZ 10 (Fig. 4). Although these species from the eastern Neo-Tethys realm have not been assigned to the SBZ before now (Serra-Kiel et al. 1998), the reason to allocate them to SBZ 10 is that the co-occurrence of *Nummulites fossulata* with *Nummulites aquitana* (SBZ 10) in France (Cizancourt 1945) provides an age of SBZ 10 for the larger foraminiferal assemblage.

At Gamba, *Alveolina ovicula* (Nuttall) and *A. moussoulensis* (Hottinger) at the top of the Zongpu limestones constrain the termination of the Zongpu Fm to SBZ 7 (Fig. 4), because *Alveolina moussoulensis* is one of the index fossils for SBZ 7 (Serra-Kiel et al. 1998).

#### **Planktonic foraminifera and Calcareous nannofossils**

At Tingri, although most of late Cretaceous and Paleocene plankton in the Youxia Fm were reworked, the presence of youngest age-diagnostic planktonic foraminifers, such as *Acarinina pseudotopilensis*, *A. soldadoensis*, *A. esnaensis* and *A. wilcoxensis* provide an age of P 6-7 for the boundary between the Zhepure Shan and Youxia Fms. Moreover, the diagnostic coccoliths in the green marls give a depositional age of NP 12 for the Youxia Fm (Fig. 5). These results fit well with the larger foraminiferal biostratigraphy (Fig. 3).

#### **4.5 Paleoenvironmental and paleobathymetric analysis**

The symbiont-bearing benthic larger foraminifera usually live in the photic zone (<120 m) of warm, oligotrophic, neritic environments. They are sensitive to depth distribution, and have been successfully used for paleoenvironmental and paleobathymetric reconstructions (Hallock and Glenn 1986; Hottinger 1997; Green et al. 2008). From the late Paleocene to early Eocene, larger foraminiferal associations with *Miscellanea-Ranikothalia*, *Alveolina-Orbitolites*, *Nummulites-Alveolina*, and *Assilina-Discocyclina* inhabited at the depths of ~40-80 m, <~40 m, ~40-80 m, and ~80-120 m, respectively (Hottinger 1997). Besides, changes of associations from *Alveolina-Orbitolites*, *Alveolina*, *Nummulites-Alveolina*, *Assilina-Discocyclina* have also been proposed to indicate a gradually deepening process on the Eocene carbonate ramp (Racey 1994; Beavington-Penney and Racey 2004).

Zhepure Shan (Tibet)	Youxia Fm																Series	
	ZT 26	Zt 25	ZT 21	ZT 19	ZT 15	ZT 13	ZT 11	ZT 9	ZT 7	ZT 6	ZT 4	ZT 2	ZT 1	9ZE8	9ZE7			
Arkhangelskiella cf. cymbiformis								R									R= rare F= few C= common	Upper Cretaceous
Cretarhabdus crenulatus						R							R					
Eiffellithus eximius								R										
Eiffellithus turrisieffeli	R		R		R	R		R					R					
Micula staurophora	R		R						R				R					
Prediscosphaera cretacea			R					R										
Watznaueria barnesae	C	C -	C +	C	F	C	C	C +	C	C	C	C	C	C	C			
Zeugrhabdodus pseudanthophorus									R		R							
Chiasmolithus danicus				R		R					R				R			
Cruciplacolithus tenuis							R	R			R							
Discoaster multiradiatus		R						R				R	R	R				
Fasciculithus sp.						R				R		R						
Rhombaster cuspis									R									
Sphenolithus anarrhopus							R		R									
Braarudosphaera bigelowii								R									NP zones	Lower/Middle Eocene
Chiasmolithus solitus	R							R					R				12 → 16	
C. cf. gammaton				R						R							12 → 14	
Coccolithus pelagicus	R	F	F	C	F	C	F	C	F	F	C	F	F	F	F			
Cyclococcolithus formosus						R				R							12 → 21	
Discoaster sp. VII/VIII							R	R						R			11 → 20	
Discolithus planus				R													12 → 14	
Sphenolithus moriformis			R								R							
Sphenolithus radians		R		R				R			R	R	R	R			12 → 18	
Transversopontis pulcher			R					R				R					12 → 14	
Tribachiatus orthostylus							R	R	R			R	R	R			10ob → 12	
Zygrhablithus bijugatus								R									12 → 25	

Fig. 5 List of coccolith abundances from the Youxia Fm at Tingri.

At Gamba and Tingri, the *Miscellanea-Ranikothalia* assemblage of SBZ 5 indicates a generally shallow-water environment. During SBZ 6, a sudden uplift and erosion occurred at Gamba, depositing a ~2 m thick conglomerate layer with a dominance of reworked pebbles derived from upper Paleocene limestones. During SBZ 7, the uplifted area started to subside gradually, however, the assemblage of *Alveolina-Orbitolites* implies that water depth was still very shallow. Above SBZ 7, a remarkable deepening occurred at Gamba, as revealed by deposition of the Youxia Fm rich in planktonic foraminifers and coccoliths. And the green marls and siltstones in the Youxia Fm are occasionally intercalated by thin-bedded limestones with reworked Paleogene larger foraminifera-bearing limestone clasts, indicating the slight erosion at some local areas nearby (Fig. 6).

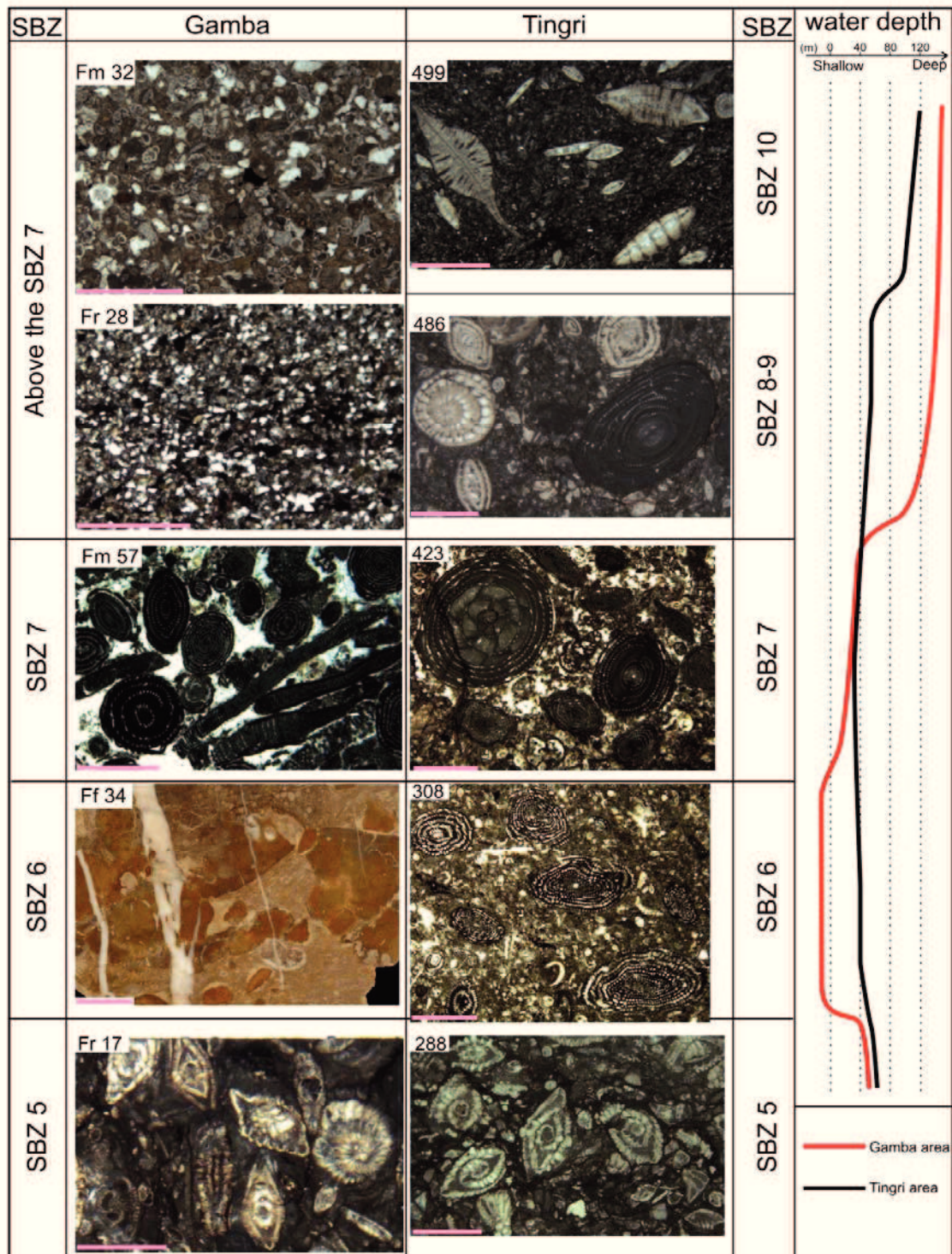


Fig. 6 Representative sedimentary facies from the latest Paleocene to early Eocene at Gamba and Tingri with paleobathymetric changes. Photo of Ff 34 was taken from a polished rock slab, the others are photomicrographs. The scale bars represent 20 mm in Ff 34, 1 mm in Fr28, and 2 mm in all other images. At Gamba, the limestones at the SBZ 5 (Fr17) are rich in late Paleocene larger foraminifera (*Miscellanea-Ranikothalia* assemblage). The conglomerate with dominant pebbles of late Paleocene limestones (Ff34) represents a flexural uplift and erosion at Gamba. Above SBZ 7, the change of depositional environments

from shallow water with *Alveolina-Orbitolites* assemblage (Fm57) to deeper water with planktonic foraminifera (Fm32) and Asian-derived siltstones (Fr28) indicates a sudden deepening event and the arrival of the foredeep to Gamba. At Tingri, a shallowing period during the SBZ 6-7 followed by an evident deepening event is also revealed by changes of the larger foraminiferal assemblages. Note that the deepening event occurred earlier at Gamba than that at Tingri.

As with Gamba, the shallowing event during the earliest Eocene is documented at Tingri as well, by the change from a *Miscellanea-Ranikothalia* assemblage in SBZ 5 to *Alveolina* in the SBZ 6-7. However, a continuous larger foraminiferal record and absence of a conglomerate layer above SBZ 5 suggest that Tingri may have had a paleotopographically deeper depositional environment. A gradual deepening started in SBZ 8-9, and afterwards the assemblage of *Assilina-Discocyclus* together with planktonic foraminifera reflected the sudden deepening at the beginning of SBZ 10 (Fig. 6).

#### 4.6 The initial India-Asia continental collision

During the late Maastrichtian up to the K/Pg boundary, both the depositions of a conglomerate layer from the Zhepure Shanpo Fm at Tingri and the Quxia conglomerate at Tso Jiangding were proposed to indicate the initial India-Asia collision (Willems et al. 1996; Ding et al. 2005) (Fig. 3). However, the upper Maastrichtian conglomerate layer at Tingri is not observed at Gamba (Willems and Zhang 1993a), implying that it represents only a local sedimentary phenomenon. Moreover, the overlying thick Paleocene-lower Eocene limestones are widely distributed across the entire northern Indian continental margin (Garzanti et al. 1987; Willems et al. 1996; Green et al. 2008), indicating a stable carbonate ramp environment during the Paleocene (Willems 1993b). Both of them conflict with the idea that the initial collision occurred at the late Maastrichtian and led to deposition of the conglomerate at Tingri. At Tso Jiangding, the K/Pg collision was originally interpreted with two contrasting models: India-Asia continental collision or India continent-island arc collision. So the possibility of the India-Asia collision at the K/Pg boundary needs more solid evidence.

In the southern Tethyan Himalaya, the Paleogene sedimentary sequences on the Indian continental margin are generally consistent from Zanskar in the west to Tingri/Gamba in the east, starting from lower Paleocene Indian-derived sandstones, to middle Paleocene-lower Eocene limestones, then to lower Eocene green marls and Asian-derived siltstones, and with red mudstones and siltstones at the top. All sedimentary sequences are roughly comparable to the underfilled trinity in the Alpine foreland basin (Sinclair 1997) (Fig. 7).

Stage	Lithology	Tethyan Himalaya		Depositional environment
		West	East	
Lower Eocene		Chulung-La Fm	Shenkeza Fm	Wedge-top
		Kong Fm	Youxia Fm	Foredeep ← Asian-derived detritus ← Sudden deepening
Paleocene		Dibling Fm	Zhepure Shan Fm	Forebulge ← Sudden shallowing
		Singe-La Fm		
		Stumpata Quartzarenite	Jidula Fm	Indian passive continental margin ← Indian-derived detritus

Fig. 7 Simplified Paleocene-lower Eocene lithostratigraphic correlation between the western (Zaskar) (Garzanti et al., 1987; Green et al., 2008) and eastern (Tingri and Gamba) Tethyan Himalaya.

During the early Eocene, the firstly shallowing and then deepening events at Gamba and Tingri occurred in the context of global sea-level rising (Miller et al. 2005; Sluijs et al. 2008), which would imply that the changes of paleo-water depths were mainly caused by regional tectonics, not eustasy. Therefore, the deepening trends recorded at Gamba and Tingri may imply transition from the forebulge to the foredeep due to the migration of flexural subsidence from the northern Tethyan Himalaya to the southern Tethyan Himalaya. As a result of our biostratigraphic and sedimentological data, onset of the deepening event occurred earlier at Gamba than that at Tingri, suggesting that Gamba was situated closer to the orogenic belt of the Asian continent and underwent earlier flexural subsidence (Fig. 8). Consequently, the appearance of the forebulge at Gamba would also predate that at Tingri, and the forebulge at Gamba can provide a better constraint on the initial India-Asia continental collision.



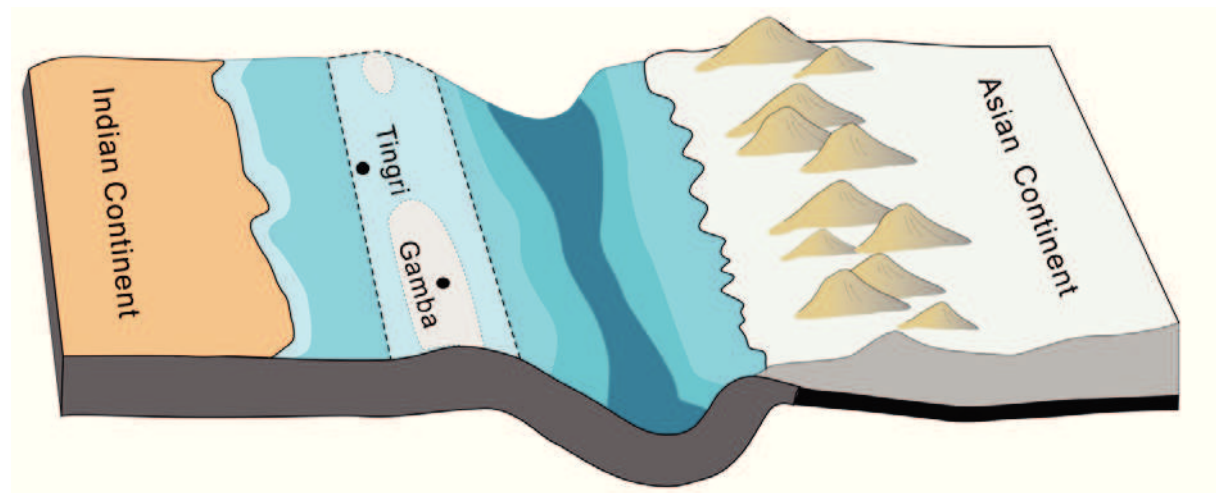


Fig. 8 The paleogeographic positions of Gamba and Tingri at the P/E boundary. Two dotted lines show the forebulge depozone with possible erosional areas (white patches). Note that Gamba was located at a paleotopographically higher position and was closer to the orogenic belt of the Asian continent. Not to scale.

At Gamba, deposition of the conglomerate layer within the Zongpu limestones was accompanied by a distinct shallowing event, which may reflect the occurrence of flexural uplift owing to the India-Asia continental collision. Coincidentally, a pronounced Carbon Isotope Excursion (CIE) appeared just below the conglomerate layer (Fig. 9). Although the assumption that the India-Asia collision triggered or partly affected the CIE still needs detailed argumentation (Higgins and Schrag 2006), time equivalence of the two events does provide an accurate age of ~56 Ma (the P/E boundary) for the India-Asia continental collision (Aubry et al. 2007; Westerhold et al. 2009; Jaramillo et al. 2010).

To the north of Gamba and Tingri (e.g., Sangdanlin), the Paleocene deep-water siliciclastic sequences in the northern Tethyan Himalaya show no evidence of flexural uplift (tectonic-induced shallowing event) for the existence of a possible older forebulge. Therefore, the P/E boundary forebulge developing at Gamba probably represents the earliest forebulge at the onset of the foreland basin, and not the one caused by the subsequent lateral migration of foreland basin (DeCelles et al. 1998). Consequently, the age of the P/E boundary recorded in the conglomerate layer of the Zongpu Fm may indicate a possibly maximum age of the initial India-Asia continental collision. Moreover, in combination with the results from Ladakh/Zaskar (Garzanti et al. 1987; Garzanti 2008; Green et al. 2008), the quasi-synchronicity of the India-Asia collision in the western and eastern Tethyan Himalaya is supported by us (Zhu et al. 2005; Green et al. 2008).

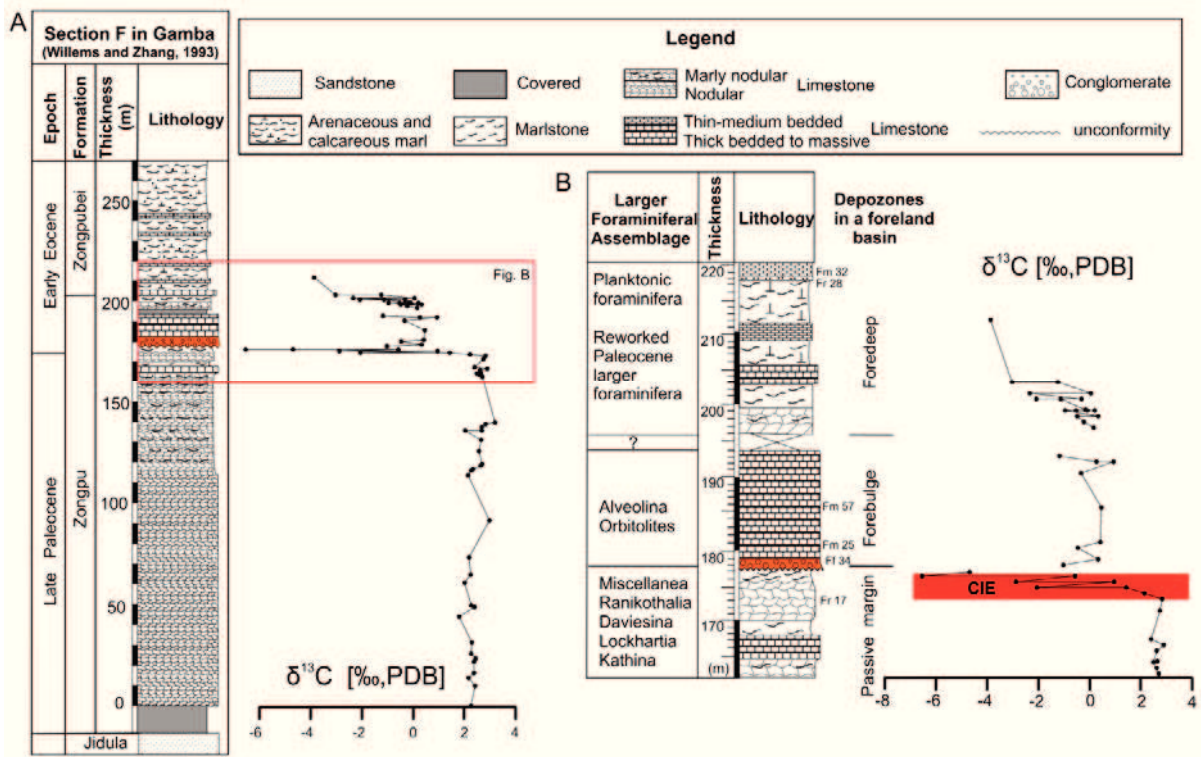


Fig. 9 (A) Upper Paleocene to lower Eocene lithological column at Gamba (Willems and Zhang, 1993a), with the  $\delta^{13}\text{C}$  curve measured from bulk carbonate. (B) An enlargement of part of Fig. 9A, showing the details of changes of lithology and carbon isotopes from the latest Paleocene to the earliest Eocene. The identification of different depozones of the foreland basin and the positions of the lithological samples for biostratigraphy and paleobathymetric analysis are presented on the right side of the lithological column. Note that the deposition of the conglomerate layer occurred coincidentally with the CIE.

In addition, although the width of a foreland basin depends on the flexural rigidity of the underlying lithosphere and the nature of the orogenic belt, the distance from the forebulge to the orogenic belt is normally less than  $\sim 500$  km (DeCelles and Giles 1996; Rowley 1998). Based on our conclusion that the conglomerate layer in the upper Zongpu Fm represents the first forebulge at the onset of foreland basin, we speculate that the maximum distance between Gamba and the southernmost part of the Asian continent was less than  $\sim 500$  km at the P/E boundary.

#### 4.7 Reinterpretation of timing of provenance change at Sangdanlin

At Sangdanlin, Wang et al. (2011) have studied petrology, detrital Cr-spinel geochemistry, and detrital zircon U-Pb ages from the Upper Cretaceous-Eocene sandstones, and provided new evidence on provenance change in the area adjacent to the Indus-Yarlung Zangbo suture zone. Lithic sandstones at the bottom of the Sangdanlin formation were proposed to record the first arrival of Asian-derived detritus (Wang et al. 2011). Because no age-diagnostic fossil were found in the sandstones, the utilization of the mean U-Pb age of the youngest detrital zircon population was used to

infer the maximum depositional age (Kapp et al. 2007; Dickinson and Gehrels 2009). Based on the original data of detrital zircon U-Pb ages (sample 06SDL14-1) from Wang et al. (2011) and the method recommended by Dickinson and Gehrels (2009), the maximum depositional age of  $54.9 \pm 1.6$  Ma was obtained for the sandstones containing the first Asian-derived detritus (Fig. 10).

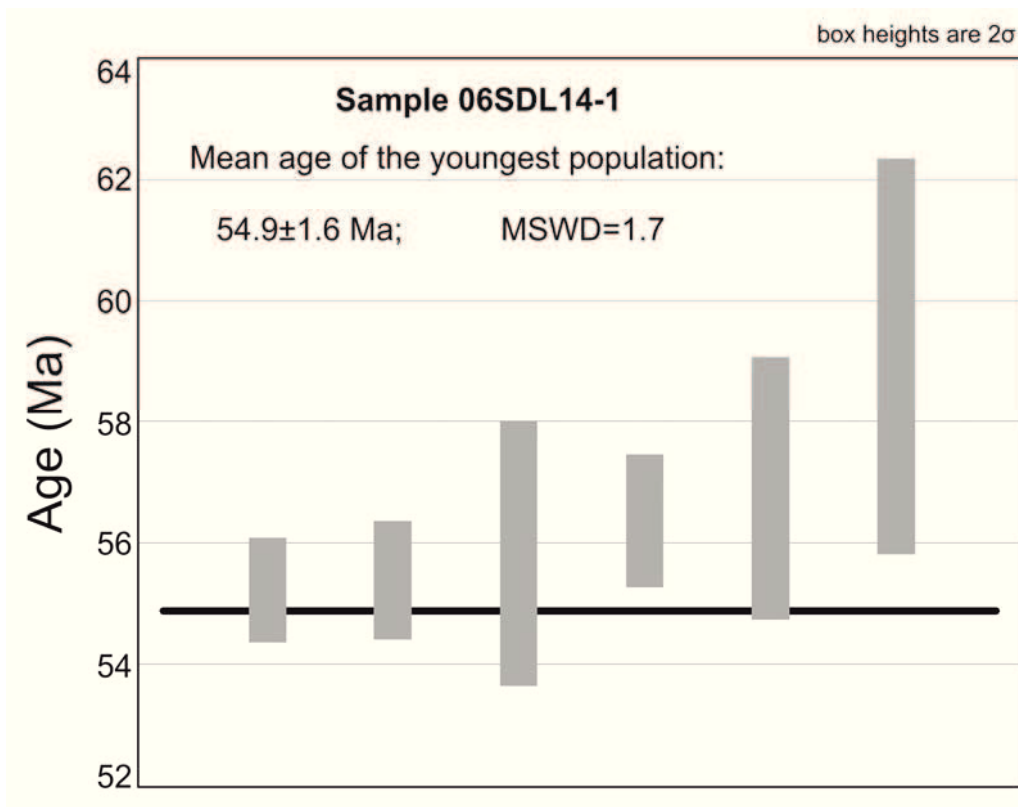


Fig. 10 The mean age of the youngest zircon grains overlapping in age at  $2\sigma$  from sandstone 06SDL14-1 at Sangdanlin. Original data from Wang et al. (2011).

The Paleocene radiolarian assemblage in the red chert immediately below the Sangdanlin formation produced a youngest age of  $\sim 56$  Ma (Ding et al. 2003). In the lower Eocene radiolarian zone  $\sim 20$  m above the lithic sandstones (Wang et al. 2011), *Buryella clinata-Thursocyrtis ampla*, was identified by Li et al. (2007). *Buryella clinata* belongs to RP8 (Sanfilippo and Nigrini 1988), providing a numerical age of  $\sim 53.2$ - $50.3$  Ma according to the 2004 geological time scale (Gradstein et al. 2004); thus the age of  $54.9 \pm 1.6$  Ma derived from isotope geochronology fits well with the biostratigraphy from both the underlying and overlying strata, and consequently provenance change at Sangdanlin may have occurred close to the P/E boundary.

## 4.8 A tectonic model for the early Paleogene India-Asia convergence

Based on our studies of the stratigraphy, paleontology and sedimentology, together with other previously published results (Garzanti et al. 1987; Willems and Zhang 1993a; Willems 1993b; Critelli and Garzanti 1994; Willems et al. 1996; Ding et al. 2005; Zhu et al. 2005; Green et al. 2008; Najman et al. 2010; Wang et al. 2011), a new tectonic reconstruction is proposed here to interpret the lower Paleogene stratigraphy on the northern Indian and southern Asian continental margins (Fig. 11).

During the Paleocene, the Neo-Tethys oceanic crust continued to subduct beneath the Asian continent. The Paleocene siliciclastic rocks in the Tethyan Himalaya (e.g., Denggang Fm at Sangdanlin, Jidula Fm at Gamba and Tingri) mainly consisted of Indian-derived detritus, indicating a passive continental margin environment on the northern Indian continent. Besides, the relatively stable environment led to the deposition of ~400 m Paleocene limestone in the southern Tethyan Himalaya. At Tso Jiangding, the Quxia conglomerate and the lower part of Jialazi limestones were deposited in the Gangdese forearc basin (Fig. 11a).

At the P/E boundary, the initial India-Asia continental collision occurred quasi-synchronously in the west (Ladakh/Zaskar) and east (Gamba), and a foreland basin formed on the northern Indian continental margin. In the northern Tethyan Himalaya, a foredeep started to develop at Sangdanlin with the deposition of the Sangdanlin Fm and the lower Zheya Fm, and an abrupt provenance change from India to Asia in the Sangdanlin Fm was detected by provenance analyses (Wang et al. 2011). To the south, flexural uplift generated the possible first forebulge at Gamba, and led to a shallowing of the depositional environment. The conglomerate layer in the upper Zongpu Fm shows that the uplift might even have exposed Gamba above sea level and formed an unconformity within the Zongpu limestones. Compared to Gamba, Tingri might have had a relatively deeper depositional environment and didn't undergo subaerial exposure, depositing the continuous limestone sequences of the Zhepure Shan Fm. At Tso Jiangding, the upper Jialazi limestones intercalated by sandstones and conglomerates were probably deposited in a subaqueous wedge-top depozone (Fig. 11b).

In the early Eocene, through the gradual migration of the foreland basin towards the Indian continent, pebbly sandstones and conglomerates of the upper Zheya Fm at Sangdanlin (Ding et al. 2005) were probably deposited in the wedge top of the foreland basin. In the southern Tethyan Himalaya, the foredeep firstly arrived at Gamba and then Tingri. The Youxia Fm rich in planktonic foraminifera and coccoliths shows a distinct provenance change from the Indian to Asian sources (Zhu et al. 2005; Najman et al. 2010), indicating the foredeep deposition in an underfilled foreland basin. The sudden

deepening of depositional environment drowned the early Eocene carbonate ramp and led to the complete disappearance of the larger foraminifera at Gamba and Tingri. To the south of Gamba and Tingri, southward migration of flexural uplift caused formation of another forebulge probably in High Himalaya (?), which resulted in erosion of the underlying marine strata and shed the reworked late Cretaceous and Paleocene plankton into the Youxia Fm (Fig. 11c).

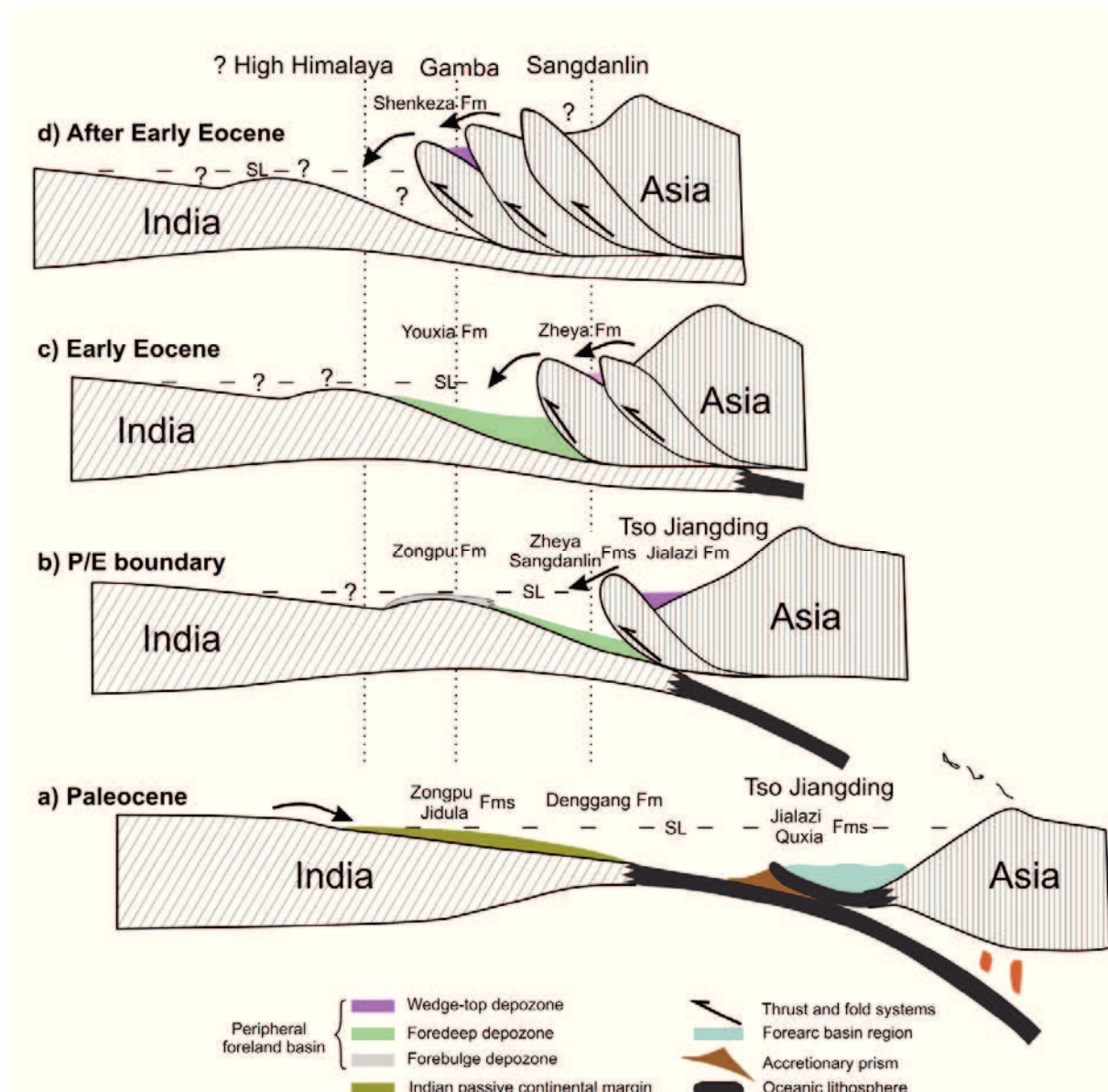


Fig. 11 Simplified plate tectonic model illustrating basin evolution from Paleocene to Eocene, not to scale. The arrows indicate sediment dispersal directions and sources, and the abbreviation of 'SL' represents sea level.

Finally, the red beds of the Shenkeza Fm at the top of Paleogene marine sequences might have been deposited in a subaerial wedge-top depozone of foreland basin or

piggy-back basin, representing the first continental sediment during the Cenozoic (Critelli and Garzanti 1994; Zhu et al. 2005) (Fig. 11d).

## 4.9 Conclusions

1. Deposition of the Paleogene larger foraminifera-bearing limestones of the Zongpu Fm at Gamba and the Zhepure Shan Fm at Tingri ceased at SBZ 7 (~54-55 Ma) and the base of SBZ 10 (~52.8 Ma), respectively, and the depositional age of the Youxia Fm at Tingri is NP 12 (~51-52.8 Ma).
2. Compared with Tingri, Gamba was located closer to the orogenic belt of the Asian continent, and exhibited a shallower water depth at the P/E boundary.
3. The conglomerate layer immediately above the SBZ 5 at Gamba represents deposition in the forebulge, which is probably the first forebulge corresponding to the onset of the foreland basin, and therefore may provide the maximum age of the initial India-Asia continental collision.
4. The coincidence of the CIE and the conglomerate layer provides a precise age of ~56 Ma for the initial India-Asia continental collision, and the quasi-synchronicity of the collision in the west (Ladakh) and east (Gamba) is supported by us.

## Acknowledgements

We thank I. Wendler and J. Wendler for providing the samples from the Youxia Formation, E. Martini for the determination of calcareous nannofossils, L. Hottinger for imparting knowledge of larger foraminifera, W. Hale for polishing the written English, B. Zhang, Z. Zhou, A. Hübner, C. Schott, F. Wieseler, J. Duda, and A. Ruppel for assistance in field and laboratory work. E. Garzanti, D. Rowley, and an anonymous reviewer are gratefully acknowledged for their careful and constructive comments. The project is funded by Deutsche Forschungsgemeinschaft (No. Wi725/26), National Science Fund for Outstanding Youths of China (40625008 to Ding Lin), and the Max-Planck Society.

## References

- Aitchison JC, Ali JR, Davis AM (2007) When and where did India and Asia collide?. *J Geophys Res* 112. doi:10.1029/2006JB004706
- Aubry MP, Ouda K, Dupuis C, Berggren WA, Van Couvering JA, Ali J, Brinkhuis H, Gingerich PD, Heilmann-Clausen C, Hooker J, Kent DV, King C, Knox RWOB, Laga P, Molina E, Schmitz B, Steurbaut E, Ward DR (2007) The Global Standard

- Stratotype-section and Point (GSSP) for the base of the Eocene Series in the Dababiya section (Egypt). *Episodes* 30 (4):271-286
- Beavington-Penney SJ, Racey A (2004) Ecology of extant nummulitids and other larger benthic foraminifera: applications in palaeoenvironmental analysis. *Earth Sci Rev* 67:219-265
- Berggren WA, Kent DV, Swisher Iii CC, Aubry MP (1995) A revised Cenozoic geochronology and chronostratigraphy. In: Berggren WA, Kent DV, Aubry MP, Hardenbol J (eds) *Geochronology, Time Scales and Global Stratigraphic Correlation* 54. SEPM Spec Pub 54, pp 129–212
- Cai F, Ding L, Yue Y (2011) Provenance analysis of upper Cretaceous strata in the Tethys Himalaya, southern Tibet: Implications for timing of India-Asia collision. *Earth Planet Sci Lett* 305:195-206
- Chen J, Huang B, Sun L (2010) New constraints to the onset of the India-Asia collision: Paleomagnetic reconnaissance on the Linzizong Group in the Lhasa Block, China. *Tectonophysics* 489:189-209
- Clementz M, Bajpai S, Ravikant V, Thewissen JGM, Saravanan N, Singh IB, Prasad V (2011) Early Eocene warming events and the timing of terrestrial faunal exchange between India and Asia. *Geology* 39:15-18
- Corfield RI, Watts AB, Searle MP (2005) Subsidence history of the north Indian continental margin, Zaskar-Ladakh Himalaya, NW India. *J Geol Soc Lond* 162:135-146
- Critelli S, Garzanti E (1994) Provenance of the lower Tertiary Murree redbeds (Hazara-Kashmir syntaxis, Pakistan) and initial rising of the Himalayas. *Sediment Geology* 89:265-284
- DeCelles PG, Giles KA (1996) Foreland basin systems. *Basin Res* 8:105-123
- DeCelles PG, Gehrels GE, Quade J, Ojha TP (1998) Eocene-early Miocene foreland basin development and the history of Himalayan thrusting, western and central Nepal. *Tectonics* 17:741-765
- De Cizancourt M (1945) Nummulites nouvelles ou peu connues d'Aquitaine. *B Soc Geol Fr* 15:643-655

- Dickinson WR, Gehrels GE (2009) Use of U-Pb ages of detrital zircons to infer maximum depositional ages of strata: A test against a Colorado Plateau Mesozoic database. *Earth Planet Sci Lett* 288:115-125
- Ding L (2003) Paleocene deep-water sediments and radiolarian faunas: implications for evolution of Yarlung-Zangbo foreland basin, southern Tibet. *Sci China Ser D-Earth Sci* 46:84-96
- Ding L, Kapp P, Wan X (2005) Paleocene-Eocene record of ophiolite obduction and initial India-Asia collision, south central Tibet. *Tectonics* 24.  
doi:10.1029/2004TC001729
- Dürr SB (1996) Provenance of Xigaze fore-arc basin clastic rocks (Cretaceous, South Tibet). *Geol Soc Am Bull* 108:669-684
- Garzanti E (2008) Comment on "When and where did India and Asia collide?" by Jonathan C. Aitchison, Jason R. Ali, and Aileen M. Davis. *J Geophys Res* 113.  
doi:10.1029/2007jb005276
- Garzanti E, Baud A, Mascle G (1987) Sedimentary record of the northward flight of India and its collision with Eurasia (Ladakh Himalaya, India). *Geodin Acta* 1:297-312
- Green OR, Searle MP, Corfield RI, Corfield RM (2008) Cretaceous-Tertiary carbonate platform evolution and the age of the India-Asia collision along the Ladakh Himalaya (Northwest India). *J Geol* 116:331-353
- Gradstein FM, Ogg JG, Smith AG (2004) *A geologic time scale 2004*. Cambridge University press, Cambridge
- Hallock P, Glenn EC (1986) Larger foraminifera: A tool for paleoenvironmental analysis of Cenozoic carbonate depositional facies. *Palaios* 1:55-64
- Higgins JA, Schrag DP (2006) Beyond methane: Towards a theory for the Paleocene-Eocene Thermal Maximum. *Earth Planet Sci Lett* 245:523-537
- Hottinger L (1997) Shallow benthic foraminiferal assemblages as signals for depth of their deposition and their limitations. *Bull Soc Géol Fr* 168:491-505
- Hottinger L (2009) The Paleocene and earliest Eocene foraminiferal family *Miscellaneidae*: neither *nummulitids* nor *rotaliids*. *Carnets de Géologie* 6:1-41
- Jaramillo C, Ochoa D, Contreras L, Pagani M, Carvajal-Ortiz H, Pratt LM, Krishnan S, Cardona A, Romero M, Quiroz L, Rodriguez G, Rueda MJ, de la Parra F, Moron



- S, Green W, Bayona G, Montes C, Quintero O, Ramirez R, Mora G, Schouten S, Bermudez H, Navarrete R, Parra F, Alvaran M, Osorno J, Crowley JL, Valencia V, Vervoort J (2010) Effects of rapid global warming at the Paleocene-Eocene boundary on neotropical vegetation. *Science* 330:957-961
- Jauhri AK (1996) *Ranikothalia nuttalli* (Davies), a distinctive early Ilerdian marker, in the Shillong Plateau. In: Pandey J, Azmi RJ, Bhandari A, Dave A (eds) Contributions to XV Indian Colloquium on Micropalaeontology and stratigraphy. Allied Printer, Dehra Dun, pp 209-218
- Kapp P, DeCelles PG, Gehrels GE, Heizler M, Ding L (2007) Geological records of the Lhasa-Qiangtang and Indo-Asian collisions in the Nima area of central Tibet. *Geol Soc Am Bull* 119:917-932
- Leech ML, Singh S, Jain AK, Klemperer SL, Manickavasagam RM (2005) The onset of India-Asia continental collision: Early, steep subduction required by the timing of UHP metamorphism in the western Himalaya. *Earth Planet Sci Lett* 234:83-97
- Li Y, Wang C, Hu X, Bak M, Wang J, Chen L (2007) Characteristics of Early Eocene radiolarian assemblages of the Saga area, southern Tibet and their constraint on the closure history of the Tethys. *Chin Sci Bull* 52:2108-2114
- Liebke U, Appel E, Ding L, Neumann U, Antolin B, Xu Q (2010) Position of the Lhasa terrane prior to India-Asia collision derived from palaeomagnetic inclinations of 53 Ma old dykes of the Linzhou Basin: constraints on the age of collision and post-collisional shortening within the Tibetan Plateau. *Geophys J Int* 182:1199-1215
- Liu G, Einsele G (1994) Sedimentary history of the Tethyan basin in the Tibetan Himalayas. *Int J Earth Sci* 83:32-61
- Martini E (1971) Standard Tertiary and Quaternary calcareous nannoplankton zonation. In: Farinacci A (ed) Proceedings of the second planktonic conference. Roma, pp 739-785
- Miller KG, Komazin MA, Browning JV, Wright JD, Mountain GS, Katz ME, Sugarman PJ, Cramer BS, Christie-Blick N, Pekar SF (2005) The Phanerozoic record of global sea-level change. *Science* 310:1293-1298
- Najman Y, Appel E, Boudagher-Fadel M, Bown P, Carter A, Garzanti E, Godin L, Han J, Liebke U, Oliver G, Parrish R, Vezzoli G (2010) Timing of India-Asia collision:

- Geological, biostratigraphic, and palaeomagnetic constraints. *J Geophys Res* 115. doi:10.1029/2010jb007673
- Patriat P, Achache J (1984) India-Eurasia collision chronology has implications for crustal shortening and driving mechanism of plates. *Nature* 311:615-621
- Patzelt A, Li H, Wang J, Appel E (1996) Palaeomagnetism of Cretaceous to Tertiary sediments from southern Tibet: evidence for the extent of the northern margin of India prior to the collision with Eurasia. *Tectonophysics* 259:259-284
- Racey A (1994) Biostratigraphy and palaeobiogeographic significance of Tertiary nummulitids (foraminifera) from northern Oman. In: Simmons MD (ed) *Micropalaeontology and hydrocarbon exploration in the Middle East*. Chapman & Hall, pp 343-370
- Rowley DB (1998) Minimum age of initiation of collision between India and Asia north of Everest based on the subsidence history of the Zhepure Mountain section. *J Geol* 106:229-235
- Sanfilippo A, Nigrini C (1998) Code numbers for Cenozoic low latitude radiolarian biostratigraphic zones and GPTS conversion tables. *Mar Micropaleontol* 33:109-156
- Searle MP, Cooper DJW, Rex AJ, Herren E, Colchen M (1988) Collision tectonics of the Ladakh--Zaskar Himalaya. *Phil Trans R Soc Lond A* 326:117-150
- Searle M, Corfield RI, Stephenson BEN, McCarron JOE (1997) Structure of the north Indian continental margin in the Ladakh--Zaskar Himalayas: Implications for the timing of obduction of the Spontang ophiolite, India--Asia collision and deformation events in the Himalaya. *Geol Mag* 134:297-316
- Serra-Kiel J, Hottinger L, Caus E, Drobne K, Ferrandez C, Jauhri AK, Less G, Pavlovec R, Pignatti J, Samsó JM (1998) Larger foraminiferal biostratigraphy of the Tethyan Paleocene and Eocene. *Bull Soc Géol Fr* 169 (2):281-299
- Sinclair HD (1997) Tectonostratigraphic model for underfilled peripheral foreland basins: An Alpine perspective. *Bull Geol Soc Am* 109 (3):324-346
- Sluijs A, Brinkhuis H, Crouch EM, John CM, Handley L, Munsterman D, Bohaty SM, Zachos JC, Reichert G, Schouten S, Pancost RD, Sinninghe Damste JS, Welters NLD, Lotter AF, Dickens GR (2008) Eustatic variations during the Paleocene-Eocene greenhouse world. *Paleoceanography* (23). doi:10.1029/2008PA001615

- St-Onge MR, Rayner N, Searle MP (2010) Zircon age determinations for the Ladakh batholith at Chumathang (Northwest India): Implications for the age of the India-Asia collision in the Ladakh Himalaya. *Tectonophysics* 495:171-183
- Wang C, Li X, Hu X, Jansa LF (2002) Latest marine horizon north of Qomolangma (Mt Everest): implications for closure of Tethys seaway and collision tectonics. *Terra Nova* 14:114-120
- Wang J, Hu X, Jansa L, Huang Z (2011) Provenance of the upper Cretaceous-Eocene deep-water sandstones in Sangdanlin, southern Tibet: Constraints on the timing of initial India-Asia Collision. *J Geol* 119:293-309
- Westerhold T, Röhl U, McCarren HK, Zachos JC (2009) Latest on the absolute age of the Paleocene-Eocene Thermal Maximum (PETM): New insights from exact stratigraphic position of key ash layers + 19 and - 17. *Earth Planet Sci Lett* 287:412-419
- Willems H (1993) Sedimentary history of the Tethys Himalaya continental shelf in south Tibet (Gamba, Tingri) during upper Cretaceous and lower Tertiary (Xizang Autonomous Region, PR China). *Bermen, FB Geowiss Univ Bremen* 38:49-140
- Willems H, Zhang B (1993) Cretaceous and lower Tertiary sediments of the Tibetan Himalaya in the area of Gamba (south Tibet, PR China). *Bermen, FB Geowiss Univ Bremen* 38:3-27
- Willems H (1996) Stratigraphy of the upper Cretaceous and lower Tertiary strata in the Tethyan Himalayas of Tibet (Tingri area, China). *Geol Rundsch* 85:723-754
- Yin A, Harrison TM (2000) Geologic evolution of the Himalayan-Tibetan Orogen. *Annu Rev Earth Planet Sci* 28:211-280
- Zhu B, Kidd WSF, Rowley DB, Currie BS, Shafique N (2005) Age of initiation of the India-Asia collision in the east-central Himalaya. *J Geol* 113:265-285

Fourth manuscript

## **5. High resolution Paleocene-Eocene carbon isotope excursion in the shallow marine environment of the Tethyan Himalaya (Tibet, China)**

**Qinghai Zhang<sup>1,2</sup>, Helmut Willems<sup>1,3</sup>, Lin Ding<sup>2</sup>, Xiaoxia Xu<sup>1</sup>**

<sup>1</sup> University of Bremen, Department of Geosciences, D-28359 Bremen, Germany

<sup>2</sup> Key Laboratory of Continental Collision and Plateau Uplift, Institute of Tibetan Plateau Research, Chinese Academy of Sciences, 100085 Beijing, China

<sup>3</sup> Nanjing Institute of Geology and Palaeontology, Chinese Academy of Sciences, 210008 Nanjing, China

To be submitted to *Geology*

## Abstract

The magnitude, duration, and pattern of the negative Carbon Isotope Excursion (CIE) are key to constraining the mass and rate of light-carbon release during the Paleocene-Eocene Thermal Maximum (PETM), which in turn play crucial roles in determining possible light-carbon sources and mechanisms triggering the PETM. Here we present a high-resolution CIE curve from the shallow marine limestones in Tibet, and the duration of each phase within the CIE has been tentatively estimated. The CIE in Tibet consists of three distinct  $\delta^{13}\text{C}$  declines and two smaller  $\delta^{13}\text{C}$  shifts. Each decline in  $\delta^{13}\text{C}$  lasted for ~1-10 kyr, and the smaller shifts had longer duration of ~25-40 kyr. The CIE curve from Tibet shows a similar pattern to the one at Ocean Drilling Program (ODP) Site 690, suggesting that the CIE throughout the entire ocean followed particular steps toward the most negative carbon isotope values. However, the magnitude of the negative CIE in Tibet is clearly larger than it is at ODP Site 690, implying that the magnitude might gradually increase from the deep seas to shallow marine environments. Our work will, to some extent, improve the current understanding of the PETM-CIE event.

## 5.1 Introduction

The PETM was a transient global warming event occurring at ~56 Ma (Kennett and Stott 1991; Zachos et al. 2001; Jaramillo et al. 2010), and generally its cause has been proposed to be a massive release of light carbon from the lithosphere into the ocean-atmosphere-biosphere system (Thomas and Shackleton 1996). The PETM was accompanied by drastic climatic and environmental perturbations as well as biotic changes (Bowen et al. 2002; Zachos et al. 2005; Nunes and Norris 2006; Schmitz and Pujalte 2007), and one of its characteristic features was an abrupt negative CIE taking place both in the ocean and on land (Kennett and Stott 1991; Bowen et al. 2001). The magnitude of the CIE reveals key information about the mass of light-carbon release and the possible mechanisms triggering the PETM (Dickens et al. 1997; Svensen et al. 2004; Higgins and Schrag 2006; DeConto et al. 2012). Past studies of the CIE suggested that there may be a difference in the magnitudes of the excursion from the deep oceans into shallow marine and terrestrial areas (McCarren et al. 2008; Tipple et al. 2011). Generally, the magnitudes of the negative CIE are relatively smaller in deep oceans (~2.5-4‰ in ODP Site 690) (Kennett and Stott 1991; Bains et al. 1999) and larger on land (~4.5-8‰ in the Bighorn Basin) (Bowen et al. 2001) (Fig. 1). Although Bowen et al. (2004) assumed the large magnitudes of the terrestrial CIE to have been amplified by increases in humidity and soil moisture, this assumption fails to explain the terrestrial-plant CIE from the wet Arctic setting (Pagani et al. 2006).

In addition, the detailed pattern of the CIE during the PETM is still uncertain because no two CIE curves with similar patterns have been reported from different sections. Although the high-resolution CIE measured from bulk carbonates at ODP Site 690 has been generally regarded as the most representative one (Bains et al. 1999), the possibility of carbonate dissolution due to ocean acidification (Zachos et al. 2005) still cannot be totally ruled out.

Most investigations on the CIE have been performed in the middle to high latitude deep seas and in terrestrial areas (McInerney and Wing 2011), but the shallow marine environment, as a possible link between land and deep sea, has been rather neglected. Here we report a high-resolution CIE curve from the Tethyan Himalaya of Tibet and discuss the magnitude, duration, and pattern of the CIE in the tropical shallow marine environment.

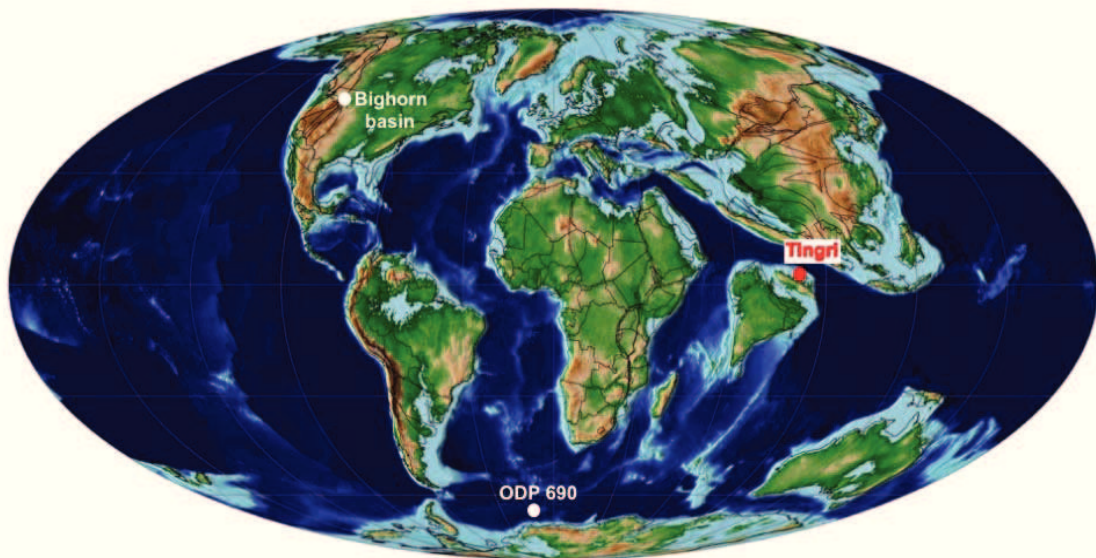


Fig. 1 Global paleogeographic map at the Paleocene-Eocene boundary (Scotese 2011). Showing our working area (Tingri) and two other representative locations for the PETM studies in deep sea (ODP Site 690) and on land (Bighorn Basin). Background colors show relative elevation/bathymetric depth.

## 5.2 Study area, materials, and methods

The study area is located near the county of Old Tingri in south Tibet, which represented the northernmost Indian continental margin when a shallow water carbonate ramp was deposited there during the early Paleogene (Willems et al. 1996) (Fig. 1). ~30 m thick nodular limestones with interbedded marls and thin-bedded limestones have been studied, and 150 limestone samples were collected with vertical sampling intervals of ~20 cm. The samples were freshly broken in order to select homogeneous micrites with

no evident reworked components or petrographically visible diagenetic alterations. The micrites were microdrilled using a dentist's drill and measured for carbon and oxygen isotopes. The  $\delta^{13}\text{C}$  and  $\delta^{18}\text{O}$  values were measured on a Finnigan MAT 251 Spectrometer at MARUM (University of Bremen), and the results were calibrated to the PDB with standard deviation of  $<0.05\text{‰}$  for the  $\delta^{13}\text{C}$  and  $<0.07\text{‰}$  for the  $\delta^{18}\text{O}$ . The measurements of Total Carbon (TC) and Total Organic Carbon (TOC) were conducted on a LECO CS200 elemental analyser at the Faculty of Geosciences (University of Bremen), and the precision for both is better than 1%. The content of  $\text{CaCO}_3$  was calculated by the equation  $\text{CaCO}_3 [\text{wt. \%}] = [\text{TC (wt. \%)} - \text{TOC (wt. \%)}] \times 8.33$ .

### 5.3 Discussion

The main CIE is preserved in the nodular limestones at Tingri, and the nodular limestones are rich in larger benthic foraminifera. The assemblages of larger foraminifera, which include the genera *Miscellanea*, *Ranikothalia*, *Lockhartia*, *Daviesina*, *Kathina* in the latest Paleocene and *Alveolina*, *Orbitolites* in the earliest Eocene (Zhang et al. 2012), indicate a water depth of  $< \sim 80$  m at the P/E boundary (Hottinger 1997). The origin of the nodular limestones at Tingri was discussed by Willems (1993), and based on paleontological, sedimentological and diagenetic evidence the nodular limestones have been interpreted as being formed by differential diagenesis, rather than allochthonous redeposition.

It is well known that  $\delta^{13}\text{C}$  and  $\delta^{18}\text{O}$  data from bulk carbonates are generally sensitive to diagenesis. However, we are confident that the effects of diagenesis on the  $\delta^{13}\text{C}$  are insignificant because (1) background values of high  $\delta^{13}\text{C}$  and low  $\delta^{18}\text{O}$  indicate that the limestones experienced water-rock interaction within a closed system such that the  $\delta^{18}\text{O}$  values were strongly altered while the pristine  $\delta^{13}\text{C}$  values were still preserved (Marshall 1992) (Fig. 2); (2) low TOC contents ( $< 0.4\%$ ) and no evident correlation between TOC% and  $\delta^{13}\text{C}$  (Fig. 3 A & B) argue against the effect of organic matter degradation on  $\delta^{13}\text{C}$ ; (3) Similarity of the patterns of the CIEs at Tingri and the geographically very distant section of ODP Site 690 is solid evidence for the good preservation of the  $\delta^{13}\text{C}$  signal at Tingri (Fig. 3 A & D); (4) The larger foraminifera as well as other fossils in the limestones are still perfectly preserved (Zhang et al. 2012).

The completeness of the CIE records from the deep seas has commonly been questioned owing to the possible effect of ocean acidification; however, the content of  $\sim 90\text{-}100\%$   $\text{CaCO}_3$  in the nodular limestones (Fig. 3C) clearly suggests that ocean acidification did not affect the shallow water carbonate deposition in Tibet. Evaluations of diagenetic overprints and high  $\text{CaCO}_3$  contents in the limestones suggest that the CIE at

Tingri probably represents a complete record of shallow water carbon isotope variations during the PETM.

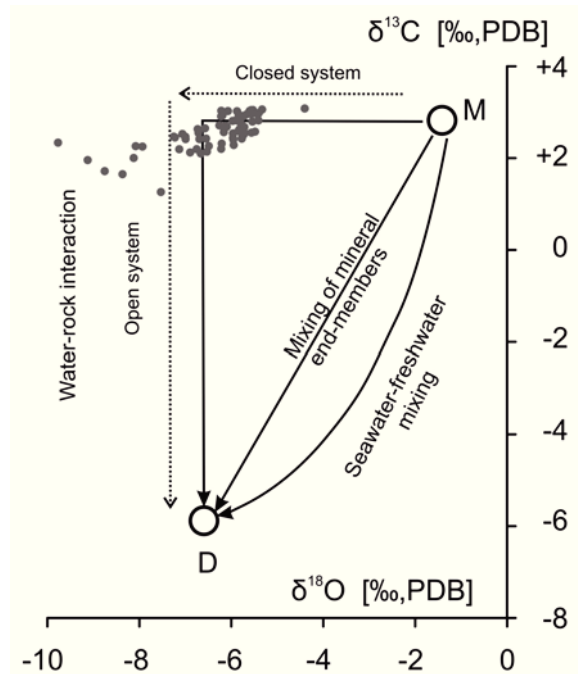


Fig. 2 Crossplot diagram of  $\delta^{13}\text{C}$  and  $\delta^{18}\text{O}$ . Possible diagenetic processes are shown by different paths from marine carbonate (M) to diagenetic limestone (D) with different effects on the original  $\delta^{13}\text{C}$  and  $\delta^{18}\text{O}$  values (Marshall 1992). Note that most of the background  $\delta^{13}\text{C}$  and  $\delta^{18}\text{O}$  values measured from bulk carbonates at Tingri fall into the junction area of the water-rock interaction between a closed system and an open system, indicating that the  $\delta^{13}\text{C}$  values were not altered by diagenetic overprints.

The pattern in the negative CIE at Tingri is nearly identical to that from ODP Site 690, except for the large magnitude and rapid recovery of the CIE in the former. Each phase of the main CIE defined at ODP Site 690 (Fig. 3D) can be recognized at Tingri (Fig. 3A). The similarity of the CIE patterns not only confirms that the CIE at ODP Site 690 (Bains et al. 1999) was not significantly affected by ocean acidification, but also implies that the CIE during the PETM probably followed certain steps throughout the ocean to attain its lowest values.

At Tingri, the magnitude of the negative CIE is  $\sim 6.5\text{‰}$ , which is distinctly larger than the magnitudes reported from deeper bathyal-abyssal environments (Bains et al. 1999; John et al. 2008), but to some degree consistent with those from terrestrial records (Bowen 2001; Pagani et al. 2006). This difference may imply that the magnitudes of the negative CIE are not uniform within the entire ocean-atmosphere-biosphere system, and probably increase gradually from the deep sea to shallow marine and land.



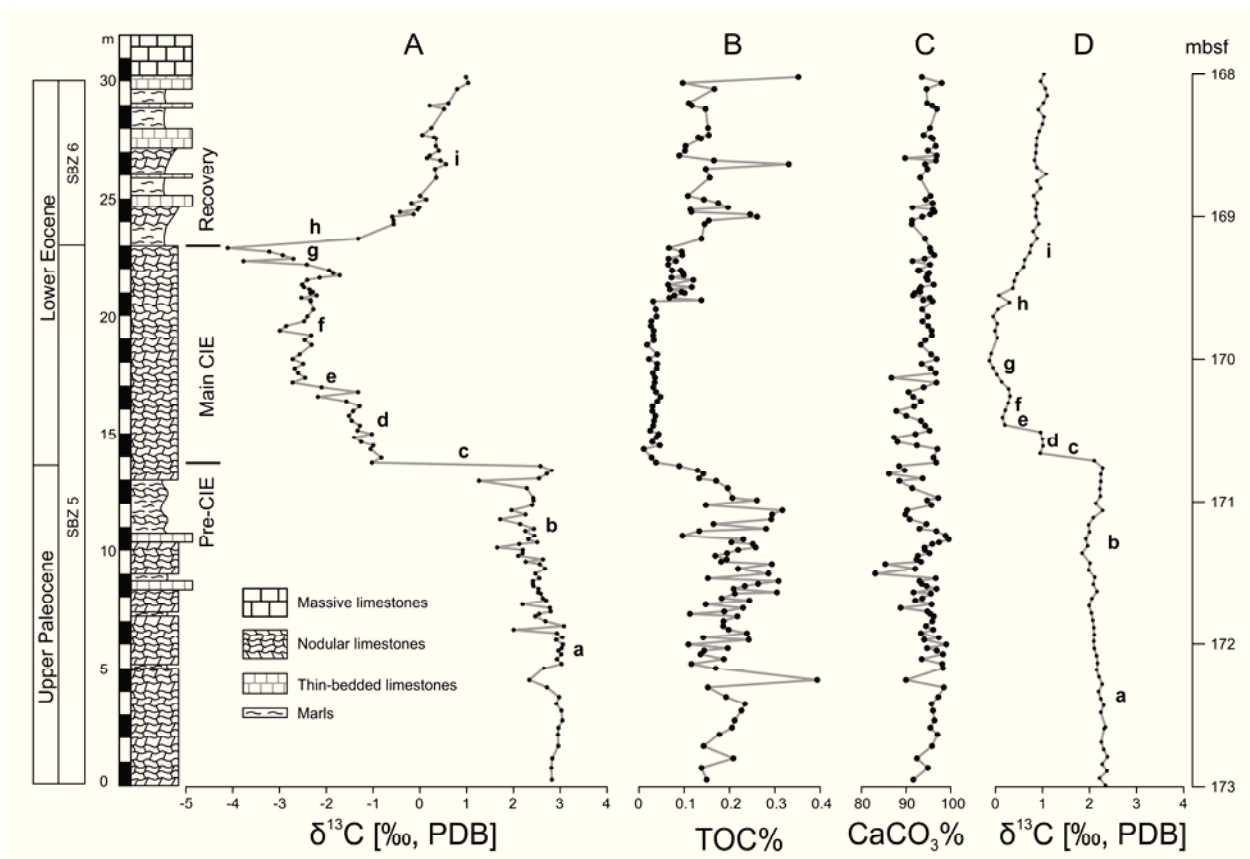


Fig. 3 The shallow marine limestones at Tingri with  $\delta^{13}\text{C}$  (A), TOC% (B), and  $\text{CaCO}_3\%$  (C). Figure D shows the  $\delta^{13}\text{C}$  curve from ODP Site 690, with lower-case letters labeling each phase in the main CIE (Bains et al. 1999). Note that the patterns of the CIEs at Tingri (A) and ODP Site 690 (D) are highly similar except for a larger magnitude and an abrupt initial recovery in the former. The SBZ refers to the Shallow Benthic Zones and the designation of the main CIE is adopted from Farley and Eltgroth (2003).

At Tingri, the main CIE is recorded in the ~9.2 m thick, highly homogeneous nodular limestones, for which we tentatively assume a constant sedimentation rate. Furthermore, there is agreement between the extraterrestrial  $^3\text{He}$  age model and the orbital age model with regard to the duration of the main CIE at ODP Site 690 (Farley and Eltgroth 2003; Röhl et al. 2007), and the two age models are adopted to indicate the duration of the CIE at Tingri owing to the similarity of their CIE patterns. Consequently, the average sedimentation rate of the nodular limestones and the duration of each phase in the main CIE at Tingri can be roughly calculated (Table 1).

At Tingri, the sedimentation rate was ~11 cm/kyr during the main CIE, and it decreased significantly to ~4 cm/kyr at the onset of the CIE recovery. This is roughly consistent with the findings at other continental margins (John et al. 2008), but in contrast to those in deep sea environments (Farley and Eltgroth 2003). The relatively high sedimentation rate during the main CIE indicates that continental margins were probably carbon sinks during the PETM.

Table 1 The CIE at Tingri with the  $^3\text{He}$  age model (Farley and Eltgroth 2003) and the orbital age model (Röhl et al. 2007). Note that the sedimentation rate and estimated ages are based on the age models and an assumed constant sedimentation rate of the homogeneous nodular limestones.

Phases of the CIE		Age models (kyr)		The CIE record in the shallow marine limestones at Tingri				
Stages	Letters	$^3\text{He}$ model	Orbital model	Lithology	Thickness (cm)	Magnitude of the CIE (‰)	Sedimentation rate (cm/kyr)	Estimated ages (kyr)
Pre-CIE	b	~45	~31	Marl + nodular Limestone	345		~7.7-11.1	
Main CIE	c	~80	~84	Highly homogeneous nodular limestone	15	-3.6	~11-11.5	1.3-1.4
	d				295	-0.3		25.7-26.8
	e				40	-1.4		3.5-3.6
	f				455	1		40-41.4
	g				115	-2.4		10-10.5
Initial Recovery	h	~30	~21	Marl	100	3.6	~3.3-4.8	

The main CIE at Tingri comprises three distinct declines (phases c, e, g) and two slightly negative or even positive shifts (phases d, f) in  $\delta^{13}\text{C}$ . Each of the  $\delta^{13}\text{C}$  declines took place within ~1-10 kyr, probably reflecting rapid and spasmodic releases of light carbon. The most abrupt and drastic light-carbon release (phase c) occurred at the onset of the CIE, lasted for ~1 kyr, and led to a ~3.6‰  $\delta^{13}\text{C}$  decline in the shallow marine environment. In contrast, the other two  $\delta^{13}\text{C}$  declines (phases e, g) show evident decreases in magnitude and increases in duration, probably implying two relatively small-scale light-carbon releases. Phases d and f lasted for a relatively longer time (~25-40 kyr), and the positive  $\delta^{13}\text{C}$  shift in phase f probably indicates there was already some positive feedback in the ocean, even during the longer-term process of generally negative drifting of the  $\delta^{13}\text{C}$ .

The initial recovery (phase h) is preserved in a ~1 m thick marl layer, and indicates an apparently rapid rebound of the carbon isotopes, which is quite contrast to the more gradual increase in  $\delta^{13}\text{C}$  values at ODP Site 690. The initial recovery led to a ~3.6‰

positive shift in  $\delta^{13}\text{C}$ , which is coincidentally identical to the magnitude of the  $\delta^{13}\text{C}$  decline at the onset of the CIE. Assuming that the  $^3\text{He}$ -based age model for the CIE is correct (Farley and Eltgroth 2003), the  $\sim 3.6\%$  positive  $\delta^{13}\text{C}$  shift within a time period of  $\sim 30$  kyr supports the premise that an accelerated sequestration of organic carbon, not by weathering of silicates alone, may exist at the initial recovery of the CIE (Bowen and Zachos 2010).

## 5.4 Conclusions

The CIE in the Tethyan Himalaya of Tibet is recorded in the  $\sim 9$  m thick limestones with a paleo-water depth of  $< \sim 80$  m. The  $\delta^{13}\text{C}$  values from bulk carbonates have not been altered by diagenetic overprints, and ocean acidification during the PETM did not affect carbonate deposition. For the first time, the CIE curves with similar patterns have been found from two geographically distant locations – Tibet and ODP Site 690, which suggests that the  $\delta^{13}\text{C}$  variations during the PETM followed certain steps throughout the ocean. However, the magnitude of the negative CIE in Tibet is clearly larger than at ODP Site 690, implying that it may increase gradually from the deep seas to shallow marine environments. The main CIE consists of three distinct  $\delta^{13}\text{C}$  declines and two minor  $\delta^{13}\text{C}$  shifts. Each  $\delta^{13}\text{C}$  decline lasted for  $\sim 1$ -10 kyr, and each minor shift had the duration of  $\sim 25$ -40 kyr. We tentatively speculate that there was already some positive feedback during the end of the main CIE, and a rapid recovery of the CIE did occur after the light-carbon release.

## Acknowledgements

We thank Anne Hübner, Christiane Schott, Friederike Wieseler, and Shun Li for assistance in laboratory and field work, Walter Hale for polishing the written English. The project is part of the Priority Programme 1372 Tibetan Plateau: Formation, Climate, Ecosystems (TiP) and is funded by the Deutsche Forschungsgemeinschaft (No. Wi725/26), and Chinese Ministry of Science and Technology (2011CB403101 to Ding Lin), Chinese Academy of Sciences (KZCX2-YW-Q09-03 to Ding Lin).

## References

- Bains S, Corfield RM, Norris RD (1999) Mechanisms of climate warming at the end of the Paleocene. *Science* 285:724-727
- Bowen GJ, Koch PL, Gingerich PD, Norris RD, Bains S, Corfield RM (2001) Refined isotope stratigraphy across the continental Paleocene-Eocene boundary on Polecat Bench in the northern Bighorn basin. In: Gingerich PD (ed) *Paleocene-Eocene*

- stratigraphy and biotic change in the Bighorn and Clarks Fork basins, Wyoming. University of Michigan papers on Paleontology 33, pp 73-88
- Bowen GJ, Clyde WC, Koch PL, Ting S, Alroy J, Tsubamoto T, Wang Y (2002) Mammalian dispersal at the Paleocene/Eocene boundary. *Nature* 295:2062-2065
- Bowen GJ, Beerling DJ, Koch PL, Zachos JC, Quattlebaum T (2004) A humid climate state during the Palaeocene/Eocene thermal maximum. *Nature* 432:495-499
- Bowen GJ, Zachos JC (2010) Rapid carbon sequestration at the termination of the Palaeocene-Eocene Thermal Maximum. *Nature Geosci* 3:866-869
- DeConto RM, Galeotti S, Pagani M, Tracy D, Schaefer K, Zhang T, Pollard D, Beerling DJ (2012) Past extreme warming events linked to massive carbon release from thawing permafrost. *Nature* 484:87-91
- Dickens GR, Castillo MM, Walker JCG (1997) A blast of gas in the latest Paleocene: Simulating first-order effects of massive dissociation of oceanic methane hydrate. *Geology* 25:259
- Farley KA, Eltgroth SF (2003) An alternative age model for the Paleocene-Eocene thermal maximum using extraterrestrial  $^3\text{He}$ . *Earth Planet Sci Lett* 208:135-148
- Higgins JA, Schrag DP (2006) Beyond methane: Towards a theory for the Paleocene-Eocene Thermal Maximum. *Earth and Planetary Science Letters* 245:523-537
- Hottinger L (1997) Shallow benthic foraminiferal assemblages as signals for depth of their deposition and their limitations. *Bull Soc Géol Fr* 168:491-505
- Jaramillo C, Ochoa D, Contreras L, Pagani M, Carvajal-Ortiz H, Pratt LM, Krishnan S, Cardona A, Romero M, Quiroz L, Rodriguez G, Rueda MJ, de la Parra F, Moron S, Green W, Bayona G, Montes C, Quintero O, Ramirez R, Mora G, Schouten S, Bermudez H, Navarrete R, Parra F, Alvaran M, Osorno J, Crowley JL, Valencia V, Vervoort J (2010) Effects of rapid global warming at the Paleocene-Eocene boundary on neotropical vegetation. *Science* 330:957-961
- John CM, Bohaty SM, Zachos JC, Sluijs A, Gibbs S, Brinkhuis H, Bralower TJ (2008) North American continental margin records of the Paleocene-Eocene thermal maximum: Implications for global carbon and hydrological cycling. *Paleoceanography* 23. doi:10.1029/2007PA001465

- Kelly DC, Bralower TJ, Zachos JC, Premoli-Silva I, Thomas E (1996) Rapid diversification of planktonic foraminifera in the tropical Pacific (ODP Site 865) during the late Paleocene thermal maximum. *Geology* 24:423-426
- Kennett JP, Stott LD (1991) Abrupt deep-sea warming, palaeoceanographic changes and benthic extinctions at the end of the Palaeocene. *Nature* 353:225-229
- Marshall JD (1992) Climatic and oceanographic isotopic signals from the carbonate rock record and their preservation. *Geol Mag* 129:143-160
- McCarren H, Thomas E, Hasegawa T, Röhl U, Zachos JC (2008) Depth dependency of the Paleocene-Eocene carbon isotope excursion: Paired benthic and terrestrial biomarker records (Ocean Drilling Program Leg 208, Walvis Ridge). *Geochem Geophys Geosyst* 9. doi:10.1029/2008gc002116
- McInerney FA, Wing SL (2011) The Paleocene-Eocene Thermal Maximum: A Perturbation of Carbon Cycle, Climate, and Biosphere with Implications for the Future. *Annu Rev Earth Planet Sci* 39:489-516
- Nunes F, Norris RD (2006) Abrupt reversal in ocean overturning during the Palaeocene/Eocene warm period. *Nature* 439:60-63
- Pagani M, Pedentchouk N, Huber M, Sluijs A, Schouten S, Brinkhuis H, Sinninghe Damste JS, Dickens GR, Expedition Scientists (2006) Arctic hydrology during global warming at the Palaeocene/Eocene thermal maximum. *Nature* 442:671-675
- Röhl U, Westerhold T, Bralower TJ, Zachos JC (2007) On the duration of the Paleocene-Eocene thermal maximum (PETM). *Geochem Geophys Geosyst* 8. doi:10.1029/2007gc001784
- Schmitz B, Pujalte V (2007) Abrupt increase in seasonal extreme precipitation at the Paleocene-Eocene boundary. *Geology* 35:215-218
- Scotese, CR (2011) The PALEOMAP Project PaleoAtlas for ArcGIS, Vol. 1; Cenozoic paleogeographic and plate tectonic reconstructions, Arlington, Texas
- Svensen H, Planke S, Malthé-Sorensen A, Jamtveit B, Myklebust R, Rasmussen Eidem T, Rey SS (2004) Release of methane from a volcanic basin as a mechanism for initial Eocene global warming. *Nature* 429:542-545
- Thomas E, Shackleton NJ (1996) The Paleocene-Eocene benthic foraminiferal extinction and stable isotope anomalies. In: Knox RWOB, Corfield RM, Dunay RE

(eds) Correlation of the Early Paleogene in Northwest Europe. Geol Soc London Spec Pub, pp 401-441

Tipple BJ, Pagani M, Krishnan S, Dirghangi SS, Galeotti S, Agnini C, Giusberti L, Rio D (2011) Coupled high-resolution marine and terrestrial records of carbon and hydrologic cycles variations during the Paleocene-Eocene Thermal Maximum (PETM). *Earth Planet Sci Lett* 311:82-92

Willems H (1993) Geoscientific investigations in the Tethyan. Universität Bremen, Bremen

Willems H, Zhou Z, Zhang B, Gräfe KU (1996) Stratigraphy of the upper Cretaceous and Lower Tertiary strata in the Tethyan Himalayas of Tibet (Tingri area, China). *Geol Rundsch* 85:723-754

Zachos J, Pagani M, Sloan L, Thomas E, Billups K (2001) Trends, rhythms, and aberrations in global climate 65 Ma to present. *Science* 292:686-693

Zachos JC, Rohl U, Schellenberg SA, Sluijs A, Hodell DA, Kelly DC, Thomas E, Nicolo M, Raffi I, Lourens LJ, McCarren H, Kroon D (2005) Rapid acidification of the ocean during the Paleocene-Eocene Thermal Maximum. *Science* 308:1611-1615

Zhang Q, Willems H, Ding L, Graefe K-U, Appel E (2012) Initial India-Asia continental collision and foreland basin Evolution in the Tethyan Himalaya of Tibet: Evidence from stratigraphy and paleontology. *J Geol* 120:175-189

## 6. Conclusions and future perspectives

### 6.1 Conclusions

The work in the thesis was based on ~900 samples collected mainly from four sections (sections ZP, ZM, and F at Gamba, and section 09ZS at Tingri) in the Tethyan Himalaya of Tibet. The studies of ~2000 thin sections and ~900 geochemical measurements of carbon and oxygen isotopes, TOC, and CaCO<sub>3</sub>% from these samples have reached the following conclusions:

1. With respect to the larger foraminifera, 72 species from 19 genera have been identified from the Paleocene-lower Eocene limestones in south Tibet, and their biostratigraphic ranges in the Shallow Benthic Zones (SBZs) have been tentatively assigned.
2. In Tibet, the Paleocene larger benthic foraminifera show high species diversity of *Lockhartia*, *Kathina*, *Daviesina*, *Miscellanea*, *Ranikothalia*, and *Operculina*. The differentiation between genera and species diversity probably started since the middle Paleocene. After that some genera had evolved more than one species in the so-called 'Lockhartia Sea', which doesn't correspond with the monospecific trait of K-strategist genera during the early period of the Global Community Maturation cycle in Europe (Hottinger 2001). In the early Eocene, some successful genera of *Alveolina*, *Orbitolites*, *Nummulites*, *Assilina*, and *Discocyclina* gained their predominance in the Neo-Tethyan Ocean, and the larger foraminifera showed a high-extent homogenization in the entire Neo-Tethyan Ocean.
3. A transient Larger Foraminiferal Extinction and Origination (LFEO) event has been found in the low latitudinal areas of the eastern Neo-Tethyan Ocean, which is characterized by the sudden disappearance of all Paleocene lamellar-perforate larger benthic foraminifera, such as *Miscellanea*, *Ranikothalia*, *Operculina*, *Lockhartia*, *Kathina*, and *Daviesina*, and the following dominance of porcellaneous forams of *Alveolina* and *Orbitolites*. It occurs at the boundary between SBZ 5 and 6, and coincides with the beginning of the CIE recovery at Tingri, which implies that some mechanisms causing the sudden CIE recovery (Bowen and Zachos 2010) probably also led to the LFEO during the PETM.
4. Following Oppel Zone's principle, 10 biozones from SBZ 1 to 10 have been established from the Zhepure Shan Formation at Tingri. At Gamba, the deposition of the Zongpu Formation started from SBZ 2 and terminated in SBZ 7.

5. High resolution carbon isotopic variations and well-defined SBZs at Tingri clearly show that the P-E boundary is located at the upper part of SBZ 5, not at the boundary between SBZ 4 and 5 proposed by some authors (Scheibner et al. 2005; Pujalte et al. 2009).
6. With special emphasis on the paleoecology of the larger foraminifera, eight microfacies types have been recognized in the Zhepure Shan Formation at Tingri. Microfacies analysis suggests there were a gradual deepening of depositional environment during the Paleocene and early Eocene and a sudden shallowing event at the Paleocene-Eocene boundary.
7. In addition to Tibet, the shallowing event at the Paleocene-Eocene boundary has also been reported from other shallow marine environments surrounding the Neo-Tethyan Ocean. Moreover, the sudden shallowing event was taking place under the background of a eustatic rise (Sluijs et al. 2008), and consequently reflects a regional tectonic uplift. The shallowing event is tentatively named 'Circum-Tethyan tectonic uplift', and in Tibet it is ascribed to the initial India-Asia continental collision.
8. High resolution CIE records have been obtained in the nodular limestones of the Zhepure Shan Formation at Tingri, and the CIE curve shows nearly identical pattern with the one from deep sea (Bains et al. 1999). However, the magnitude of the negative CIE in the shallow marine is evidently larger than it is from the deep sea (Kennett and Stott 1991; Bains et al. 1999), but to some extent consistent with the magnitudes from terrestrial records (Bains et al. 2003; Pagani et al. 2006). We propose that the CIE in the entire ocean has followed certain regular steps to reach the most negative carbon isotope values during the PETM, and the magnitude of the negative CIE may gradually increase from the deep sea to shallow marine and land.

## 6.2 Future perspectives

The investigations of the lower Paleogene larger foraminiferal limestones in the thesis have demonstrated the great potential of the shallow-water limestones for studying biostratigraphy, paleoenvironment and paleoclimatology as well as basin evolution. However, in order to further understand the lower Paleogene limestones in south Tibet, the following aspects still need to be paid more attention.

1. The origin of the nodular limestones in Member C of the Zhepure Shan Formation



The nodular limestones have been reported from different time periods during the geologic history, such as in the Devonian, Permian, Jurassic, and Paleocene, which usually exhibit densely packed nodules with only few matrix or scattered nodules floating in a matrix with like/unlike character. The nodular limestones could be formed in deeper marine and slope environments (such as the Jurassic 'Ammonitico rosso' facies of the Alpine-Mediterranean region) or shallow marine environments (such as Member C of the Zhepure Shan limestones on a carbonate ramp). Broadly speaking, the origins of the nodular limestones have been explained by diagenetic, sedimentary and tectonic processes (Flügel 2004). In the Tingri area, the detailed pattern of the CIE curve recorded in the nodular limestones are nearly identical to the one from the reference section ODP 690 (Bains et al. 1999), which implies that the up-down sequences of different nodules during their depositional processes are still kept orderly in the nodular limestones. Thus, allochthonous redeposition through mechanical processes during sedimentation can be generally excluded from the possible origins. However, how diagenetic and/or tectonic processes resulted in the formation of the nodular limestones still need further study.

## 2. The impact of the PETM-CIE on the shallow marine environment

The knowledge of the response of shallow marine environments to the PETM-CIE is relatively rare, which to a great extent owes to the lack of the findings of complete, in-situ shallow marine sedimentary sections covering the P-E boundary. In Spain, tectonic uplift during the PETM-CIE led to the deposition of continental sediments in most of shallow marine sections, such as Campo and Trespalacios sections (Pujalte et al. 2009). And in Egypt, most of the studied sections in the Galala Mountains are located in continental slopes (Scheibner and Speijer 2009), where redeposition of carbonate sediments and fossils during the period of sedimentation was inevitable. All those blur not only the precise location of the P-E boundary in the SBZs but also the response of shallow marine environments to the PETM-CIE. In the Tingri area of south Tibet, we found the perfect paleontological, sedimentary, and carbon isotopic records from the shallow marine environment during the PETM. Our present results suggest that the Paleocene larger foraminifera showed no response to the onset of the CIE, however, a sudden change of larger foraminiferal assemblages (LFEO) coincides with the initial recovery of the CIE. Therefore, how to understand the biotic changes in the shallow marine environment during the PETM will be the focus of our research in the next step.

## 3. The implication of diachronous terminations of the limestones at Tingri and Gamba

In Tibet, our studies suggest that the lower Paleogene larger foraminiferal limestones both at Tingri and Gamba were drowned in the early Eocene owing to the arrival of

foredeep depozones, which in turn was interpreted to be a result of progressively southward migrations of a foreland basin. Moreover, biostratigraphic evidence shows that the termination of the limestones at Gamba (~54-55 Ma) is ~1 Ma earlier than that at Tingri (~52.8 Ma). The ~ 1 Ma time lag of the limestones' termination between Gamba and Tingri implies that the Gamba area might fall into the foredeep depozone ~ 1Ma earlier than the Tingri area. If we take the average convergence velocity (between India and Asia) of ~50-100 Km/Ma during the early Eocene into account (Klootwijk et al. 1992; Guillot et al. 2003), a general conclusion can be reached that Gamba area was located at least ~50-100 Km closer to the suture zone than Tingri in the early Eocene. However, comparison of the actual locations of the two areas shows that Tingri is even slightly closer to the suture zone than Gamba at present. Therefore, changes of the positions of Gamba and Tingri relative to the suture zone since ~55 Ma probably contain important information for understanding the paleotopography of the southernmost Asia and the northernmost India before the India-Asia collision and the kinematic processes during the India-Asia collision.

#### 4. Further studies of the PETM-CIE in Tibet

In Tibet, the shallow marine section at Tingri records an extended, complete CIE with its detailed pattern almost identical to that from ODP 690 (Bains et al. 1999). In order to improve the understanding of the PETM-CIE in the shallow marine environments and make the best use of the section at Tingri, further multidisciplinary studies, such as <sup>3</sup>He-based and cycle-based age models (Röhl et al. 2007; Murphy et al. 2010), lipid biomarkers (Peckmann and Thiel 2004; Birgel and Peckmann 2008) for the possible evidence which may directly reveal the sources of light-carbon release, boron isotopes for paleo-seawater pH and atmospheric CO<sub>2</sub> concentrations (Pearson and Palmer 2000; Kasemann et al. 2005), and strontium isotopes for seawater chemistry and high resolution isotopic stratigraphy (Veizer et al. 1999; McArthur et al. 2001), are worth re-investigating on the nodular limestones of Member C in the Zhepure Shan Formation.

## References

- Bains S, Corfield RM, Norris RD (1999) Mechanisms of climate warming at the end of the Paleocene. *Science* 285:724-727
- Bains S, Norris RD, Corfield RM, Bowen GJ, Gingerich PD, Koch PL (2003) Marine-terrestrial linkages at the Paleocene-Eocene boundary. In: Wing SL, Gingerich PD, Schmitz B, Thomas E (eds) *Causes and consequences of globally warm climates in the early Paleogene*. *Geol Soc Am Spec Pap* 369, 1-9

- Birgel D, Peckmann J (2008) Aerobic methanotrophy at ancient marine methane seeps: A synthesis. *Organ Geochem* 39:1659-1667
- Bowen GJ, Zachos JC (2010) Rapid carbon sequestration at the termination of the Palaeocene-Eocene Thermal Maximum. *Nature Geosci* 3 (12):866-869
- Flügel (2004) *Microfacies of carbonate rocks: analysis, interpretation, and application*. Springer, Heidelberg Dordrecht London New York
- Guillot S, Garzanti E, Baratoux D, Marquer D, Mahéo G, de Sigoyer J (2003) Reconstructing the total shortening history of the NW Himalaya. *Geochem Geophys Geosyst* 4. doi:10.1029/2002gc000484
- Hottinger L (2001) Learning from the past. In: Levi-Montalcini R (ed) *Frontiers of life*. Academic Press, London & San Diego, pp 449-477
- Kasemann SA, Hawkesworth CJ, Prave AR, Fallick AE, Pearson PN (2005) Boron and calcium isotope composition in Neoproterozoic carbonate rocks from Namibia: evidence for extreme environmental change. *Earth Planet Sci Lett* 231:73-86
- Kennett JP, Stott LD (1991) Abrupt deep-sea warming, palaeoceanographic changes and benthic extinctions at the end of the Palaeocene. *Nature* 353:225-229
- Klootwijk CT, Gee JS, Peirce JW, Smith GM, McFadden PL (1992) An early India-Asia contact: Paleomagnetic constraints from Ninetyeast Ridge, ODP Leg 121. *Geology* 20:395-398
- McArthur JM, Howarth RJ, Bailey TR (2001) Strontium isotope stratigraphy: LOWESS Version 3: Best fit to the marine Sr-Isotope curve for 0-509 Ma and accompanying Look-up Table for deriving numerical age. *J Geol* 109:155-170
- Murphy BH, Farley KA, Zachos JC (2010) An extraterrestrial <sup>3</sup>He-based timescale for the Paleocene-Eocene thermal maximum (PETM) from Walvis Ridge, IODP Site 1266. *Geochim Cosmochim AC* 74:5098-5108
- Pagani M, Pedentchouk N, Huber M, Sluijs A, Schouten S, Brinkhuis H, Sinninghe Damste JS, Dickens GR, Expedition Scientists (2006) Arctic hydrology during global warming at the Palaeocene/Eocene thermal maximum. *Nature* 442:671-675
- Pearson PN, Palmer MR (2000) Atmospheric carbon dioxide concentrations over the past 60 million years. *Nature* 406:695-699

- Peckmann J, Thiel V (2004) Carbon cycling at ancient methane-seeps. *Chem Geol* 205:443-467
- Pujalte V, Schmitz B, Baceta JI, Orue-Etxebarria X, Bernaola G, Dinarès-Turell J, Payros A, Apellaniz E, Caballero F (2009) Correlation of the Thanetian-Ilerdian turnover of larger foraminifera and the Paleocene-Eocene thermal maximum: confirming evidence from the Campo area (Pyrenees, Spain). *Geol Acta* 7:161-175
- Röhl U, Westerhold T, Bralower TJ, Zachos JC (2007) On the duration of the Paleocene-Eocene thermal maximum (PETM). *Geochem Geophys Geosyst* 8. doi:10.1029/2007gc001784
- Scheibner C, Speijer RP, Marzouk AM (2005) Turnover of larger foraminifera during the Paleocene-Eocene Thermal Maximum and paleoclimatic control on the evolution of platform ecosystems. *Geology* 33:493-496
- Scheibner C, Speijer RP (2009) Recalibration of the Tethyan shallow-benthic zonation across the Paleocene-Eocene boundary. *Geol Acta* 7:195-214
- Sluijs A, Brinkhuis H, Crouch EM, John CM, Handley L, Munsterman D, Bohaty SM, Zachos JC, Reichert G, Schouten S, Pancost RD, Sinninghe Damste JS, Welters NLD, Lotter AF, Dickens GR (2008) Eustatic variations during the Paleocene-Eocene greenhouse world. *Paleoceanography* 23. doi:10.1029/2008PA001615
- Veizer J, Ala D, Azmy K, Bruckschen P, Buhl D, Bruhn F, Carden GAF, Diener A, Ebneth S, Godderis Y, Jasper T, Korte C, Pawellek F, Podlaha OG, Strauss H (1999)  $^{87}\text{Sr}/^{86}\text{Sr}$ ,  $\delta^{13}\text{C}$  and  $\delta^{18}\text{O}$  evolution of Phanerozoic seawater. *Chem Geol* 161:59-88

# 格物致知

<<礼记·大学>>